



THE UNIVERSITY OF
SYDNEY

School of Civil Engineering

Vulnerability to Flooding in Cities at Local Scale: New
Methodology with Application to a Local Council in Sydney

by Tanvir Ahmed

A thesis submitted for the Degree of Master of Philosophy

The University of Sydney

Declaration

This is to certify that to the best of my knowledge, the content of this thesis is my own work. This thesis has not been submitted for any degree or other purposes. All the assistance received in preparing this thesis and sources have been acknowledged.

Signed: Tanvir Ahmed

Date: 26th November 2018

Abstract

Background. Flood studies are conducted mostly at city or catchment scales. While such studies are necessary for developing flood policies, municipalities require, in addition, place-specific data and strategies that can identify population at risk and develop tailored measures to reduce vulnerability and increase resilience. Local authorities commonly conduct their own flood studies, concentrating on the geophysical aspects of floods without considering their differential social impacts. Different communities and individuals may be at risk for different reasons and for effective flood risk management and better adaptation to floods, it is important to know not only how significant the aggregate flooding risk is, but who is at risk and what are the drivers of their vulnerability.

Objectives and Methods. The objective of the study is to develop a new methodology for assessing urban flood risk at local scale by constructing a Flood Social Vulnerability (FSV) model and use it to assess the extent to which vulnerability to flooding is likely to change under different scenarios of climate change. The model is based on a hybrid approach, combining hydrological and hydraulic flood simulations with social vulnerability and built-environment indicators. The methodology is tested by applying it to the Marrickville Study Region (MSR), which consists of a number of suburbs in Sydney's Inner-West known to be prone to flooding. The study area is divided into a set of local spatial units, determined by the smallest unit at which aggregated data is available. This is, in the case of MSR, the SA1 scale of the Australian Bureau of Statistics. A set of indicators under each dimension of a flood risk pyramid – hazard, exposure and social vulnerability – are extracted from simulation analyses and socio-economic databases, for each local unit, and combined into a flood social vulnerability index (FSVI). Moreover, this research investigated how vulnerability might change in the future due to the impact of climate change under today's demographic, socioeconomic and built-environment conditions. To test the suitability of FSVI in informing flood mitigation policy making within a local government, results were discussed with the local government authority (the Inner-West Council) of the MSR.

Findings. FSVI developed in this study helped in detecting local flood vulnerability hotspots. There was little overlap between the spatial distribution of the three sets of indicators (hazard, exposure and social vulnerability). Hence, drawing on socio-economic information to assess vulnerability to flooding was found to be useful. Simulation of climate change

scenarios show noticeable increases in the duration of floods, but limited changes in flood depths, velocities and extents. Stakeholders at the Inner-West Council stated that the study's findings could inform the Council's current flood management planning, especially in relation to emergency services.

Acknowledgements

All praises are due to the Almighty Allah Who has provided me with the opportunity to complete this research.

This thesis could have never been completed without the valuable support of my supervisor Prof. Abbas El-Zein. I wish to express my heartfelt and sincere gratitude to him, who spent much time on reviewing the chapters of this thesis and offering direction and assistance throughout all phases of this research project. His continuous encouragement, constructive advice, and contribution to improving my writing throughout this research have been of inestimable value.

I gratefully acknowledge the grant received towards my research from the Civil Engineering Research Development Scheme (CERDS) at The University of Sydney. My sincere thanks to Dr Federico Maggi and Dr Kenneth Chung from School of Civil Engineering, the University of Sydney for their initial support during the research. I would like to have some words for Dr Fahim Nawroz Tonmoy, Griffith Centre for Coastal Management (GCCM), Griffith University for his generous support for reading draft at various stage of the research, suggesting valuable resources regarding the topic and offering me advice about publishing.

I am profoundly grateful to the stakeholders from Inner-West Council, Sydney especially to Ryan Hawken for his unstinting support including discussion time, feedback, models and flood data. I would like to acknowledge the support of Chris Huxley, Senior Engineer from BMT WBM for his valuable support of understanding the TUFLOW model and to Watercom for providing access to Drains software.

A very special thanks to my wife Aruba Azam, son Zayan Ahmed and daughter Aqeedah Ahmed. Without Aruba's continuous support, sacrifices and patience during my long spent hours at work, this research would not be possible. Finally, I would like to thank my father Tasir Uddin Ahmed and mother Jahanara Begum. Everything that I do today would not be possible without the sacrifices that my parents have made for me, throughout their life.

.

List of Book Chapter

Ahmed, T., El-Zein, A., Tonmoy, F. N., Maggi, F., & Chung, K. S. K. (2019). Flood Exposure and Social Vulnerability for Prioritizing Local Adaptation of Urban Storm Water Systems. In *Asset Intelligence through Integration and Interoperability and Contemporary Vibration Engineering Technologies* (pp. 41-49). Springer, Cham.

Notation and Abbreviation

1D	One Dimensional
2D	Two Dimensional
ABS	Australian Bureau of Statistics
AEP	Annual Exceedance Probability
ALS	Airborne Laser System
BSR	Broad Study Region
CC	Climate Change
DEM	Digital Elevation Model
F _E	Exposure Index
F _H	Hazard Index
FVI	Flood Vulnerability Index
FSVI	Flood Social Vulnerability Index
GHG	Greenhouse gases
GPS	Global Positioning System
h	Hour
HD	Hydrodynamic
IPCC	International Panel on Climate Change
m	Meter
MSR	Marrickville Study Region
NEXIS	National Exposure Information Systems
NSW	New South Wales
PCA	Principal Component Analysis
RCPs	Representative Concentration Pathways
SV	Social Vulnerability

SoVI Social Vulnerability Index
SRES Special Report on Emission Scenarios

Table of Content

Declaration	i
Abstract.....	ii
Acknowledgements.....	iv
List of Book Chapter	v
Notation and Abbreviation.....	vi
Table of Content	viii
1 Background and Aims	16
1.1 Introduction	16
1.2 Socio-Economic Flood Risk Assessment Framework.....	17
1.3 Objectives	20
2 Literature Review	22
2.1 Urban Flood Modelling.....	22
2.1.1 Urban Flood	22
2.1.2 Modelling Approaches	23
2.1.3 Climate Change Implication on Urban Flooding.....	27
2.1.3.1 Climate Change Scenario.....	28
2.2 Vulnerability Concept.....	29
2.2.1 Social Vulnerability (SV).....	30
2.2.2 Measurement of Social Vulnerability.....	31
2.2.2.1 Indicators selection.....	31
2.2.2.2 Quantitative measure of Social Vulnerability	32
2.3 Composite Indices of Vulnerability to Flood	35
3 Indicator-Based Flood Social Vulnerability Model.....	37
3.1 Introduction	37
3.2 Methods.....	38

3.3	Social Vulnerability Index (SoVI)	40
3.4	Exposure Index (F_E).....	41
3.5	Flood Hazard Index (F_H)	41
3.6	Software	42
4	Application of Flood Social Vulnerability Model.....	43
4.1	Study Area	43
4.1.1	Background.....	43
4.1.2	Drainage Systems	47
4.1.3	Land Use.....	49
4.2	Scope of Study.....	49
4.3	SoVI for Marrickville Valley.....	50
4.3.1	Indicator Selection	51
4.3.2	Principal Component Analysis (PCA)	54
4.3.3	Normalisation of Principal Components	55
4.4	Flood Exposure Index for Marrickville Valley.....	56
4.5	Flood Hazard Index for Marrickville Valley	57
4.5.1	Flood Simulation	57
4.5.2	Design Storm	58
4.5.3	F_H construction.....	59
4.6	Flood Social Vulnerability Index (FSVI) for Marrickville Study Region.....	60
5	Result and Discussion.....	61
5.1	Vulnerability to flooding in Marrickville.....	61
5.1.1	Social Vulnerability Index (SoVI)	61
5.1.1.1	Sensitivity Analysis of SoVI.....	68
5.1.2	Flood Exposure Index	72
5.1.3	Flood Hazard	75

5.1.3.1	Hydrological Analysis.....	75
5.1.3.2	Hydraulic Analysis.....	76
5.1.3.3	Climate Change Impacts.....	83
5.1.3.4	Approach.....	85
5.1.3.5	Climate change results.....	86
5.1.3.6	Flood Hazard Index.....	93
5.1.3.7	Sector-specific flood hazard index (SF _H).....	96
5.1.4	Flood Social Vulnerability Index (FSVI).....	98
5.2	Feedback from Inner-West Council.....	104
5.3	Discussion.....	105
5.3.1	Usefulness of Combined Indices.....	106
5.3.2	Vulnerability to Flooding under Climate Change in Marrickville.....	107
5.3.3	Vulnerability Assessment in Policy Making.....	109
5.3.4	Future Research.....	110
A.	Appendix A.....	111
B.	Appendix B.....	114
	References.....	127

Table of Figures

Figure 1-1: Risk Pyramid	19
Figure 2-1: Overall schema of combined hydrological/hydrodynamic modelling; rectangular shapes represent computer model/simulation tools; circular shapes represent the major input to and/or output of simulation tools.....	24
Figure 2-2: Depiction of a general 1D model of the river channel coupled with a 2D model of the floodplain (Source: Gilles et al., 2012)	25
Figure 2-3: Social vulnerability of Norway (Source: Holand et al., 2011); 0.5 standard deviations (Std.Dev) are used as breakpoints and highlight the areas that score over 0.5 or under -0.5 Std.Dev from the mean score. The areas above 0.5 Std.Dev represent higher than average levels of vulnerability, and vice versa)	34
Figure 3-1: Research design	37
Figure 4-1: Marrickville Study Region.....	45
Figure 4-2: Broader Study Region.....	46
Figure 4-3: Sub-catchments of Marrickville valley (Source: GRAY, 2011).....	47
Figure 4-4: Topography of the study area.....	48
Figure 4-5: Land use of Marrickville Valley.....	49
Figure 4-6: SA1 Map.....	55
Figure 5-1: Scree plot.....	62
Figure 5-2: Different components of SoVI and composite SoVI within Marrickville.....	66
Figure 5-3: a) SoVI of Marrickville Valley in comparison to its surrounding suburbs b) Zoom to Marrickville valley.....	67
<i>Figure 5-4: Variation of sample size of SA1 to check sensitivity of SoVI.....</i>	<i>68</i>
<i>Figure 5-5: Composite SoVI of MSR after changing sample size of SA1</i>	<i>70</i>
<i>Figure 5-6: Change in level of Social Vulnerability</i>	<i>72</i>
Figure 5-4: Exposure Index within Marrickville Valley	73

Figure 5-5: a) F_E of Marrickville Valley in comparison to its surrounding suburbs b) Zoom to Marrickville Valley.....	74
Figure 5-6: Comparison of rainfall intensities of ARR 1987 and ARR 2016 design storms for Marrickville valley	76
Figure 5-7: Provisional hazard categories (Source: NSW floodplain development manual).77	
Figure 5-8: 1% AEP design flood event: Peak flood depth	79
Figure 5-9: 1% AEP design flood event: Peak velocity vector.....	80
Figure 5-10: 1% AEP design flood event: Flood Duration	81
Figure 5-11: 1% AEP design flood event: Provisional Flood Hazard	82
Figure 5-12: Locations of Natural Resource Management Clusters, source: Bates et al. (2016).....	84
Figure 5-13: Confluence of Cooks River.....	85
Figure 5-14: 1% AEP design flood event, Climate Change Scenario, RCP 8.5 (2080): Peak flood depth	88
Figure 5-15: Change in flood depth due to CC in comparison to base condition.....	88
Figure 5-16: 1% AEP design flood event, Climate Change Scenario, RCP 8.5 (2080): Peak velocity vector.....	89
Figure 5-17: Change in flood velocity due to CC in comparison to base condition.....	89
Figure 5-18: 1% AEP design flood event, Climate Change Scenario, RCP 8.5 (2080): Flood Duration.....	90
Figure 5-19: Change in flood duration due to CC in comparison to base condition	90
Figure 5-20: 1% AEP design flood event, CC Scenario, RCP8.5 (2080): Provisional Flood Hazard.....	91
Figure 5-21: Change in provisional flood hazard zone due to CC in comparison to base condition	91
Figure 5-22: Correlation of flood hazard index between base condition Vs different climate change scenarios.....	94
Figure 5-23: Flood Hazard Index: 1% AEP design flood event.....	95

Figure 5-24: Flood Hazard Index: RCP 8.5 (2080).....	95
Figure 5-25: Residential flood hazard index for 1% AEP design event.....	97
Figure 5-26: Industrial flood hazard index for 1% AEP design event.....	97
Figure 5-27: Correlation between different indices.....	98
Figure 5-28: Flood Social Vulnerability Index for different weight combination: additive aggregation.....	99
Figure 5-29: Flood Social Vulnerability Index for different weight combination: multiplicative aggregation	100
Figure 5-30: Percentage of area and population exposed under each categories of F_H	101
Figure 5-31: percentage of high/very high categories of FSVI with different weight combination.....	101
Figure 5-32: FSVI _E : Equal Weight (additive aggregation) with four selected SA1s.....	102
Figure B-1: 1% AEP design flood event, Climate Change Scenario, RCP 4.5 (2060): Peak flood depth	115
Figure B-2: 1% AEP design flood event, Climate Change Scenario, RCP 4.5 (2080): Peak flood depth	116
Figure B-3: 1% AEP design flood event, Climate Change Scenario, RCP 8.5 (2060): Peak flood depth	117
Figure B-4: 1% AEP design flood event, Climate Change Scenario, RCP 4.5 (2060): Peak velocity vector.....	118
Figure B-5: 1% AEP design flood event, Climate Change Scenario, RCP 4.5 (2080): Peak velocity vector.....	119
Figure B-6: 1% AEP design flood event, Climate Change Scenario, RCP 8.5 (2060): Peak velocity vector.....	120
Figure B-7: 1% AEP design flood event, Climate Change Scenario, RCP 4.5 (2060): Flood Duration.....	121
Figure B-8: 1% AEP design flood event, Climate Change Scenario, RCP 4.5 (2080): Flood Duration.....	122

Figure B-9: 1% AEP design flood event, Climate Change Scenario, RCP 8.5 (2060): Flood Duration..... 123

Figure B-10: 1% AEP design flood event, CC Scenario, RCP4.5 (2060): Provisional Flood Hazard..... 124

Figure B-11: 1% AEP design flood event, CC Scenario, RCP4.5 (2080): Provisional Flood Hazard..... 125

Figure B-12: 1% AEP design flood event, CC Scenario, RCP8.5 (2060): Provisional Flood Hazard..... 126

Table of Tables

Table 4-1: Vulnerability related questions and answer.....	50
Table 4-2: Social Vulnerability Indicators Selected for the Study	52
Table 4-3: Flood Exposure Indicators.....	57
Table 4-4: FSVI with different weight combination	60
Table 5-1: Extracted Principal Component.....	63
Table 5-2: Extracted Principal Component after changing sample size of SA1.....	71
Table 5-3: Flows for the 1% Annual Exceedance Probability for ensemble storms.....	75
Table 5-4: % of Area Flooded Under Different Flood Indicators (Base Condition)	83
Table 5-5: Projected Rainfall Change for the Year 2060 and 2080 relative to the period 1986-2005	84
Table 5-6: Projected Sea Level Rise in meter for the Year 2060 and 2080 relative to 1986 - 2005	85
Table 5-7: Climate change scenarios.....	86
Table 5-8: Percentage of Area Flooded under Different Flood Indicators due to Base and RCP8.5 (2080).....	92
Table 5-9: Percentage of Area Flooded Under Different Flood Hazard Zone due to Base and RCP8.5 (2080).....	92
Table 5-10: Comparison of indicators/component score between four selected SA1s.....	103
Table A-1	112
Table A-2.....	113

Chapter 1

Background and Aims

1.1 Introduction

Global flood losses are increasing due to a number of factors, including changes in climate patterns as well as growing population and economic development in flood-prone areas (Ashley et al., 2005; Muis et al., 2015). The reported average annual global losses between 1980 and 2012 exceeded \$23 billion (Jongman et al., 2015). Climate change is likely to significantly increase weather-related hazards including flood hazards and associated economic damage (Muller, 2007) due to a change in rainfall patterns and an increase in the frequency and intensity of extreme weather events (Jongman et al., 2015). Considering only projected population growth, urbanization and growth in economic activity, but without taking into account increases in flood frequency and intensity, the average annual global flood losses are set to increase approximately ninefold from 2005 to 2050. If the effects of climate change are considered as well, then annual losses in 2050 would be expected to increase by more than 17 times relative to 2005 (Hallegatte et al., 2013).

A rich literature has helped us to understand the physical behavior of floods and predict future flooding scenarios (Zhou, 2014; Domingo et al., 2010; Patro et al., 2009; Sole et al., 2008; Phillips et al., 2005; Ashley et al., 2005; Overton, 2005; Hallegatte et al., 2013). In addition, a number of studies have proposed and/or analysed flood management strategies aimed at reducing economic damage and assisting communities in adapting to flooding events (Muis et al., 2015; Liu et al., 2015; Tavares et al., 2015; Garbutt et al., 2015; Hunt and Watkiss, 2011; Charlesworth, 2010). However, most flood studies are conducted at city or catchment scales. As far municipal government is concerned, city-scale flood management

strategies are important and useful but not sufficient. Municipalities require locally-specific data and strategies that can identify population at risk and develop specific measures to reduce vulnerability and increase resilience. Such strategies are typically inscribed within, and informed by, larger-scale strategies but are not entirely determined by them.

In some cases, local authorities have conducted their own flood studies. However, these studies typically concentrate on the geophysical aspects of flooding by determining frequency and areal extent of flooding and providing recommendations for improving drainage paths and upgrading storm water infrastructure (e.g. Cornelius, 2012; GRAY, 2011; Reid et al., 2014). However, different communities and individuals may be at risk for different reasons (e.g., living in low-lying areas, poor mobility, poor access to financial resources in times of flood). Hence, for effective flood risk management and for better adaptation to floods, it is important to know not only how significant the aggregate flooding risk is, but who is at risk and what are the drivers of their vulnerability (Koks et al., 2015). While the literature on flooding has recognized the importance of incorporating institutional and socio-economic factors in determining vulnerability to flooding, conducting such assessments at local scale remains limited.

The goal of this project is to develop and apply a new methodology for assessing vulnerability to flooding in urban areas at local scale. More specifically, this thesis aims to advance our understanding of the relative importance of geophysical, institutional and socio-economic factors within local communities that make them vulnerable to flooding. A hybrid approach, combining hydrological and hydraulic analyses with social vulnerability analyses, is adopted. The methods developed here are tested and validated by applying them to Marrickville Study Region (MSR) located into Sydney's Inner-West council that is known to be prone to flooding events.

1.2 Socio-Economic Flood Risk Assessment Framework

A number of geophysical factors affect the intensity and distribution of flooding, such as meteorology, hydrology, hydraulics, climate change, topography and patterns of land use etc. However, the impact of flooding (damage to properties, loss of lives, spread of diseases etc.) depend not only on such factors but also on the characteristics of the built environment, demography and the socioeconomic conditions of communities affected by

the flood. These factors, together, can have a strong effect on the ability of individuals, communities and institutions to adapt and respond to the floods. Flood risk assessment is an important tool for an effective flood risk management process, and is usually the first step towards the development and implementation of short and long-term flood risk reduction plans, that operate both before and after floods have occurred (Floodsite, n.d.).

Flood risk mitigation can be broadly divided into structural and non-structural approaches (Thampapillai and Musgrave, 1985). Often, risk due to flood cannot be fully prevented by the application of structural measures only, even those designed for rarely extreme events. This is because there is always a chance of residual risks due to the failure of technical flood protection systems or natural and human-induced modifications of land form and land use (Plate, 2002; Cutter et al., 2013). Structural protection measures rarely eliminate all flood risk and preparedness is therefore an important part of flood risk management (Plate 2002). For example, early warning systems which forecast information about upcoming floods are an essential part of flood management which provide vital lead time to control reservoir levels and prepare evacuation in advance (Chau et al., 2005; Cloke and Pappenberger, 2009). Conjunctive use of structural and non-structural measures is important for reducing flood risk and implementing this strategy at local level requires strong organizational capacity by local government, including data collection and vulnerability assessment (Brody et al., 2010).

A number of different conceptual frameworks exist for analysing flood risk and vulnerability. Methodologies that have been applied in prior flood risk assessments are implemented within probabilistic and/or deterministic analyses. The most traditional, and still most commonly used, flood risk evaluation framework is based on a definition of risk as the product of the probability of occurrence of the flood and its likely impact. Typically, the probability of occurrence - evaluated from past time series or climate change projection is expressed as exceedance probabilities (Apel et al., 2004; Tapsell et al., 2002; Koks et al., 2015; van Manen and Brinkhuis, 2005). A commonly-used approach to quantify economic damage and estimate the number of casualties is based on water depth-damage functions. The quantitation is usually based on expert analysis of impacts of previous flood events (Muis et al., 2015; van Manen and Brinkhuis, 2005). This approach does not usually consider social ramifications of risk (other than those implied by economic cost, injury and

death) or differential exposure to the hazard within communities nor does it assess the spatial distribution of the risk, relying instead on aggregate indicators. Some approaches extend the risk framework by considering all possible flood events, with their probability of occurrence and likely impacts, while taking into account various uncertainties associated with the risk (Apel et al., 2004).

The impacts of a flood, as well as the capacity to deal with it through preparedness, depends on, in addition to the intensity of the flood and the extent of exposure, the infrastructure systems and institutional capacity in place and, more generally, the ability of populations to cope with and adapt to the hazard (Koks et al., 2015). Hence, damage or loss of life due to flood can be seen as the outcome of interactions between the local ecology, physical environment, socio-economic factors and institutional arrangements (Mileti, 1999). Therefore, any assessment of flooding must take into account all of these factors and not just the geophysical ones – and this can be challenging from a methodological point of view because data and information on the different factors are different in nature and in quality (Schanze, 2006). This is the case for studies conducted at country or catchment levels, but equally for those conducted at local scale.

Another conceptual framework – used by a number of studies in the literature – defines flood risk as a pyramid in which the impact of floods is the outcome of the interaction between hazard, exposure and social vulnerability (Crichton, 2002; Dwyer et al., 2004; Lindley et al., 2006; Dang et al., 2011; Kaźmierczak and Cavan, 2011)

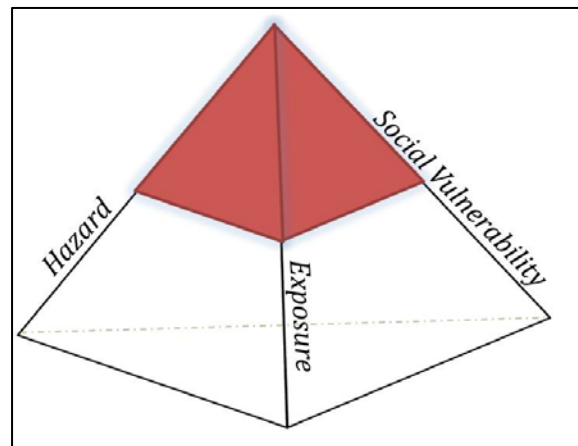


Figure 1-1: Risk Pyramid

(see Figure 1-1). Hazard is typically characterized by its probability of occurrence (Dwyer et al., 2004) and most commonly represented by the areal extent and depth of flooding in time and space under different scenarios (Plate, 2002; Schanze, 2006). “Exposure” is the extent to which valued aspects of a community’s life (e.g., health, prosperity, security) are likely to be affected by the flood (Field, 2009; Koks et al., 2015; Dwyer et al., 2004; GeoscienceAustralia, n.d.). Often, characterizing exposure consists of identifying key economic and livelihood elements of a community in GIS-type data management systems.

On the other hand, social vulnerability (SV) refers to the intrinsic characteristics of the exposed elements which determine their potential to be harmed and their capacity to cope with, and adapt to, the hazard (Sarewitz et al., 2003). Cutter et al. (2003) defines social vulnerability as demographic and socioeconomic features of people, community and infrastructures that reflect their poor ability to prepare for, respond to and recover from hazard and disaster. The concept helps explain why two communities equally exposed to the same hazard may experience its impacts in very different ways (Cutter et al., 2013). SV was often neglected because of the difficulty in quantifying it (Cutter et al., 2003). Social vulnerability can be quantified by constructing a social vulnerability index (SoVI) where the index value is calculated by aggregating a set of indicators reflecting various elements of vulnerability information. Including social vulnerability in flood risk assessment allows for a more comprehensive characterization of the impacts of flood, as represented by the three dimensional risk pyramid shown in Figure 1-1 where each face of the pyramid represents one the three dimensions discussed earlier, hazard, exposure and social vulnerability (Dwyer et al., 2004). Hence, increasing the magnitude of any of these dimensions increases the volume of the pyramid which reflects a higher overall risk. The aim of this study is to develop a flood social vulnerability index which combines all three dimensions of the risk pyramid and can be used at a municipal scale to provide useful planning information for local government. The index will allow spatial units within a locality to be compared to each other in terms of their vulnerability to flooding. Natural hazards such as floods, cyclones and earthquakes cannot be fully prevented, but their impacts can be mitigated by identifying social groups vulnerable to their effects and assisting them through preparedness and emergency planning measures process (Solangaarachchi et al., 2012). Since, ultimately all impacts of flooding are experienced locally, preparedness requires detailed information at a local scale that can help local government planners to develop specific, differentiated mitigation plans, rather than simply adopting homogenous flood mitigation measures based on larger-scale studies.

1.3 Objectives

The objective of the study is to develop a new methodology for assessing urban flood risk at local scale by developing a Flood Social Vulnerability (FSV) model. The developed

methodology can be used by local government authorities as an input for better adaptation strategies for flood and climate change issues. The output of the FSV model will be a flood social vulnerability index (FSVI) that will allow a comparison of vulnerabilities of different spatial units. A detailed hydrological and hydraulic analysis will be conducted, as part of the methodology, in order to characterize the hazard and exposure dimensions of the risk pyramid, under climate change projections. Results from the flood analysis are combined with a newly-constructed social vulnerability index to produce the FSVI at local scale. The term “local”, as used here, refers to the lowest possible spatial resolution at which social and flood vulnerability index can be determined based on available data resolution. The following specific objectives will be pursued:

Build a hydrological and hydraulic model to quantify the magnitude of the hazard under different climate scenarios.

1. Build an exposure indicator based on built-environment data.
2. Build a social vulnerability index based on a combination of socio-economic and demographic indicators.
3. Combine the above three indicators into an FSVI and analyse the possible future evolution of the FSVI.
4. Apply the methodology to Marrickville Study Region (MSR) and identify vulnerable groups, sources of vulnerability as well as measures likely to reduce vulnerability.

The study will hence seek to answer the following research questions:

1. Does an index combining geophysical and socio-economic elements of flood risk provide useful information on vulnerable groups, over and above that found in more conventional flood studies?
2. How does the spatial pattern of flooding in the Marrickville valley change under various scenarios of climate change and what kind of adaptation measures are most likely to reduce vulnerability to flooding under climate change?
3. How useful are vulnerability assessments, such as the one conducted here, for municipal planning for flooding?

Chapter 2

Literature Review

2.1 Urban Flood Modelling

2.1.1 Urban Flood

Urban flooding is increasing worldwide due to rapid urbanization and change in hydrological and meteorological condition in cities (Koop and van Leeuwen, 2017; Miller and Hutchins, 2017; Huong and Pathirana, 2013; Bruni et al., 2015; Ashley et al., 2005). In addition, many cities around the world are experiencing flooding due to insufficient drainage capacity, lower standard of drainage systems, financial constraints and limited ability to modify existing underground drainage systems (Mark et al., 2004). There are a number of negative consequences of urban flooding, including damage to assets and loss of lives. Other impacts of urban flooding include economic losses due to disruption of traffic, decreased productivity, spread of water-borne diseases and decline in property values (König et al., 2002).

An urban flood can be defined as a situation in which water remains on the surface because the stormwater drainage system cannot discharge it in a timely fashion, i.e. when runoff generated by rainfall or upstream water flow exceeds the capacity of the drainage systems (Schmitt et al., 2004). Sometimes the underground pipe systems may have sufficient capacity and the surface intake capacity may be the limiting factor. In that case, at the time of heavy rainfall, a major portion of the runoff will flow above surface while the pipe systems are only partially filled. Hence, the duration of the flood depends on the capacity of the total system including the surface and underground components (Mark et al., 2004).

The surface drainage component of an urban drainage system may include curb/street gutters, drainage swales, road side channels, water ways, road reserves, detention/retention basins and water bodies like lakes, ponds etc. The roofs of houses and buildings, streets, parking lots, yards etc. are also a part of surface drainage components that are connected with the sewer system via inlets and street gutters. On the other hand, the closed underground sewer network contains inlets, pipes, junction pits, access chambers and outlet structures (Schmitt et al., 2004; QUDM, 2013).

Urban geometry is highly complex as it contains artificial morphology with a number of barriers like curbs, footpaths, fences which divert the shallow water flows in different directions. An urban catchment is comparatively smaller than a rural catchment and is characterized by a fast hydrological response due to a high percentage of imperviousness (McGrane, 2016; Bruni et al., 2015). The impervious surface decreases the infiltration capacity of the system which eventually increases the surface runoff and higher peak discharge occurs more rapidly in comparison to a natural catchment. On the other hand, though small natural streams are reduced or paved over in urban areas, the overall drainage density increases with the increasing number of artificial channels (Paul and Meyer, 2001).

It is clear, therefore, that any attempt at understanding vulnerability to flooding in cities must take into account the complex network of systems and features affecting runoff and drainage, whether they are an intentional part of the urban storm-water system or not (Hsu et al., 2000). Flood models are commonly used to simulate rainfall events in specific urban settings. The output of these models are flood depth and extent, water velocity profiles and flood duration (Schmitt et al., 2004; Rauch et al., 2002; QUDM, 2013). The models can be calibrated against historical records of flooding and can be used to simulate flooding dynamics under different climate change scenarios. In addition, they allow planners to consider the effects on flooding risk of specific modifications to the built environment.

2.1.2 Modelling Approaches

Flood models are based on a combination of hydrological and hydrodynamic approaches, according to overall schema shown in Figure 2-1.

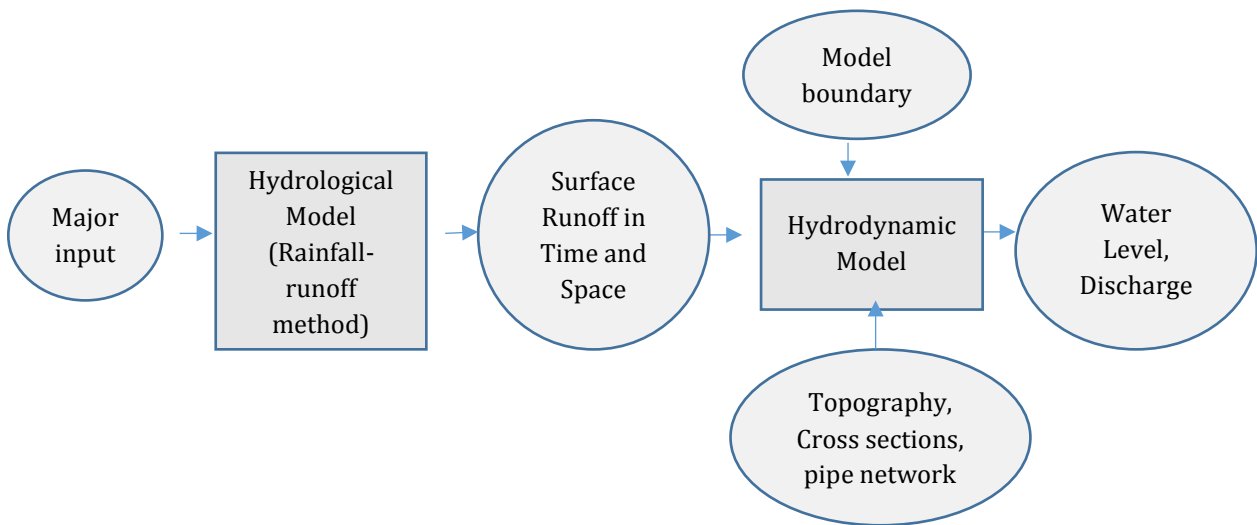


Figure 2-1: Overall schema of combined hydrological/hydrodynamic modelling; rectangular shapes represent computer model/simulation tools; circular shapes represent the major input to and/or output of simulation tools.

Hydrological models take rainfall as a major input and calculate the surface runoff that becomes an input to the hydrodynamic model. Hydrological simulations are important because the spatial and temporal resolution of rainfall affects time shifts of modelled runoff peaks (Bruni et al., 2015). Hydrology can be modelled using a separate rainfall-runoff model. Alternatively, rather than conducting a separate hydrological simulation prior to the hydrodynamic one, as shown in Figure 2-1, the hydrology can be characterized through the 2D hydrodynamic model using the rain-on-grid method. Both approaches (rainfall-runoff and rain-on-grid) have already been successfully applied in a number of studies (Phillips et al., 2005; Cornelius, 2012; Johnson, 2013) and either can be used provided adequate calibration has been performed (Johnson, 2013). A major advantage of rainfall-runoff models is that significant knowledge has accrued because of their long history. The advantage of the rain-on-grid method, on the other hand, is that it removes the need to build and run a separate hydrological model. However, it is a comparatively new technology, can increase hydraulic modelling runtime significantly, and require detailed digital terrain information. Furthermore, only a limited amount of research has been undertaken in support of this approach.

The hydrodynamic (HD) behaviour of the water system can be modelled either by one dimensional (1D) HD or two dimensional (2D) HD or 1D and 2D (1D-2D) coupled hydrodynamic modelling techniques (Figure 2-2). Both the 1D and 2D modelling techniques are based on solving the Saint Venant equations which are derived from principles of

conservation of mass and momentum. In a 1D model, the cross-sectional average Saint Venant equations describe the evolution of water depth and discharge or mean velocity by solving one continuity and one momentum equation. In 2D models, the depth average Saint Venant equations (also known as shallow water equations) describe the evolution of water depth and two Cartesian velocity components by solving one continuity equation and two momentum equations (Petersen et al., 2002; Gharbi et al., 2016).

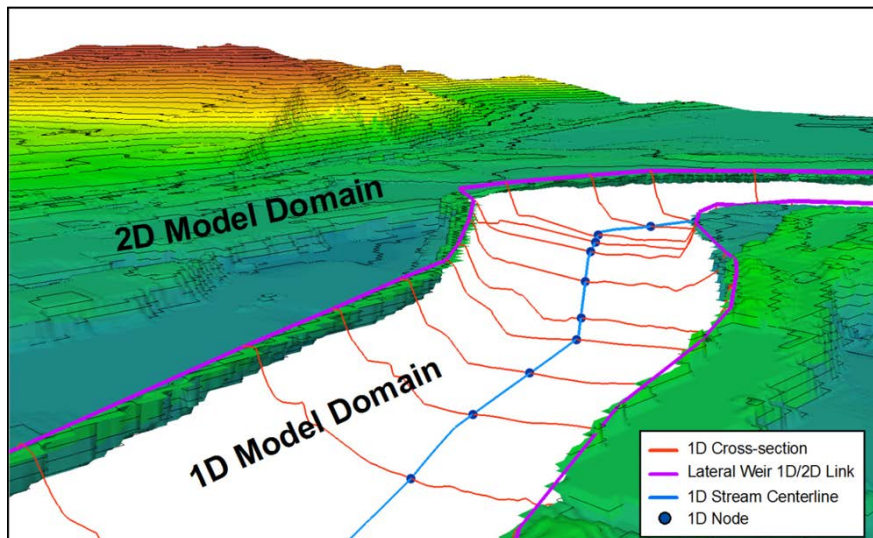


Figure 2-2: Depiction of a general 1D model of the river channel coupled with a 2D model of the floodplain (Source: Gilles et al., 2012)

Topography is one of the major inputs for the HD model. The geographic information in the 1D model is described by the cross-section data while in 2D model it is described by a digital elevation model (DEM). DEM is the digital representation of natural topography as well as man-made features located on the surface of the earth in raster format (Vaze and Teng, 2007; Gupta, 2018). The higher the resolution, the more accurate will be the real-world representation. On the other hand, the computational requirements of the model, including simulation time, will increase with increasing resolution of DEM (Sole et al., 2008). Airborne Laser System (ALS) is a technique designed to quickly produce DEM using instruments such as GPS, laser scanners and video cameras fastened to aircraft. The ALS technique produces high quality of DEM with an accuracy of ± 25 cm (Sole et al., 2008). The required resolution of DEM depends on the type of catchment that is being modelled. To model a rural flood plain, 30m (30 m \times 30 m) resolution of the DEM usually produces good results (Karim et al., 2011). Even 90m resolution DEM has been used for river basin modelling (Patro et al., 2009). But for urban terrain, micro scale topography requires 1 to 5

m resolution in order to adequately represent complex flow paths around different urban features (Hunter et al., 2008).

There is a rich body of literature describing urban drainage models based on the above-mentioned three approaches (1D or 2D or 1D-2D). The selection of a correct HD model depends on the purpose and complexity of the watershed systems. 1D models can simulate both surface networks and buried pipe networks. These two types of networks are dynamically interconnected and the flow exchange between the two systems is simulated by inlets (Mark et al., 2004; Leandro et al., 2016; Chang et al., 2015). 1D models are easy to setup, calibrate and explain but they cannot be applied in all types of geography. To model a flood plain or an urban terrain in 1D, it is necessary to widen cross-sections of a channel (Vojinovic and Tutulic, 2009). However, this may not be a realistic assumption, in flat areas with large variations in water depth. 2D models provide a more valid description of flow by describing the spatial distribution of flow (Petersen et al., 2002; Fatichi et al., 2016). For example, in an urban catchment, when the water overtops the curb, flow direction can change due to a change in slope and this kind of effect is best simulated in 2D (Leandro et al., 2009). This is why, for pipe flow, artificial open channels, creeks and rivers, where flow paths are well defined, 1D hydrodynamic models are recommended. 2D models, on the other hand, are better used to model the effects of more complex urban features (Vojinovic and Tutulic, 2009; Cornelius, 2012; QUDM, 2013). An added disadvantage of 1D models is that generation of flood maps requires extra effort because longitudinal profiles of channel water levels need to be extrapolated through the flood plain to generate water surface maps (using the GIS software). In 2D models, no extrapolation is required and the results can be directly presented on a 2D map (Petersen et al., 2002; Vojinovic and Tutulic, 2009). Again, a 2D model may not be suitable for the purpose of flood forecasting as it takes longer time to simulate in comparison with a 1D model.

Modelling an urban surface drainage system exclusively in 2D HD is computationally very expensive. Representing the micro topography such as small creeks and artificial drainage systems, requires very high resolution of topography data which increases the number of computational points and computation time (Petersen et al., 2002). An increasingly popular alternative is the use of a hybrid 1D-2D coupled hydrodynamic modelling approach in which the channels and pipe systems are modelled in 1D while runoff and flooding over the

topography are modelled in 2D and the flow between the two layers are dynamically interconnected (Mark and Djordjevic, 2006; Petersen et al., 2002).

A number of 1D-2D HD coupling software are commercially available that can be used to model the urban stormwater drainage system. Most of these software are integrated with a Geographic Information System (GIS) platform. The most important difference between the different software is the choice of the numerical solution technique. MIKE URBAN is an urban drainage modelling software that has been specifically developed for urban areas and is able to cover all water networks in a city including pipe networks (MikeUrban, n.d.). MIKE FLOOD is a 3 way coupling software that is good for mixed urban areas, whereas MIKE 21 is used for flood plains, overland flow paths, open channels. MIKE 11 is used for simulating significant hydraulic structures (Cornelius, 2012).

TUFLOW (sometimes referred as TUFLOW Classic) has been developed for the modelling of 2D flows in coastal zones, riverine and urban areas. In a benchmark testing of six 2D HD model including TUFLOW, Hunter et al. (2008) concluded that all models produce plausible result in a densely urban area. TUFLOW has the capacity to dynamically link with a number of 1D HD engines such as ESTRY, Flood Modeller, XP-SWMM and 12D. Besides, it can be integrated with a number of commercial and free GIS software (BMT-WBM, 2016).

The storm-water of Marrickville valley sub-catchment drains its water through a curb/gutter system, to a pipe system and finally into four major outfalls including a tunnel into the Cooks River. The area is highly impervious with high density residential and light-density industrial developments, as well as a number of major and minor roads. As the total drainage system consists of open channel and underground pipe systems, so the flood analysis will be done by the 1D-2D coupling method, using the software TUFLOW. In addition to the advantages of TUFLOW discussed earlier, an important reason for selecting TUFLOW is that the Inner West council (previous Marrickville council) has investigated urban flooding using the software and has provided the author of this study with a set of data that can be readily run with TUFLOW.

2.1.3 Climate Change Implication on Urban Flooding

Anthropogenic climate change is caused mainly by greenhouse gases emissions and deforestation. As a result, decreases in cold temperature extremes, increases in warm

temperature extremes, accelerated sea levels rise and increase in the number of heavy precipitations events have been observed in a number of regions since the middle of the last century. Greenhouse gas (GHG) emissions are driven by growth in population size and economic activity, changes in lifestyle, energy use, land use pattern, technology, as well as the existence or not of climate policy. Continuous increase of greenhouse gas emissions will cause further warming and long-lasting changes in the climate system and a number of future climate scenario projections have been made in reports by the International Panel on Climate Change (IPCC, 2014a).

2.1.3.1 Climate Change Scenario

Future scenarios of climate change are constructed from the output of Global Circulation Model (GCMs), based on different pathways of changes in greenhouse gas emissions/concentrations in these GCMs. GCMs are mainly constructed for large scale study (continental/hemisphere/global). To use these models at local scale requires downscaling. These models are have good accuracy when simulating temperature and sea level rise but are less accurate for simulating rainfall and windstorm. Better accuracy of rainfall depends on the aggregation of model grid point and average across time (CoastAdapt, n.d.).

In 2010, the International Panel on Climate Change (IPCC) in its fourth assessment report (AR4), outlined the future climate change projections with the term Special Report on Emission Scenarios (SRES) based on the emissions of greenhouse gases. By 2100, a warming of 3.4°C and 1.8°C are projected under scenarios SRES A2 and SRES B1. In 2013, the IPCC released its fifth assessment report (AR5) in which SRES were replaced with Representative Concentration Pathways (RCPs). The RCPs take into account uncertainty in projecting future emissions. The RCPs include four different climate change scenarios; i) RCP2.6, ii) RCP4.5 iii) RCP6.0 and iv) RCP8.5. The RCP8.5 and RCP2.6 are respectively the most and least severe scenarios. RCP2.6 keeps increases in average global temperatures below 2°C relative to pre-industrial levels through strong and effective greenhouse reduction measures, while RCP8.5 represents a business-as-usual scenario with very high levels of greenhouse gas emissions (CoastAdapt, n.d.).

In this research, the future flooding scenario will be projected both for the low and high emission condition by considering both the rainfall change and sea level rise projection. This projected rainfall and sea level rise data will be used as input to the flood model

described in the previous section to determine the future flooding hazard of the Marrickville Study Region.

2.2 Vulnerability Concept

Vulnerability can be defined, in the most general sense, as the degree to which a system is likely to experience harm due to exposure to a hazard (Turner et al., 2003). However, practitioners from different disciplines interpret such a definition in different ways which in turn leads to diverse methods for assessing vulnerability (Alwang et al., 2001). Research on vulnerability assessment has been conducted from within a number of disciplines, including geography, economics, sociology, disaster management, environmental science and health.

From a detailed analysis of the literature on vulnerability to natural hazards, Rygel et al. (2006) identified two major perspectives on vulnerability. The first perspective focuses on the potential exposure to hazards. Studies conducted by following this theme, try to assess the impact of hazards and degree of loss of life and property resulting from a particular event (Muis et al., 2015; van Manen and Brinkhuis, 2005; Tapsell et al., 2002). The second major perspective highlights differential impacts and attempts to explain why two different communities exposed to the same magnitude of hazard may experience its impacts in different ways and to different extents (Cutter et al., 2013).

Under this perspective, a high degree of importance is attributed the social vulnerability of individuals, households and communities. Social vulnerability can be defined, after Sarewitz et al. (2003), as the intrinsic characteristics of the exposed elements that determine their potential to be harmed, independently of the magnitude and frequency of occurrence of the hazard. The impacts of a flood, as well as the capacity to deal with it through preparedness, depends on, in addition to the intensity of the flood and the extent of exposure to it, the ability of a system to cope with it when it occurs, and to adapt to it over the longer term (Koks et al., 2015). Hence, vulnerability can be seen to be made of two dimensions, a geophysical one which depends on the characteristics of the hazard and the physical landscape over which it occurs and a socio-economic one which is a function of institutional and socio-economic characteristics. The word vulnerability has been used in the literature to denote either the total concept incorporating both its geophysical and socio-economic

and institutional dimensions, or to refer only to the latter. In this thesis, the first meaning is employed (total vulnerability) with the two dimensions referred to as geophysical and social vulnerability, respectively.

2.2.1 Social Vulnerability (SV)

Natural hazards such as floods, cyclones and earthquakes cannot be fully prevented, but their impacts can be mitigated by identifying social groups vulnerable to their effects and assisting them through preparedness and emergency planning measures process (Solangaarachchi et al., 2012). Empirical evidence from historical flood analysis has shown that particular social groups tend to carry a higher burden of death, injury and relative economic impact from floods. For example, low income populations and ethnic groups in Texas, USA experienced a high number of casualties due to flooding (Zahran et al., 2008). Specific population groups have been found to have lower levels of disaster preparedness and are less likely follow disaster warning and evacuation plans due to existing health problems, limited economic support and lack of access to resources at the time of disaster (Garbutt et al., 2015). Cutter et al. (2003) defines social vulnerability as the demographic and socioeconomic features of people and communities, and characteristics of the built environment in which they live, that reflect a deficiency in their ability to prepare for, respond to and recover from a hazard. Identifying socially vulnerable groups allows planners to develop targeted and differentiated mitigation plans to reduce the risk from floods.

Indicator-based assessments of social vulnerability typically use different types indicators that measure institutional, socio-economic, demographic and built-environment characteristics associated with high vulnerability to natural hazards. Built-environment characteristics such as high settlement density, poor quality of infrastructure, poor availability of medical facilities etc., that may or may not be dependent on social characteristics, but can lead to worse impacts from natural hazards (Borden et al., 2007; Holand et al., 2011). As an example, settlements with poor and insufficient drainage infrastructure services can lead to higher water levels during flood events. In order to reflect that social vulnerability and built-environment vulnerability will be assessed separately, in this study. This will allow further detailed characterisation of urban geophysical vulnerability to natural hazards at local scale.

2.2.2 Measurement of Social Vulnerability

2.2.2.1 Indicators selection

Measurement of social vulnerability is complex as it involves a large number of factors that determine the degree to which people's lives and assets are at risk due to natural hazards (Holand et al., 2011). The accuracy of the analysis depends on the selection of the right number and types of indicators (Tavares et al., 2015). The most common types of indicators that have been used in previous studies are i) dependency on others due to age or disability, ii) gender iii) economic disadvantage iv) occupation category v) limited access to resources including technology and transportation v) accommodation vi) immigration status vii) language barriers and vii) race and ethnicity (Fatemi et al., 2017; Frigerio and De Amicis, 2016; Garbutt et al., 2015; Cutter et al., 2003; Tavares et al., 2015; Fekete, 2009; Solangaarachchi et al., 2012; Koks et al., 2015; Holand et al., 2011; Schmidlein et al., 2008; Cutter et al., 2013; Borden et al., 2007).

People who are highly physically dependent on others often have limited capacity to adapt to changes and may require special support during and after disaster (O'Sullivan et al., 2009). The physically-impaired or physically-dependent may sometimes be overlooked at the time of recovery due to their low visibility. Examples of this group can be drawn from young children and aged population (Cutter et al., 2000; O'Brien and Mileti, 1992), persons who require special assistance or live alone in a household, single parent-family with dependent children etc. (Blaikie et al., 2014). Age is one of the major factors in determining SV as young children and the elderly have mobility constraints and may require extra care at the time of hazard. Aged people may also have pre-disaster medical conditions that further contribute to increased vulnerability. Females may be disadvantaged during recovery from natural hazard because of lower earnings and extra family care responsibilities and household tasks (Fekete, 2010; Cutter et al., 2003).

People with low socioeconomic status usually have higher dependence on welfare which limits their capacity to adapt to post-disaster conditions (Cutter et al., 2003; Burton, 1993). On the other hand, people with high socioeconomic status have a better capacity to recover from the impacts of the hazard due to insurance, social networks and social safety nets. A number of indicators such as household's income, employment status, type of profession and home ownership can be used as a proxy to measure socioeconomic status. Workers in

low-skilled sectors may be at higher risk of losing their jobs during or after disasters, compared to high-skilled professionals, sometimes leading to slower recovery. Similarly, household with low rent may indicate lower socioeconomic status, in contrast with owner-occupier households, with or without mortgage.

In some countries, education is a critical factor linked to socioeconomic status where high level of educational attainment means better employment opportunities (White, 2000). In Australia, education may not always be directly linked with economic status. However, individuals with higher education levels may be better able to access, interpret and act upon information and evacuation plans and times of disaster to make an evacuation plan (Morrow, 1999; Solangaarachchi et al., 2012). Race, ethnicity and migration status are also important factors that may partly determine vulnerability during a hazard (Pulido, 2000; O'Sullivan et al., 2009). Poor familiarity of the new migrants with the place of residence, as well as language barriers, could make it harder for them to access the country's emergency services. Other miscellaneous indicators include, for example, motor vehicle ownership and access to the internet, both of which enhance access to information and transport during a hazard (O'Sullivan et al., 2009). Furthermore, households with a relatively large number of members may find it more difficult to evacuate and/or adapt to hazards, compared to smaller households.

2.2.2.2 Quantitative measure of Social Vulnerability

Both qualitative and quantitative measurement of SV is evident in the literature. Dwyer et al. (2004) computed SV based on a risk perception questionnaire, including perceived amount of time required to recover from various natural-hazard events. However, data collection and analysis of qualitative surveys is a time consuming process. The outcome depends on the skills of the researcher and can be influenced by the researcher's personal biases. On the other hand, quantitative approaches are popular in the literature and usually lead to the calculation of a social vulnerability index (SoVI) (Cutter et al., 2003). The index value for one spatial unit is calculated by aggregating a set of indicators into a single value reflecting vulnerability. This is particularly useful when the purpose is to develop a relative assessment of vulnerability, i.e. a comparison of the social vulnerabilities of different spatial units. The actual spatial units depend on the purpose of the study and the spatial scale of at which information is available, usually from census data.

The approach of developing index has been conducted for a large number of spatial scales; e.g. from municipal scale to continental level. For a continental-level study, SoVI is computed for each country. For example, using this approach, Vincent (2004) compared the social vulnerability to climate change of African nations. Cutter et al. (2003) analysed comparative SVs to environmental hazards among 3141 counties of the United States. Holand et al. (2011) and Garbutt et al. (2015) conducted similar studies to Cutter et al. (2003) but using a higher spatial resolution by comparing social vulnerability among different local government areas. Local level social vulnerability analysis is possible when census data is available for household levels. For example, the Australian Bureau of Statistics (ABS) provides publicly available aggregate demographic and socioeconomic data for units including between 200 to 800 households. Tavares et al. (2015) and Koks et al. (2015) conducted local-scale assessments of vulnerability to flooding by comparing SoVIs at census block level. Solangaarachchi et al. (2012) conducted a similar local-level assessment in the context of bushfire risk in two local councils in Sydney. SoVI is typically displayed on GIS maps (Figure 2-3) to compare the vulnerability from one place to another.

The number of indicators for constructing SoVI is large and some of them may be correlated. Therefore, in order to eliminate correlated variables and reduce variables into a more manageable number of components, researchers apply statistical techniques, such as the principal component analysis (PCA). PCA is multivariate regression analysis technique for variables reduction. The technique derives a set of components that capture most of the variability using a smaller number of variables (Fekete, 2009). For example, in the construction of SoVI, Tavares et al. (2015) initially included 126 variables. After checking the multicollinearity between different pairs of variables, total 34 variables were retained for the PCA analysis. After PCA, a total 8 components were extracted where the number of variables under each component varies from 1 to 8. Koks et al. (2015), on the other hand, did not use PCA, but started instead with a small number of variables.

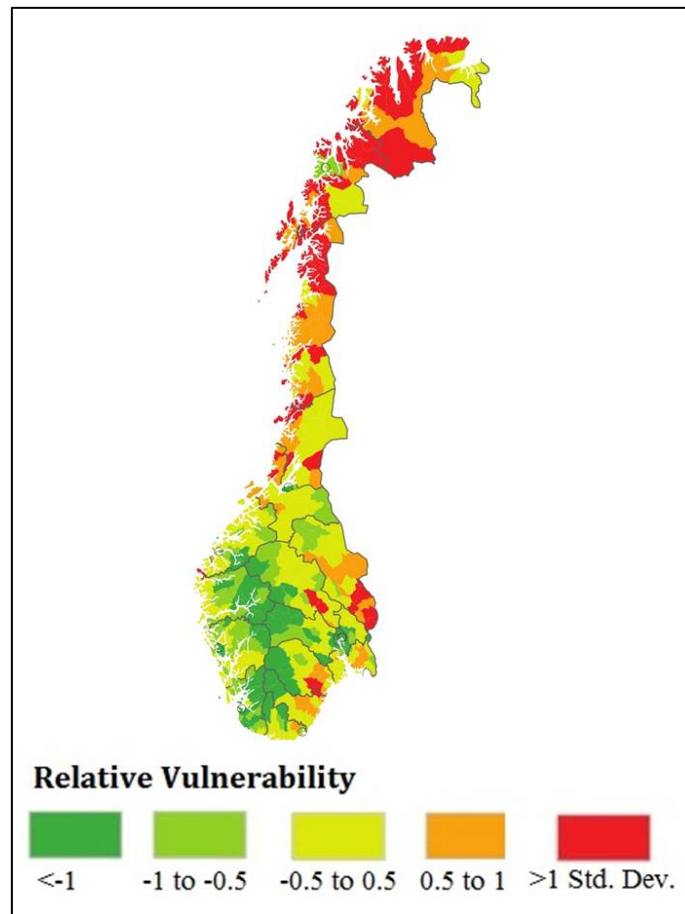


Figure 2-3: Social vulnerability of Norway (Source: Holand et al., 2011); 0.5 standard deviations (Std.Dev) are used as breakpoints and highlight the areas that score over 0.5 or under -0.5 Std.Dev from the mean score. The areas above 0.5 Std.Dev represent higher than average levels of vulnerability, and vice versa)

In this research, a quantitative approach of SV analysis developed by Cutter et al. (2003) will be followed and the census data provided by Australian Bureau of Statistics (ABS) will be used as a source of social vulnerability indicators. One important question in aggregating indicators or components from PCA is whether equal or different weights are applied to different indicators or components. This is a subject of debate in the social vulnerability literature. Cutter et al. (2003) did not find any defensible method for assigning weights and gave equal importance to each component in the aggregate model. Many researchers followed the same concept of equal contribution of each component. Solangaarachchi et al. (2012) provided weights to each component (ranging from 0 to 1) based on the percentage of variance explained. In a study of sensitivity analysis of SoVI, Schmidlein et al. (2008) on the other hand, chose to include the first component only, since it explains the largest amount of variation in the original data. This amounts to assigning a

weight of 1 to the first component and 0 to all others. Tavares et al. (2015) argued that despite different percentages of variance explained by different components, it is difficult to provide a scientifically solid basis for assigning unequal weights to components. For a more detailed discussion of problems of weights, the reader is referred to El-Zein and Tonmoy (2015). In this study, equal weights will be assigned in all aggregations, including those involving indicators and components, as well as aggregation of the three indices (geophysical, exposure and social vulnerability) into a final flood vulnerability index. It's important to keep in mind the limitations of SoVI. SoVI does not give an absolute assessment. Instead, vulnerability assessment is done by comparing the index value between different spatial units yielding a relative assessment. In addition, SoVI may identify a social group or geographical at higher risk but does not tell exactly what adaptation measures are required. Another challenge is to evaluate temporal trends of SoVI as it is based on the census data which is only updated over long time intervals (1 in 5 years).

A similar approach is used for constructing an exposure index (F_E) based on the built environment data. PCA will be not required for computing F_E because only a small number of indicators are available for the study area.

2.3 Composite Indices of Vulnerability to Flood

Social vulnerability has been used in several studies as a tool for assessing vulnerability to floods (Koks et al., 2015; Cutter et al., 2013; Tavares et al., 2015; Garbutt et al., 2015; Fekete, 2009). However, only a few of these studies went on to develop a composite index which includes indicators reflecting different components of risk such as physical, social, economic or environmental components. Fernandez et al. (2016) developed a Flood Vulnerability Index (FVI) based on both Cluster Analysis and PCA. To develop the composite index, in addition to social and economic dimensions of vulnerability, they incorporated the geophysical and environmental dimension. The geophysical component represented the potential of physical impact on the built environment and the environmental dimension referred the potential impacts on the natural environment and ability of the ecosystem to cope and recover from hazard impacts. However, they did not use any outcomes of flood simulation such as flood depth, velocity etc. Connor and Hiroki (2005) developed an FVI by combining indicators of meteorological, hydrogeological, socioeconomic and

countermeasure components, using multiple linear regression analyses. The countermeasure component represented the extent of protection against flood through river improvement and community preparedness. Zachos et al. (2016) developed a separate index for each component (physical, social, economic, environmental) and finally combined them to develop a composite index using a weighted-sum approach. They applied their index to the study of vulnerability to flooding at the basin level, for the Lower Mississippi River Valley. However, the geophysical component of risk was based only on elevation above or below a base flood datum, extracted from 100-year flood level, rather than any detailed flooding simulations. Balica et al. (2009) also computed FVI with the aim of assessing the conditions which influence flood damage at various spatial scales, such as river basin, sub-catchment and urban area. Their approach for determining the composite index was similar to that of Zachos et al. (2016). However, depending on the scale of the analysis for determining the geophysical component of risk, various physical indicators were considered, such as heavy rainfall, flood duration, evaporation rate, flow velocity, river discharge, storm surge, flood water depth and sedimentation load. In a different study, Balica et al. (2012) focused on developing Coastal City Flood Vulnerability Index based on the hydrogeological, socio-economic and politico-administrative components to demonstrate which cities are most vulnerable to coastal flooding. To the best of the author's knowledge, no composite index of vulnerability to flooding, incorporating both geophysical and socio-economic dimensions of risk and using hydrologic simulations of floods, was developed at a local municipal scale. The need for such an index has been discussed earlier and will be the subject of this thesis.

Chapter 3

Indicator-Based Flood Social Vulnerability Model

3.1 Introduction

A structure of indicators is developed, based on the risk pyramid framework described in Section 1.2. The structure, shown in Figure 3-1, is made of three indices corresponding to the three dimensions of risk in the pyramid: i) the flood hazard index (F_H), ii) the flood exposure index (F_E) and iii) the social vulnerability index (SoVI). The three indices are finally combined, leading to the Flood Social Vulnerability Index (FSVI) which assesses relative vulnerability to flooding among different spatial units of a flood-prone region.

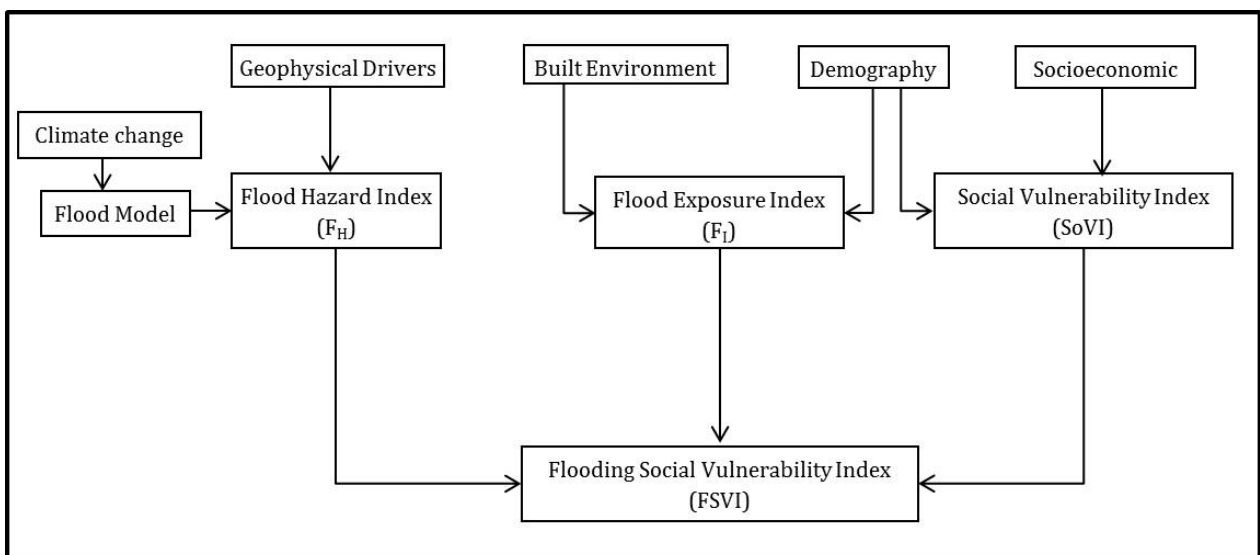


Figure 3-1: Research design

3.2 Methods

The FSVI is developed through the following steps:

- i. The study area is subdivided into a number of spatial units/blocks. These are typically the smallest geographical unit for which demographic and socioeconomic data is available. The sizes of the spatial units can vary from a few of households to hundreds or thousands of households.
- ii. Each vulnerability dimension is quantified as an index value by a set of indicators. The indicators are selected to capture major elements of that particular vulnerability dimension. The indicators are standardised with a mean of 0 and standard deviation of 1 (Equation 3-1). The individual index is calculated as a weighted average of its standardised indicators (Equation 3-2)

$$I_{si} = \frac{I_i - \mu_i}{\sigma_i} \quad \text{Equation 3-1}$$

Where I_{si} is the standardised value of the indicator I_i

μ_i and σ_i are the mean and standard deviation of I_i indicator for all the spatial units within the study area

$$F_m = \sum_{i=1}^{N_m} w_i I_{si} \quad \text{Equation 3-2}$$

Where

F is the index of the dimension m (i.e., flood hazard, flood exposure or social vulnerability),

I_{si} is the standardised value of the i -th indicator

w_i is the weight of indicator I_i .

N_m is the number of indicators for dimension m .

- iii. The index value of each of the three vulnerability dimensions is normalized and converted into a value between 1 and 10, where 1 indicates the lowest vulnerability and 10 the highest.

iv. Finally, the three indices are combined to calculate a Flood Social Vulnerability Index (FSVI). Most common means of combining or aggregating multiple vulnerability indicators into a single utility function or vulnerability index is based on an additive or multiplicative approaches. This method for building indices has generated some debate in the literature. For example, by analysing the additive and multiplicative approaches, Ebert and Welsch (2004) identified that both approaches should produce identical rankings when different normalisations and standardisations are used. They found that multiplicative aggregations have better validity than additive ones, and better reflect synergetic processes between indicators. However, multiplicative aggregation can be difficult to communicate to stakeholders and experts (El-Zein and Tonmoy, 2017; El-Zein and Tonmoy, 2015). Yet another advantage of the multiplicative approach in calculating indices relative to a more conventional additive approach is that it magnifies cases in which more than one index is pointing to high vulnerability and yields a small index in cases in which any one of the indices indicates very low vulnerability. This research applies both additive, and multiplicative approach for calculation of FSVI and results are compared and implications of results and limitations of both approaches are discussed in the result section. The following additive and multiplicative equations are used for this study.

Additive aggregation:

$$FSVI_{Ai} = w_h F_{Hi} + w_e F_{Ei} + w_s SoVI_i \quad \text{Equation 3-3}$$

Where, w_h , w_e and w_s are weight of the three indices

Multiplicative aggregation:

$$FSVI_{Mi} = F_{Hi}^{p_h} \times F_{Ei}^{p_e} \times SoVI_i^{p_s} \quad \text{Equation 3-4}$$

Where p_h , p_e and p_s are the multiplication weights of the three indices. The detailed methodology followed in generating the 3 indices SoVI, F_E and F_H is described in Sections 3.3 to 3.5.

3.3 Social Vulnerability Index (SoVI)

An indicator-based Social Vulnerability Index (SoVI) is developed using available socioeconomic and demographic data, at the smallest possible spatial scale. Representation of social vulnerability requires the selection of suitable set of indicators (Tavares et al., 2015). These indicators quantify characteristics of communities and households that can either amplify or reduce their susceptibility to a climatic event and/or their capacity to cope with and adapt to it. These characteristics may pertain to the communities or households themselves, or to systemic biases and inequities in the broader institutional and socio-economic environments in which they exist. A number of socioeconomic indicators have been used in the literature. Examples can be drawn from, without being limited to i) age, gender and special needs ii) race and ethnicity iii) family structure iv) socioeconomic status v) occupations vi) housing and purchasing power vii) mobility and communication and viii) urban context (Cutter et al., 2003; Fekete, 2009; Tavares et al., 2015; Solangaarachchi et al., 2012; Koks et al., 2015). Choice of social vulnerability indicators is often guided by a number of factors, including questions such as what is the specific research question being addressed and within which policy framework, what is the system under analysis, what data is available and so on.

The most comprehensive source of socioeconomic and demographic data in Australia is the Census data from the Australian Bureau of Statistics (ABS), collected and updated every five years. The Census data provides information on the key dimensions of income, education, employment, occupation, housing and other miscellaneous indicators. It provides aggregated socioeconomic and demographic information for persons, families or dwellings in different spatial units designed by the Australian Statistical Geography Standard (ASGS). The latest census has been conducted in 2016 and data will only be available in late 2017. Therefore, data from the previous census (2011) have been used in this research.

Mesh block is the smallest ASGS region but ABS only provides total population and dwelling counts at the mesh block level to protect the privacy of residents. The second smallest geographical region is the Statistical Area Level 1 (SA1) for which a wide range of Census data is released. Hence, SA1 is adopted as the unit of analysis here. The whole of Australia is covered by a total of 54805 SA1 and, typically, each SA1 contains between 200 and 800

capita with an average population of about 400. The areal extent of SA1 varies between regional and metropolitan zones.

The construction of SoVI involves a large number of socioeconomic and demographic variables. To reduce the number of variables to a manageable size, a multivariate statistical technique, the Principal Component Analysis (PCA) is applied. The PCA helps in simplifying the management of the data set by reducing the number of variables with minimal loss of original information. In addition, the PCA clusters the data into a number of uncorrelated principal components, hence providing new avenues of interpretation of data on social vulnerability. Each principal component is expressed as a linear combination of original variables.

3.4 Exposure Index (F_E)

A flood exposure index, F_E , based on characteristics of the built environment, is developed. The exposure index is meant to reflect different aspects of the built environment (high settlement density, poor quality of infrastructure, poor availability of medical facilities) that can magnify the negative impacts of natural hazards. The National Exposure Information System (NEXIS) designed by Geoscience Australia provides aggregate information about the residential, commercial and industrial structures that can be used to better understand elements at risk. The NEXIS data are also available for SA1, among which the building density, the old building density and population density are three indicators that used in this study to develop F_E .

3.5 Flood Hazard Index (F_H)

The flood hazard index is based on indicators of extreme flood events such as areal extent of flood, depth of flood above the ground surface, water velocity and flood duration. The flood events are simulated by means of a hydrological model and a hydraulic modelling technique, as described next. The primary output of a hydrological model is runoff from a particular rainfall event, which then becomes one of the key inputs to a hydraulic model. The hydraulic model calculates flood levels and flow patterns, taking into account the complex effects of backwater, overtopping of embankments, waterway confluences, bridge constrictions and other hydraulic structure behaviour. Projected climate change scenarios

are also applied to the hydrological model to determine the future flood hazard. This provides an assessment of changes in flood vulnerability with time.

The output of flood analyses is generated as averages over areas of 9m². This is a much smaller area than the area of any SA1 in our analyses. Hence, flood analysis results are upscaled to the SA1 level in order to build the composite indicator FSVI.

3.6 Software

Five software packages are used in the analyses. The “Statistical Package for the Social Sciences” (SPSS) is a statistical software used here to analyse demographic and socioeconomic data, perform the PCA and construct the social vulnerability index (Field, 2009).

Drains is a hydrological/hydraulic modelling software that can carry out hydrological analyses, in conjunction with hydraulic modelling systems (O’Loughlin and Stack, 2014). Drains is used in this study to generate stormwater runoff hydrographs from rainfall and routes these through surface and pipe networks.

TUFLOW, also known as TUFLOW Classic, is a grid-based two-dimensional hydrodynamic free surface solver suited for simulating 2D flood behaviour. In addition to 2D, TUFLOW is also dynamically linked to 1D networks using the hydrodynamic solutions of ESTRY which is a separate 1D engine (TUFLOW, 2016). In the simulations conducted here, TUFLOW uses as input the runoff data generated by Drains model, and generates flow and inundation patterns of urban terrains where the flow behaviour is two-dimensional. The narrow open channels, stormwater pipes, culverts, bridges and pumps are modelled with the inbuilt ESTRY engine.

Finally, ARC MAP and QGIS are two GIS tools used here for processing, analysing, mapping and visualising spatial data and model results.

Chapter 4

Application of Flood Social Vulnerability Model

4.1 Study Area

4.1.1 Background

The methodology described in Chapter 3 is applied to the major part of the Marrickville valley located in New South Wales in Inner West local government area (LGA). To be specific about the study region, the following two definitions will be used:

1. Marrickville Study Region (MSR), which consists of the Marrickville valley except for some portion of northeast part (Figure 4-1). This portion is excluded because the data required for the flood modelling could not be accessible. The SoVI, F_E , F_H and FSVI are all determined over the MSR.
2. The Broader Study Region (BSR), consists of entire Sydney Inner West, Sydney City and Inner South and Sydney Inner South West (Figure 4-2). Only SoVI and F_E are determined over the BSR.

The MSR has experienced significant flooding as recently as 2012 (Mckenny et al, 2012). It has medium-density residential housing and light-density industrial facilities, as well as major and minor roads. The MSR covers (parts or all of) the suburbs of Petersham, Stanmore, Enmore, St Peters, Tempe, Marrickville and Dulwich Hill. The stormwater system of the Marrickville Valley drains runoff through a curb/gutter system, to a pipe system, and finally into four major outfalls including a tunnel discharging into the Cooks River. The suburbs within Marrickville valley falls into a geographical area managed by Sydney's Inner

West council. Prior to 2016, when a new local government structure was introduced in New South Wales, the Marrickville suburb fell under the Marrickville Council.

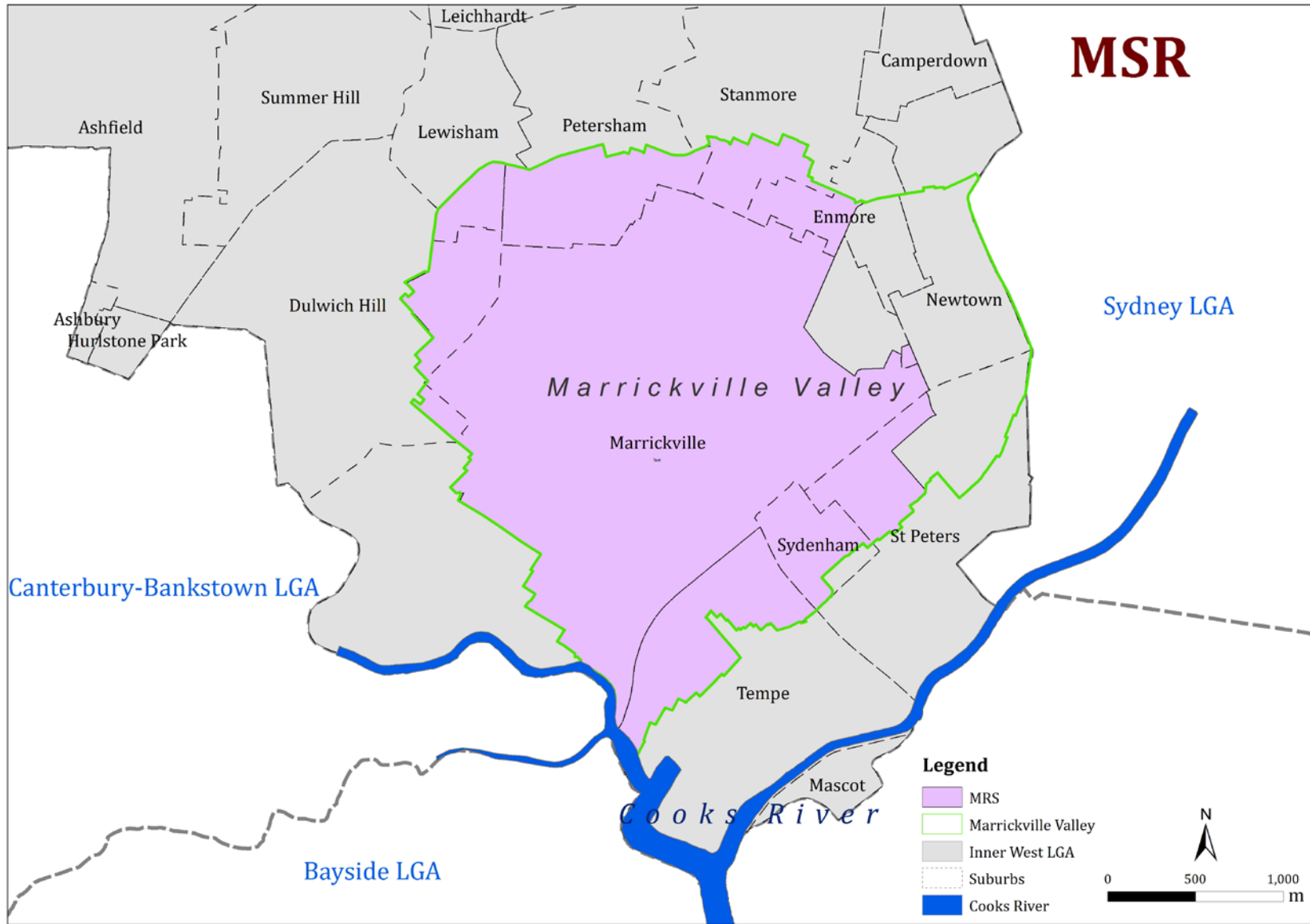


Figure 4-1: Marrickville Study Region

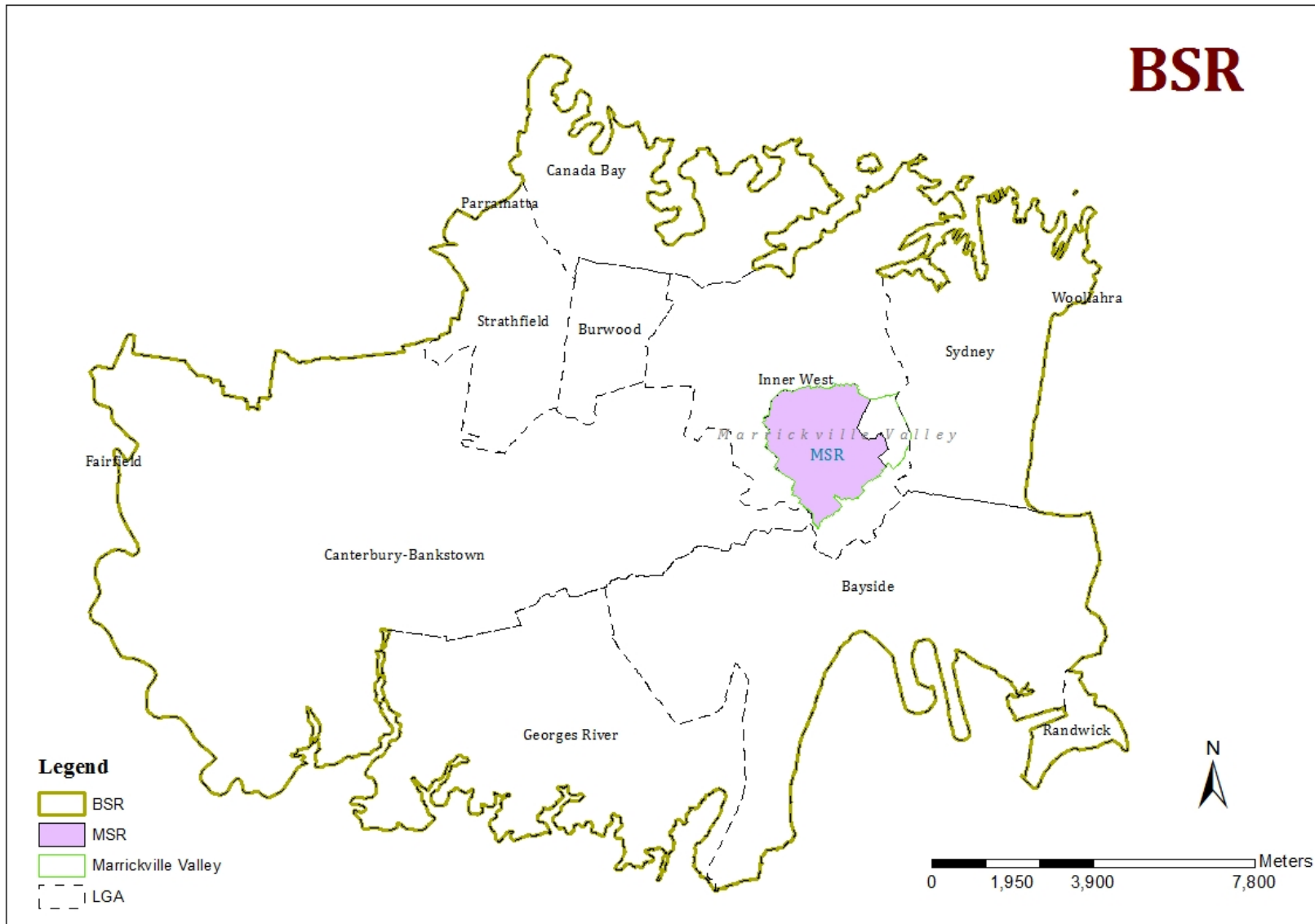


Figure 4-2: Broader Study Region

4.1.2 Drainage Systems

The Marrickville valley consists of 9 sub-catchments. These are: i) eastern channel north (ECN), ii) eastern channel east (ECE), iii) eastern channel west (ECW) iv) eastern channel south (ECS) v) eastern channel 2 (EC2), vi) western channel (WC), vii) central channel (CC), viii) Malakoff Street (MK) and ix) Malakoff Tunnel (MT). Among this 9 sub-catchment, the ECE is excluded from the MRS due to data unavailability. Figure 4-3 shows the sub-catchments of the Marrickville valley except for ECS, ECE and MT (GRAY, 2011).

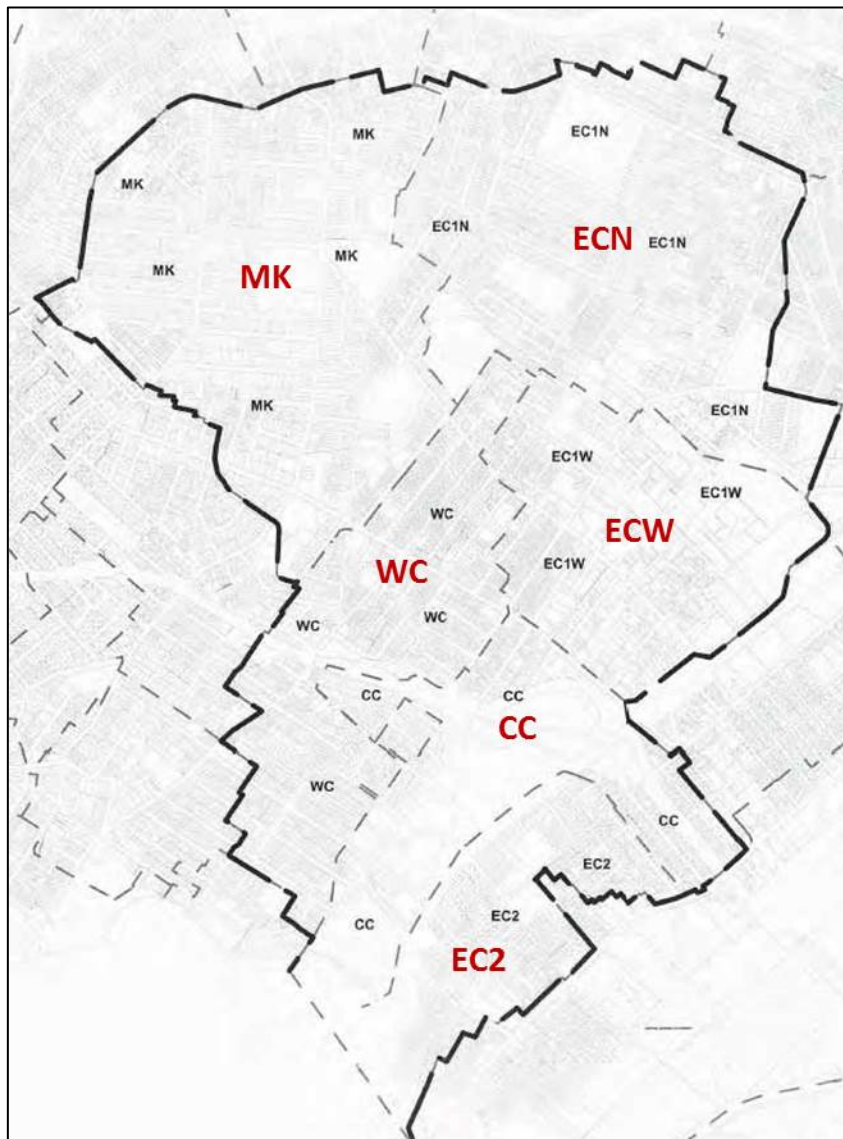


Figure 4-3: Sub-catchments of Marrickville valley (Source: GRAY, 2011)

The topography of the area derives from the Airborne Laser Survey (ALS), and varies from 5.5 to 50.8 mAHD (Figure 4-4). Due to this variation, water flows from the northern side to the southern Cooks River with the aid of major and minor drainage systems. Property

drainage systems (pipe/gutter) are linked with the pits/pipe systems when the water is conveyed to the trunk drainage system before it discharges to the Cooks River. The four major trunk drainage systems that direct water towards the Cooks River are Eastern Channel, Central Channel, Western Channel and Malakoff Street tunnel.

For the temporary storage of water, the Marrickville Oval is used as a flood retarding basin. The Sydenham storage pit is served the same purpose, but two pumps are installed in this pit to divert high flood water to the eastern channel. One pump is used to divert flood water to the Cooks River from the low lying area of the central channel catchment, and another one transfers water from the central channel to the eastern channel. When the flood flow this region exceeds the drainage capacity, the excess water is either conveyed by roadway or stored in the road or other downstream locations. Except under extreme flood events, overland flow towards the Cooks River is not possible due to urban barriers (GRAY, 2011).

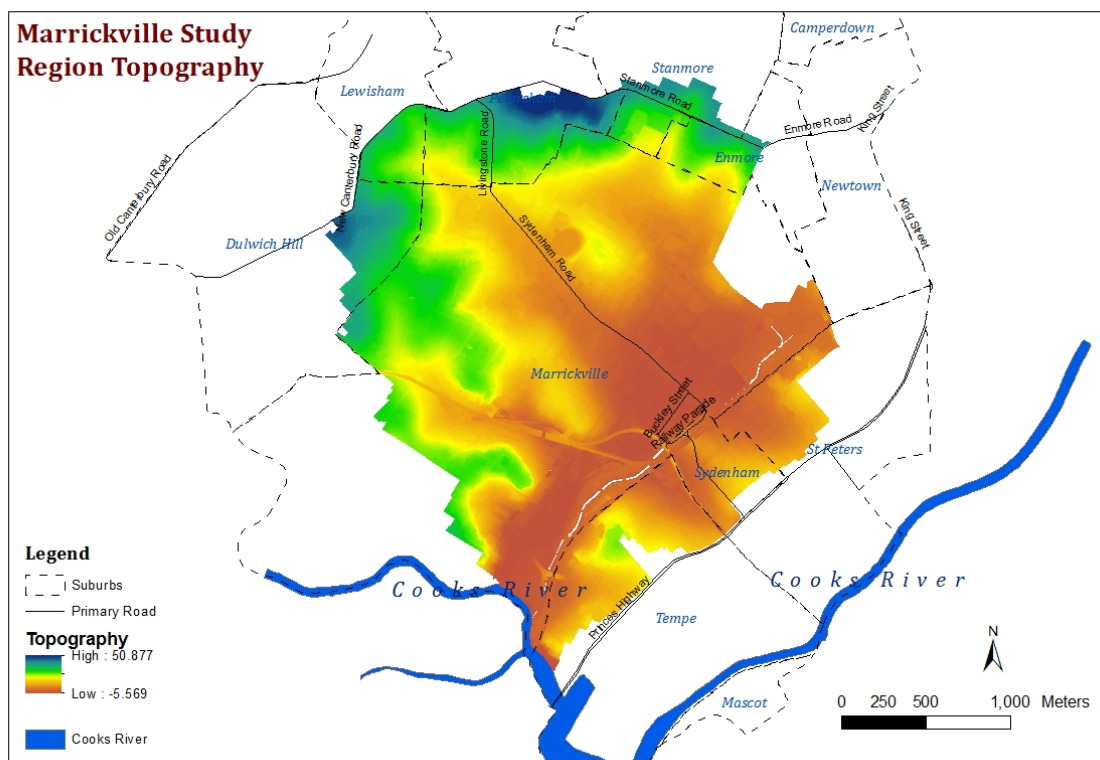


Figure 4-4: Topography of the study area

4.1.3 Land Use

Based on NEXIS data at mesh-block scale, 63% of the MSR land is residential and 21% is industrial. The remaining land use is parkland, commercial, educational and transport routes. Figure 4-5 shows the land use map of Marrickville Valley.

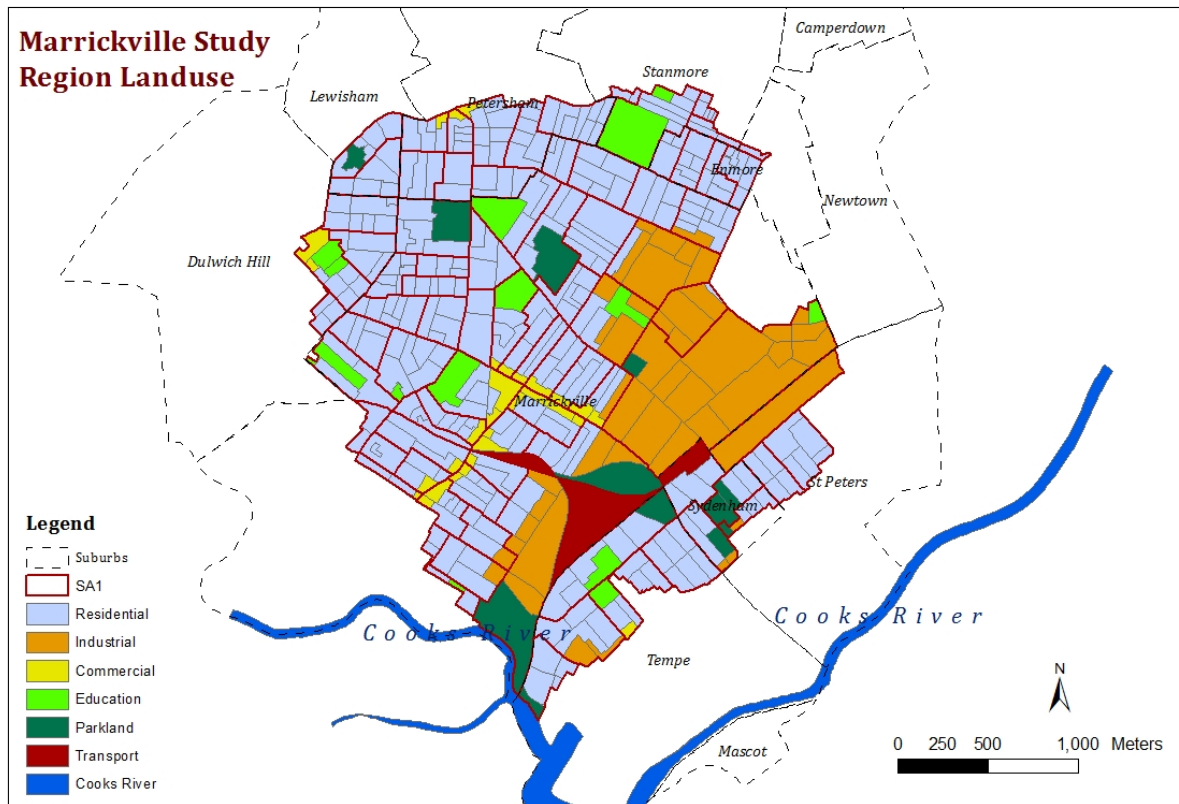


Figure 4-5: Land use of Marrickville Valley

4.2 Scope of Study

The scope of the vulnerability study is defined at the outset by providing answers to a set of fundamental questions, shown in Table 4-1 (El-Zein and Tonmoy, 2015; Tonmoy et al., 2014).

Table 4-1: Vulnerability related questions and answer

Question	Answer
1. Whose vulnerability is assessed?	Marrickville Study Region (MSR)
2. The vulnerability of <i>which valued attribute</i> of the socio-ecological system is assessed?	Well-being, including economic prosperity, of Marrickville residents
3. Vulnerability to <i>which hazard</i> , under <i>what scenarios</i> of future climatic, institutional and socio-economic change, is assessed?	Flooding as a result of heavy rainfall events under <i>future</i> climate change scenarios, given <i>current</i> socio-economic conditions.
4. What is the <i>temporal scale</i> of assessment?	Social vulnerability for the present day. Flood analysis for present day and for the period between 2060 and 2080 subject to climate change projections.
5. What is the standard <i>spatial unit</i> of the analyses?	Statistical Area Level 1 (SA1) (a total of 84 SA1 in the MSR and 2575 SA1 in the BSR)
6. <i>How will vulnerability be assessed</i> , specifically: a. What are the dimensions of vulnerability considered? b. How will they be quantified?	Dimensions i) Geophysical vulnerability: e.g. flood hazard indicators determined through hydrological and hydraulic simulations ii) Social vulnerability and vulnerability associated with the built environment vulnerability: assessed through indicators.

4.3 SoVI for Marrickville Valley

The following steps have been followed for the computation of SoVI in the Marrickville valley.

- i. Select social vulnerability indicators based on the literature
- ii. Conduct PCA analyses for reducing and clustering the large number of indicators into manageable components
- iii. Calculate the score of the principal components
- iv. Calculate the SoVI by aggregating the principal components scores

4.3.1 Indicator Selection

The social vulnerability assessment conducted here is formally independent of the specific hazard in question, i.e., it can in principle be applied to identify vulnerability to a number of hazards (e.g., flooding, heatwaves, earthquakes). The selection of an initial set of candidate indicators is an essential first step in index-building exercise. A rich literature exists on indicators of SV in Australia and overseas. Indicators of social vulnerability found in the literature broadly fall into eight categories, i.e. i) dependency on others due to age, gender or disability ii) race, ethnicity and familiarity with place of residence iii) family structure – household demography iv) educational level v) accommodation categories and household resources vi) socioeconomic disadvantage vii) occupation class viii) urban context.

The literature surveyed for this study encompasses a number of hazards including flooding (Koks et al., 2015; Cutter et al., 2013; Tavares et al., 2015; Garbutt et al., 2015; Fekete, 2009) sea level rise (Wu et al., 2002) and bushfire (Solangaarachchi et al., 2012). There are numbers literature where the vulnerability assessment is independent to any specific natural hazard (Cutter et al., 2003; Dwyer et al., 2004; Holand et al., 2011; Schmidlein et al., 2008; Zhou et al., 2014). Based on this survey, a total of 37 indicators, shown in Table 4-2, are selected. Each indicator is assumed to have a monotonic relationship with vulnerability, and the direction of correlation of the indicator with vulnerability (whether vulnerability increases or decreases with increasing indicator) has been identified based on the literature and shown in Table 4-2.

The selected indicators are extracted from the ABS database. All selected indicators are expressed as percentages relative to total population of the SA1, total families in the SA1 or total dwellings in the SA1, depending on the indicator in question. The denominator for each indicator is shown in Table 4-2.

Table 4-2: Social Vulnerability Indicators Selected for the Study

No	Indicators	Indicators in Short Form	Unit	Direction of Correlation with Vulnerability*
1	Number of children below 5 years of age	CHLD_AGE	As a % of total population	+
2	Number of people over 65 years of age	PPL_AGE	As a % of total population	+
3	Number of people between 35 and 39 years	MED_AGE	As a % of total population	-
4	Number of females	GEND	As a % of total population	+
5	Number of people requiring special assistance	SPC_ASST	As a % of total population	+
6	Number of non-citizens	NON_CIT	As a % of total population	+
7	Number of recent migrants (previous 8 months)	REC_MIGR	As a % of total population	+
8	Number of people with low speaking proficiency in English	LOW_ENG	As a % of total population	+
9	Number of people who moved residence in the last year	NEW_RES	As a % of total population	+
10	Number of people employed as managers	EMP_MNG	As a % of total population aged 15 years and over	-
11	Number of people employed as professional	EMP_PRF	As a % of total population aged 15 years and over	-
12	Number of people employed as laborers	EMP_LBR	As a % of total population aged 15 years and over	+
13	Number of people employed as machinery operators or drivers	EMP_DRV	As a % of total population aged 15 years and over	+
14	Number of households with above-median household income	HH_INCMED	As a % of total households	-
15	Number of households with negative or nil income	HH_INCNIL	As a % of total households	+
16	Number of people with weekly income less than \$300	PPL_INCLOW	As a % of total population aged 15 years and over	+
17	Number of people with weekly negative or nil income	PPL_INCNIL	As a % of total population aged 15 years and over	+
18	Number of people who are unemployed	PPL_UNEMP	As a % of total population aged 15 years and over	+
19	Number of dwellings occupied by 5 individuals or more	DWL_5PPL	As a % of total households	+

20	Number of dwellings occupied by single individuals	DWL_1PPL	As a % of total households	+
21	Number of household with 2 or more families	DWL_2FAM	As a % of total households	+
22	Number of dwellings owned with mortgage	DWL_MORT	As a % of total households	-
23	Number of dwelling owned outright or being purchased	DWL_OWN	As a % of total households	-
24	Number of cooperative, community, or church housing units	DWL_COPT	As a % of total households	+
25	Number of houses with weekly rent over the median household rent	HH_MEDRNT	As a % of total households	-
26	Number of houses with weekly rent below \$150	HH_LOWRENT	As a % of total households	+
27	Number of dwellings with no internet connection	DWL_NOINT	As a % of total households	+
28	Number of dwellings with no motor vehicle	DWL_NOVEH	As a % of total households	+
29	Number of single-parent families with children under 15	FAM_SNGLPAR	As a % of total families	+
30	Number of couple families with more than 2 dependent children	FAM_DEPCHLD	As a % of total families	+
31	Number of unemployed families	FAM_UNEMP	As a % of total families	+
32	Number of couple families with one person unemployed	FAM_1UNEMP	As a % of total families	+
33	Number of people who never went to school	NO_SCHL	As a % of total population aged 15 years and over	+
34	Number of people whose highest level of education is year 11	EDU_YR11	As a % of total population aged 15 years and over	+
35	Number of people whose highest level of education is Bachelor degree or above	EDU_BACH	As a % of total population aged 15 years and over	-
36	Number of people whose highest level of education is Diploma or Advanced Diploma	EDU_DIP	As a % of total population aged 15 years and over	-
37	Number of people whose highest level of education is Certificate Level (Certificate 1, 2, 3 or 4)	EDU_CERT	As a % of total population aged 15 years and over	+

* A positive sign next to an indicator implies that vulnerability increases with increasing value of the indicator; a negative sign indicates the opposite.

4.3.2 Principal Component Analysis (PCA)

An initial selection of 37 socioeconomic and demographic indicators (Table 4-2) is made for the 2,575 SA1's of Marrickville valley and its surrounding suburbs (Figure 4-6). All the indicators are then standardised using Equation 3-1. The PCA is applied to reduce the number of indicators (with minimal loss of information) and to cluster the data in a new set of uncorrelated orthogonal variables called principal components. PCA also provides weights for each indicator to calculate the components score. The SPSS software is used for the PCA analysis.

Correlation between pairs of indicators and multicollinearity in a sub-group of indicators play a vital role in extracting the total number of principal components and to cluster the indicators under each component. Very low or very high correlation or multi-collinearity as well as singularities (perfect correlation) can cause significant problems for PCA. It is advised, for example, that an indicator that does not correlate with other indicators be excluded from the analysis (Field, 2009). The determinant of the correlation matrix helps in identifying the problems generated by multicollinearity.

There are no straightforward rules in a PCA analysis for detecting which variables should be retained. Several trials and errors are usually required to identify which variables ought to be eliminated from the analysis. This process is performed iteratively, and the outcomes of each iteration are evaluated with Kaiser-Meyer-Olkin (KMO) measures of sampling adequacy and Bartlett's test of sphericity. These two tests provide guidance concerning the number of retained indicators appropriate for the dataset in question.

The number of components extracted from the PCA is based on the eigenvalues associated with each component and the shape of the scree plot (eigenvalue vs component number curve). This is discussed further in the results chapter.

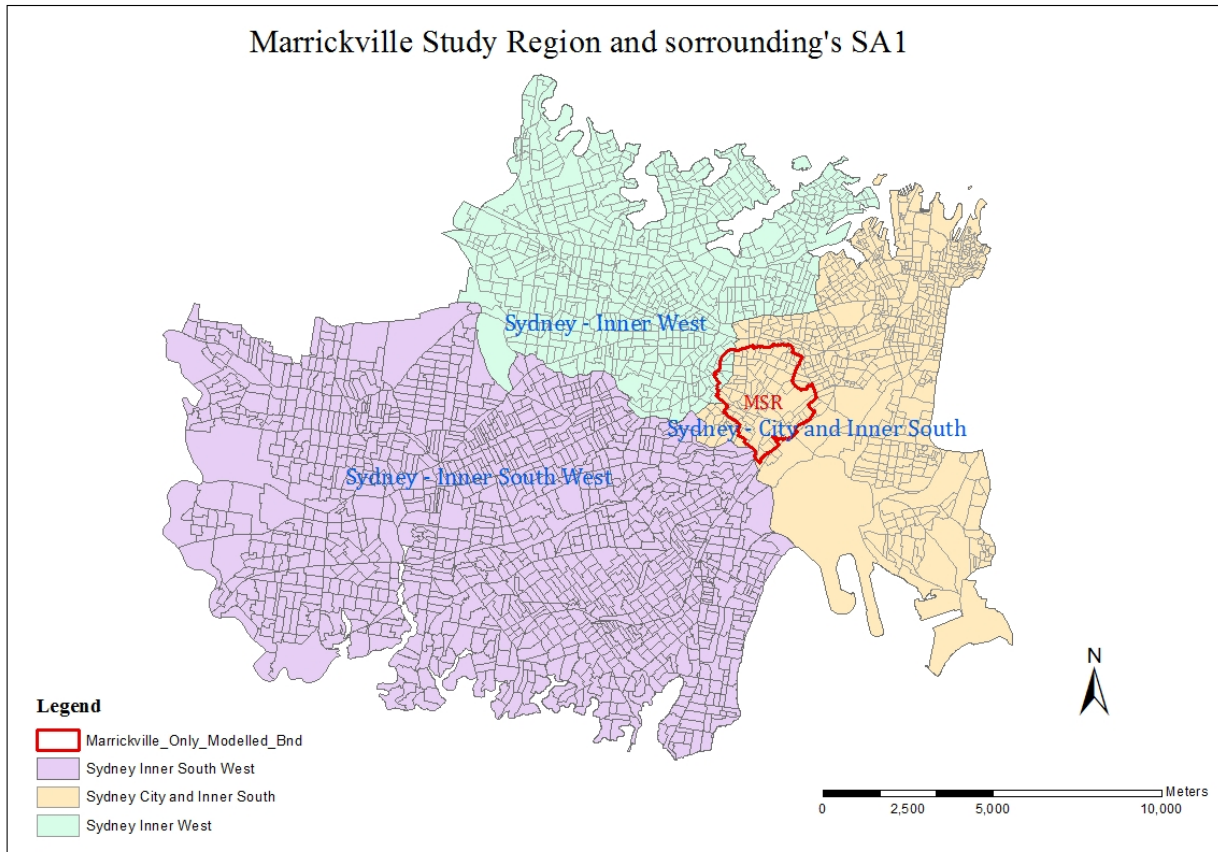


Figure 4-6: SA1 Map

4.3.3 Normalisation of Principal Components

Vulnerability is a social construct that is influenced, but not entirely determined, by physical phenomena. Hence, vulnerability cannot be measured in the same way that physical entities such as mass and length are measured. On the other hand, socioeconomic indicators, and associated composite indices, provide a relative assessment of vulnerability, rather than an absolute, objective measure. Therefore, it is important to be clear about the benchmark of comparison, i.e., relative to what is vulnerability being assessed. Each of the social vulnerability components obtained from the PCA (Section 4.3.2) for each SA1 is normalized relative to the minimum and maximum value of that component in a region of reference, using the following relationship:

$$\bar{C}_i = (b - a) \frac{C_i - C_{min}}{C_{max} - C_{min}} + a \quad \text{Equation 4-1}$$

Where

\bar{C}_i is the normalised value of the i-th indicator from the desired range of “a to b”; for this study, all indices are normalised to a range between 1 and 10; i.e. a = 1 and b = 10;

C_i is the component score of i-th component for each SA1;

$C_{\min i}$ and $C_{\max i}$ are the minimum and maximum score of the i-th component among all SA1s in the study region (MSR or BSR).

Two approaches are followed in the selection of $C_{\min i}$ and $C_{\max i}$. In the first approach, the region of reference is MSR itself and the $C_{\min i}$ and $C_{\max i}$ are the maximum and minimum value of that component within the 84 SA1 of MSR (red boundary in Figure 4-6). Principal components normalised using this approach provide measures of relative vulnerability within the MSR. They convey how vulnerable a given SA1 is relative to other SA1s in MSR. In the second approach, the region of reference is the entire Sydney Inner West, Sydney City and Inner South and Sydney Inner South West shown in Figure 4-2 (broader Sydney region), and including 2575 SA1. In other words, each principal component is normalized relative to the minimum and maximum value of that component in the entire Sydney region and can, therefore, help situate the vulnerability of Marrickville SA1s in the broader context of part of the Sydney metropolitan area hence it is possible to get a sense of how vulnerable Marrickville SA1s relative to the wider region to which MSR belongs.

Finally, SoVI is constructed using an additive aggregation of all Principal Component's scores by providing equal weight to each component and results are presented in Section 5.1.1. The reason for providing the equal weight is already discussed in the literature review (Section 2.2.2.2).

4.4 Flood Exposure Index for Marrickville Valley

The Flood Exposure Index (F_E) is developed for the Marrickville valley following the same approach that is used for constructing SoVI. Exposure index which represents vulnerability driven by the built environment has been quantified by previous researchers using indicators such as population density, quality and magnitude of residential, commercial and industrial properties, transport facilities and lifelines such as hospitals, schools, electric power, potable water facilities etc. (Mileti, 1999; Chang, 2003; Gilbert et al., 2003; Parfomak, 2005; Borden et al., 2007; Holand et al., 2011). The most comprehensive source of built environment data for the Marrickville Study Region (MSR) are the ABS and National

Exposure Information System (NEXIS) of Geoscience Australia. Three indicators are selected from these two sources as reflecting a dimension of vulnerability mediated by the built environment for the year 2011 (Table 4-3). No PCA analysis is required in this case because the number of indicators is small. Like ABS, the NEXIS provides aggregate information for Statistical Area Level 1 (SA1).

Table 4-3: Flood Exposure Indicators

Indicators	Data Source	Direction of Correlation with Vulnerability
Population density per square km	ABS	+
Building density per square km	NEXIS	+
Old building (constructed before 1980) density per square km	NEXIS	+

Each indicator is standardised using Equation 3-1, then the indicators are combined by additive aggregation to construct FE. The F_E values are again normalised to a range of 1 to 10 by using the same concept described in Section 4.3.3 and the results are described in the Section 5.1.2.

4.5 Flood Hazard Index for Marrickville Valley

4.5.1 Flood Simulation

The previous Marrickville council (now part of the Inner West council) of Sydney has developed Drains hydrological/hydraulic model and TUFLOW two-dimensional 1D/2D hydraulic model for the flood analysis of MSR. The same flood models are used in this study to generate flooding scenarios from extreme rainfall and climate change events. To generate the flooding scenarios the most up-to-date design rainfall data following the guidelines of

Australian Rainfall 2016 guidelines are used. Total 1035 hydrological sub-catchments were generated based on the Airborne Laser Survey (ALS) with the assumption that runoff generated from those sub-catchments would flow towards pits. The purpose of the Drains model is to generate surface flows arriving at each pit and route these stormwater hydrographs to pipes and surface water networks (GRAY, 2011).

The runoff from the sub-catchments is then input as pit inflow into the TUFLOW hydraulic model. TUFLOW is dynamically coupled with 1D ESTRY engines and takes consideration of urban features such as urban topography, roads, levees, infrastructures, including the urban stormwater drainage systems with its natural channels, pits, pipes, barriers, culverts, trunk drainage systems, pumps, weirs and bridges. The output from the TUFLOW model can be used to estimate extent and level of flooding, as well as velocities of water and flow patterns. Due to the non-availability of historical gauge water level and discharge data, the model results were verified based on the council knowledge of drainage hot spots, community questionnaire results and comparison of results with the previous studies. Among the nine sub-catchments, data for ECE sub-catchments is not accessible for this research and is therefore excluded from the model (GRAY, 2011).

TUFLOW does not have its own graphical user interface, but GIS software can be used for the creation and editing of spatial data and viewing of results (TUFLOW, 2016). The council's TUFLOW model was developed using the MapInfo Professionals GIS software and simulated with the hydrodynamic computational engine released in 2010. For the current study, the TUFLOW model is simulated with hydrodynamic computational engine released in 2016 and for convenience, the ArcGIS environment is used for data building and editing (starting from the MapInfo data files provided by the Council, and converted to ArcGIS).

4.5.2 Design Storm

A first step of conducting a flood hazard modelling is to an appropriate design rainfall event that suits the study objectives. As the objective in this study is to identify flood hazard under extreme conditions, a 1% Annual Exceedance Probability (AEP) which has only 1% chance of occurring in a given year is selected as our design storm event. There are five classes of design rainfalls; a 1% AEP rainfall event falls into the category of Rare Design Rainfall (Green et al., 2016). Design rainfall depths and temporal patterns are derived from the Intensity Frequency Duration (IFD) curves/charts, released by Australian Bureau of

Meteorology (BOM), which is a probabilistic-based estimation of average rainfall depth at a particular location within a defined duration.

The hydrological and hydraulic models for the Marrickville Valley Flood Study, 2011 (GRAY, 2011) are used in this research as a starting point and modified as well as updated where necessary. This initial modelling was conducted using a previous set of guidelines, namely the Australian Rainfall-Runoff (ARR), 1987 guidelines and its corresponding IFDs (Pilgrim, 1987). However, ARR 1987 IFDs are superseded by the recent published ARR 2016 IFDs (Babister et al., 2016) with new sets of temporal patterns, known as ensemble storms. Existing flood models are therefore updated in this research by using new ARR 2016 guidelines and its corresponding IFDs.

In the previous ARR guideline (i.e. ARR 1987), only one temporal storm pattern per duration for a given AEP was available for analysis. On the other hand, new ARR 2016 uses a more extensive database and provides guidelines for using ensemble event, which delivers ten temporal storm patterns per duration for a given AEP. ARR 2016 recommended the use of flood models with an ensemble of storms (i.e. use multiple storm patterns) and to find the median of ensemble storms that will be considered as the design storm event for a particular AEP. As this covers a broader range of possible rainfall scenarios, it provides a relatively more robust estimation of 1% AEP design storm, compared to previous ARR 1987.

4.5.3 F_H construction

The Flood Hazard Index (F_H) is developed from the flood simulation results discussed in the previous section. The F_H is constructed following the same approach described for F_E in section 4.4. From the flood simulation results, the following four indicators have been extracted for each SA1:

- i. Extent of flooding as percent of total area that is flooded;
- ii. Average maximum flood depth;
- iii. Average maximum velocity;
- iv. Average flood duration;

Any increase in any of the above-mentioned indicators will increase the hazard index of that particular SA1. Each of the indicators is standardised using Equation 3-1 and aggregated

(additive) to construct the F_H . The F_H values are then normalised into 1 to 10 scale by applying the same concept described in Section 4.3.3 and the results are outlined in the Section 5.1.3.

4.6 Flood Social Vulnerability Index (FSVI) for Marrickville Study Region

Finally, the FSVI is developed following both additive and multiplicative aggregations as explained in Section 3.2. One of the most significant hurdles of indicator-based vulnerability assessment is to assign relative importance (weights) to the indicators. When indicators are aggregated, the majority of quantitative-based studies in the literature adopts equal weights, while others assign weights based on expert judgment or PCA (Tonmoy, 2014). The PCA is often applied when a large number of indicators are used. For a similar reason, this research used PCA for developing SoVI index as SoVI combines a large number of indicators, and weights derived from the PCA were used in building SoVI. However, the other three indices of this study (FSVI, F_E and F_H) are based on a small number of indicators, therefore PCA is not used and, equal weights are adopted. Nevertheless, different combinations of weights are tested to check their impact on final results (Table 4-4) which was also a recommendation of the stakeholders of Inner-West Council where the MSR is located (See Section 5.2). The results of the various FSVI scenarios are outlined in the results Section 5.1.4.

Table 4-4: FSVI with different weight combination

Scenario	Weights			
	F_H	SoVI	F_E	Description
FSVI _E	1	1	1	Equal weights
FSVI _{FH50}	1.5	1	1	50% weight increase of F_H
FSVI _{FH100}	2	1	1	100% weight increase of F_H
FSVI _{SoVI_Wt_Zero}	1	0	1	0 weights to SoVI
FSVI _{FE_Wt_Zero}	1	1	0	0 weights to F_E

Chapter 5

Result and Discussion

5.1 Vulnerability to flooding in Marrickville

5.1.1 Social Vulnerability Index (SoVI)

37 socioeconomic and demographic indicators, discussed in Section 4.3.1 are initially selected for the construction of SoVI. Following a standard practice of PCA (discussed in Section 4.3.2), indicators that have high correlation (multicollinearity) or do not have any correlation with other indicators are excluded from the analysis. As a result 16 indicators are removed and 21 are retained. Three tests are conducted on the retained indicators. The determinant of the correlation coefficient matrix for the retained 21 indicators is 2.57×10^{-5} which is greater than the minimum recommended value of 10^{-5} (Field, 2009), indicating an acceptable level of multicollinearity. The Bartlett's test of sphericity is found to be highly significant ($P < 0.001$), indicating that the correlation matrix of indicators is significantly different from an identity matrix. In an identity matrix, the indicators are perfectly independent because the correlation between them is zero. In the absence of correlations, no clusters can be identified. Finally, the Kaiser-Meyer-Olkin measure of sampling adequacy (KMO) was found to be 0.815. The KMO result indicates that the sample is adequate for PCA to yield distinct and reliable component (Kaiser, 1970).

Next, a cluster analysis is conducted to identify major subgroups or components with eigenvalues greater than 1 using Kaiser's criteria (Kaiser, 1960). The scree plot (Figure 5-1), shows that the point of inflexion is at component 5 after which the slope changes significantly. Five components, shown in Table 5-1, are selected, including the point of inflexion (Cattell, 1966), although some authors suggest its exclusion (e.g., Field (2009)). The five principal components explain 66% of the variance. All 21 variables present

commonality extraction values greater than 0.5, which indicates that in all the variables, at least 50% of the variance is explained by the resulting principal component.

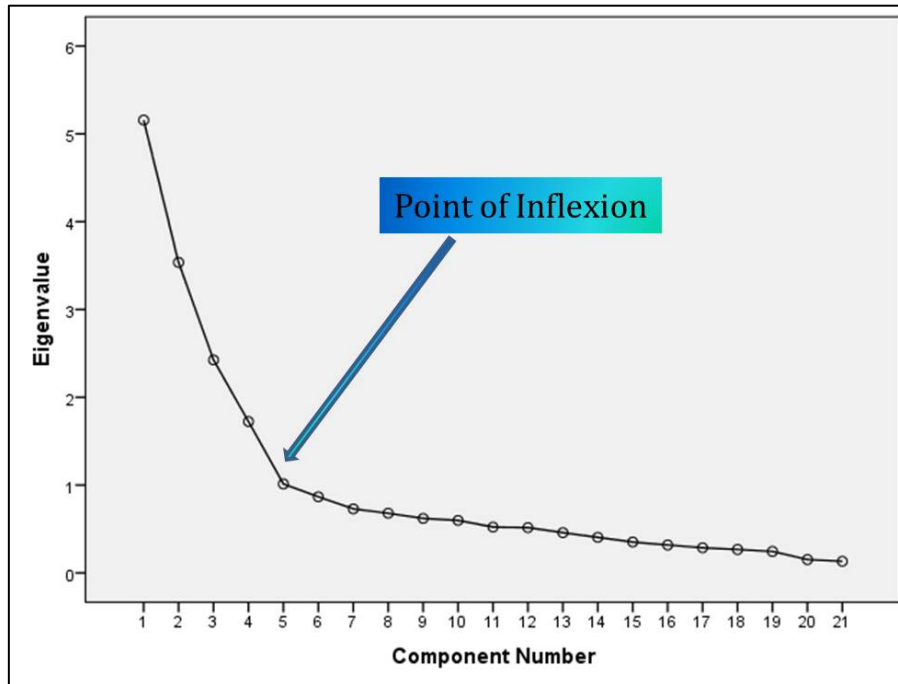


Figure 5-1: Scree plot

The resulting five principal components can be seen to reflect five different aspects of social vulnerability. Each aspect is given a label based on the indicator with the highest factor loading. The factor loading is the correlation between the indicator and the component (Field, 2009). Most indicators have significant loadings on all or most components. This characteristic makes the interpretation of components difficult, and that is why the factor rotation technique (varimax orthogonal rotation) is applied which ensures that variables are loaded maximally to only one factor. Table 5-1 shows the five principal components with the rotated factor loadings. In addition, Appendix A, shows the matrix of loadings of each indicator on each component before and after rotation.

Table 5-1: Extracted Principal Component

Principal Component	Eigen Values	Indicators	Factor Loading after rotation
1. Household demography	5.157	Number of dwellings occupied by 5 individuals or more	.773
		Number of household with 2 or more families	.726
		Number of dwellings occupied by single individuals	-.655
		Number of people with low speaking proficiency in English	.630
		Number of couple families with more than 2 dependent children	.623
		Number of people who never went to school	.605
2. Immigration and income status	3.536	Number of non-citizens	.843
		Number of households with negative or nil income	.747
		Number of recent migrants (previous 8 months)	.743
		Number of people with weekly negative or nil income	.706
		Number of houses with weekly rent over the median household rent within the study region	.542
3. Low rented households, dependent and unemployed families	2.425	Number of houses with weekly rent below \$150	.812
		Number of single-parent families with children under 15	.633
		Number of unemployed families	.575
		Number of dwellings owned with mortgage	-.562
		Number of dwelling owned outright or being purchased	-.500
4. Age distribution	1.724	Number of people over 65 years of age	-.741
		Number of people between 35 and 39 years	.685
		Number of children below 5 years of age	.531
5. Educational status	1.013	Number of people whose highest level of education is year 11	.814
		Number of people whose highest level of education is Certificate Level (Certificate 1, 2, 3 or 4)	.508

The factor loading of each indicator is divided by the square root of the eigenvalue to get the weight (Pink, 2011). The index value of each social vulnerability component is then determined by the summation of the product of the weight and standardised indicators values (Equation 5-1).

$$C_i = \sum_{j=1}^p \frac{L_j}{\sqrt{\lambda_i}} \times I_{sj} \quad \text{Equation 5-1}$$

where

C_i is the index value of i-th component for the SA1

I_{sj} is the standardised value of the j-th indicator for the SA1

L_j is the factor loading for the j-th variable

λ_i is the eigenvalue of the i-th principal component

p is the total number of indicators in the index

Though the factor loading has both +/- sign, its absolute value is used in determining the weight. Where indicators decrease with increasing vulnerability, the inverse of the indicator is used to ensure all indicators increase with increasing vulnerability. The indices of each component (C_i) are then converted into a 1 to 10 scale using Equation 4-1 where 1 denotes the lowest vulnerability and 10 the highest. Note that the index value of a given SA1 only represents the relative rank of its vulnerability and does not carry proportionality. In other words, an SA1 with an index value of 10 is not expected to be 10 times more vulnerable than one with an index value of 1. The composite social vulnerability (SoVI) is determined by the arithmetical sum of each component score by applying an equal weight (Equation 3-2). The reason for providing equal weights has been discussed in the Literature Review Section 2.2.2.

In order to present the relative vulnerability of SA1s within MSR, the SoVI within the study region is converted to a 1 to 10 scale (Figure 5-2). For the convenience of graphical representation, the SoVI is then classified into the following 5 categories by subdividing the index value into 5 equal intervals.

- i. Very low
- ii. Low

- iii. Moderate
- iv. High
- v. Very High

Figure 5-2 shows that higher social vulnerability occurs mostly within the western part of the MSR. Several factors seem to combine to produce a ranking of high vulnerability. For example, the SA1s marked as 1 and 2 in Figure 5-2 are classified as highly socially vulnerable as a result of the component school of household demography and age distribution but not, significantly, education status, low value of rental or employment type. Specifically, in these two SA1s, there is a relatively large proportion of dwellings occupied by i) more than 5 individuals, ii) more than 1 family, iii) single individuals, iv) aged individuals and v) individuals with low English proficiency. On the other hand, the SA1 marked as 3 in Figure 5-2, is ranked as highly vulnerable for different reasons, namely high proportions of migrants, low-income households and individuals with lower educational levels. Conversely, the SA1s in the eastern part of the MSR, marked as 4 and 5, rank low on social vulnerability as a result of the very low number of residential dwellings and the predominantly industrial land use this part of MSR.

Figure 5-3 shows social vulnerability of MSR in comparison to its surrounding suburbs. The figure indicates that although some SA1s in the western part of the Marrickville have relatively high social vulnerability, the most disadvantageous SA1's are those in the inner-west around Bankstown and Canterbury not Marrickville.

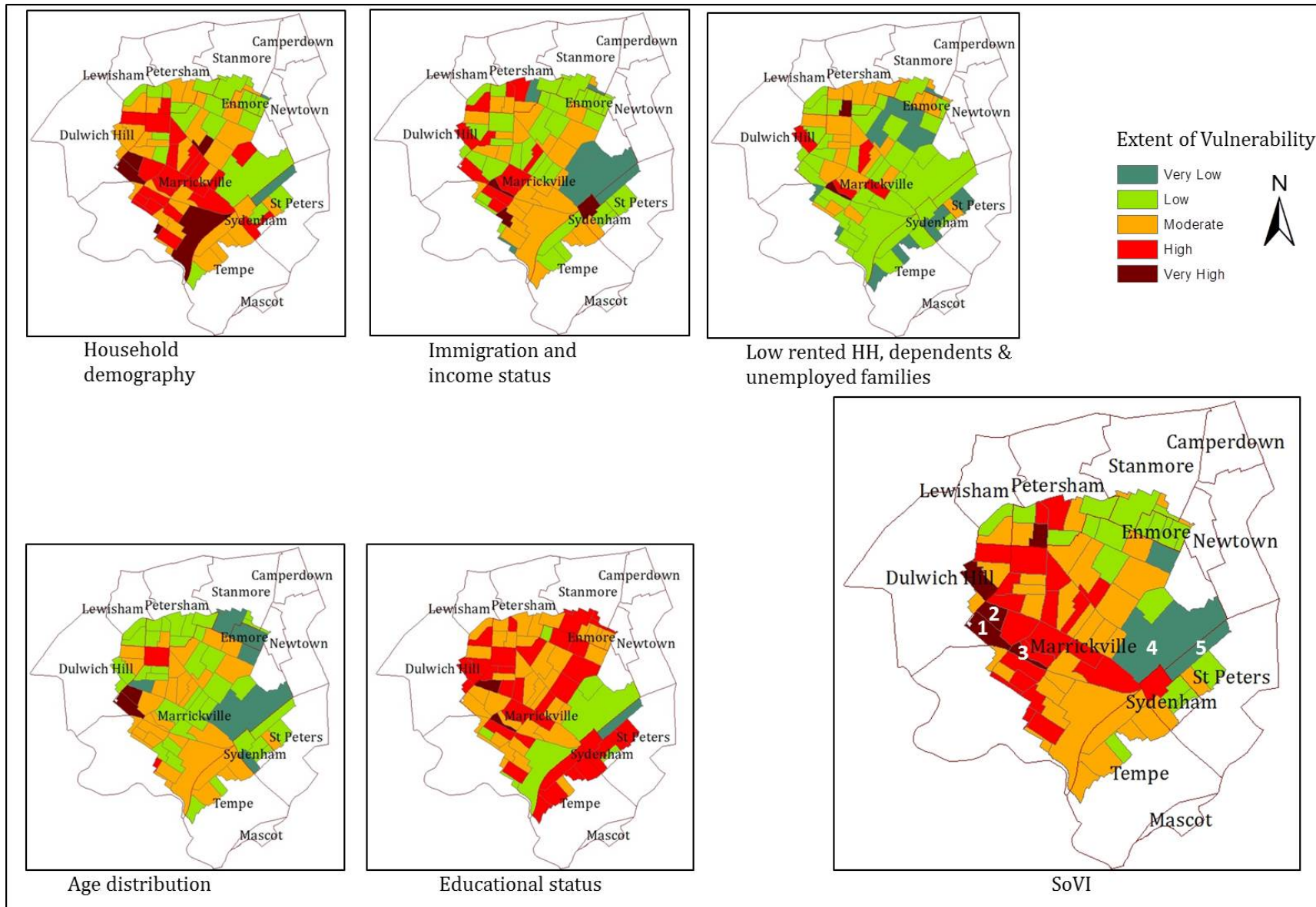


Figure 5-2: Different components of SoVI and composite SoVI within Marrickville

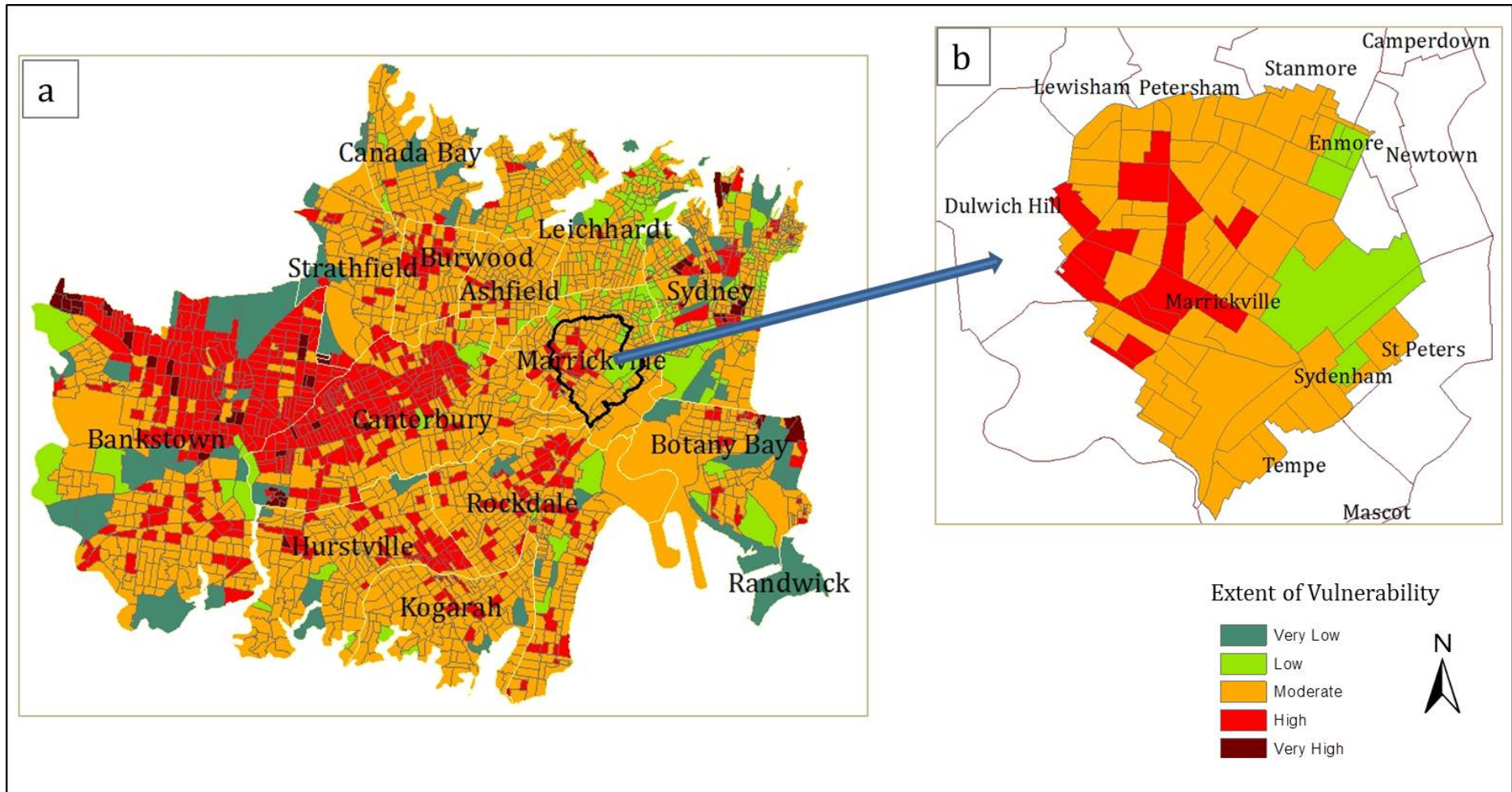


Figure 5-3: a) SoVI of Marrickville Valley in comparison to its surrounding suburbs b) Zoom to Marrickville valley

5.1.1.1 Sensitivity Analysis of SoVI

The SoVI of the Marrickville Study Region is determined (Figure 5-2) based on the initial selection of 37 socioeconomic and demographic indicators with a sample size of 2575 SA1's of Marrickville valley and its surroundings suburbs. In addition, a sensitivity analysis has been done to check how the ranking of SoVI of different SA1s varies when the sample size of SA1 is changed. To do this, a total 548 number of SA1s have been selected from a smaller geographic area in comparison to the previous analysis. This new geographical area has been selected by considering a 2500 meter buffer from the boundary of MSR (Figure 5-4). The SA1s from this new geographical area cover a smaller portion of the Sydney-Inner West, Sydney-Inner South West and Sydney-City and Inner South.

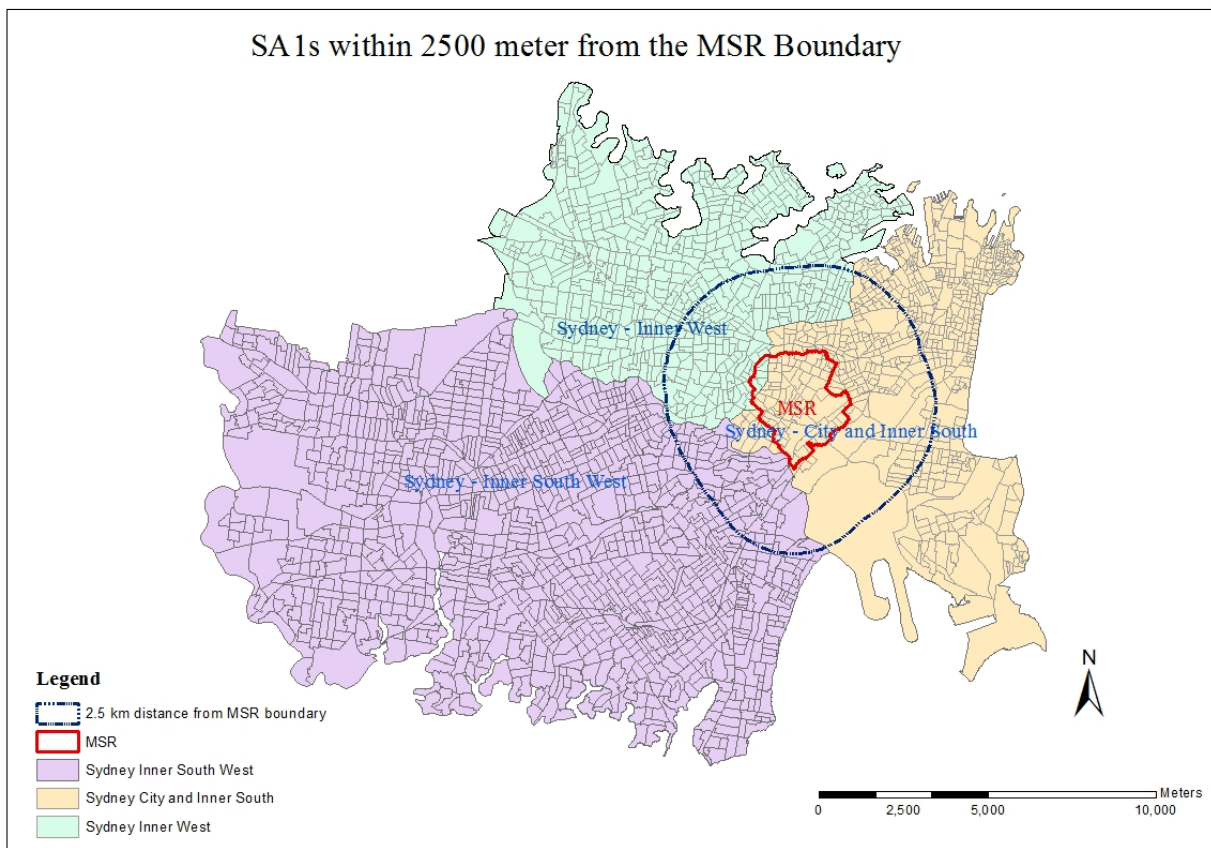


Figure 5-4: Variation of sample size of SA1 to check sensitivity of SoVI

By following the standard practice described in Section 4.3.2, a total 21 indicators were retained by the PCA. With the new sample size, the retained indicators were found to be almost the same as those obtained from the previous analysis covering a bigger geographical area. Only two new indicators emerged (number of dwellings with no motor vehicle, number of people employed as machinery operators or drivers) which had not been

retained in the previous analysis and two indicators were dropped (number of people with weekly negative or nil income, number of unemployed families) which had been retained in the previous analysis. The Principal Component Analysis (PCA) was then conducted with the 21 indicators with the varimax orthogonal rotation. The results of the three tests conducted on the 21 indicators are as follows which satisfied the criteria of PCA described in Section 5.1.1:

- i. Determinant of the correlation matrix = 2.96×10^{-5}
- ii. The Bartlett's test of sphericity is found to be highly significant ($P < 0.001$)
- iii. KMO = 0.803

From the principal component analysis, five different dimensions of social vulnerability were extracted (Table 5-2) explaining 64.4% of the variance. The different indicators that were retained under each component differed from the previous analysis (Table 5-1). However, the SoVI of MSR with the new sample size was highly similar to the one obtained from the larger set (see Figure 5-5). In nine SA1's, vulnerability increased to the next level and in 4 SA1's it moved one level down. Hence, less than 15% of MSR's SA1s were affected and only by one level.

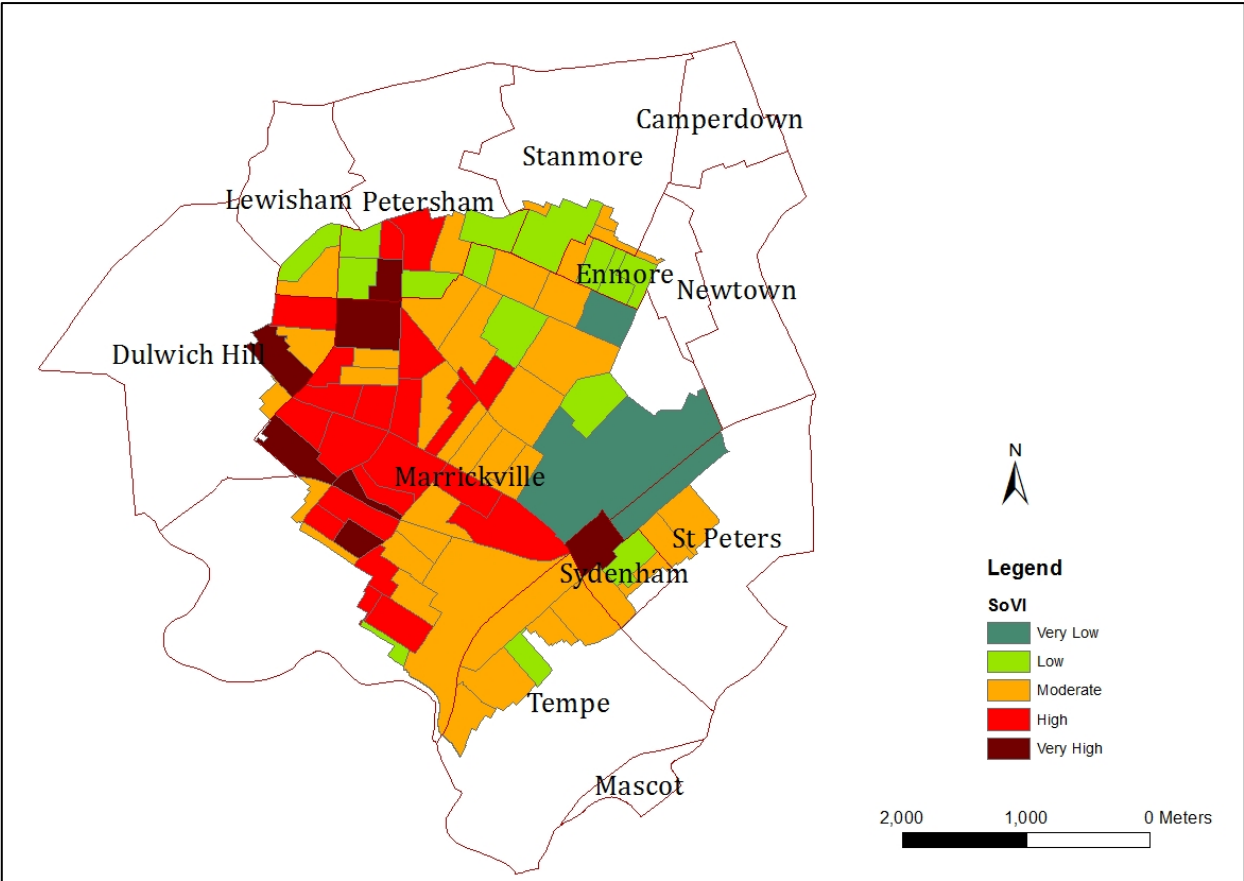


Figure 5-5: Composite SoVI of MSR after changing sample size of SA1

Table 5-2: Extracted Principal Component after changing sample size of SA1

Principal Component	Eigen Values	Indicators	Factor Loading after rotation
1	5.798	Number of non-citizens	-.781
		Number of houses with weekly rent over the median household rent within the study region	-.745
		Number of dwelling owned outright or being purchased	.744
		Number of people over 65 years of age	.722
		Number of recent migrants (previous 8 months)	-.568
		Number of couple families with more than 2 dependent children	.492
2	3.148	Number of people with low speaking proficiency in English	.820
		Number of household with 2 or more families	.788
		Number of people who never went to school	.680
		Number of dwellings occupied by 5 individuals or more	.657
		Number of people employed as machinery operators or drivers	.565
		Number of single-parent families with children under 15	.491
3	1.973	Number of houses with weekly rent below \$150	.788
		Number of dwellings with no motor vehicle	.716
		Number of dwellings occupied by single individuals	.706
		Number of dwellings owned with mortgage	-.632
4	1.507	Number of children below 5 years of age	-.716
		Number of households with negative or nil income	.631
		Number of people between 35 and 39 years	-.600
5	1.10	Number of people whose highest level of education is year 11	.804
		Number of people whose highest level of education is Certificate Level (Certificate 1, 2, 3 or 4)	.448

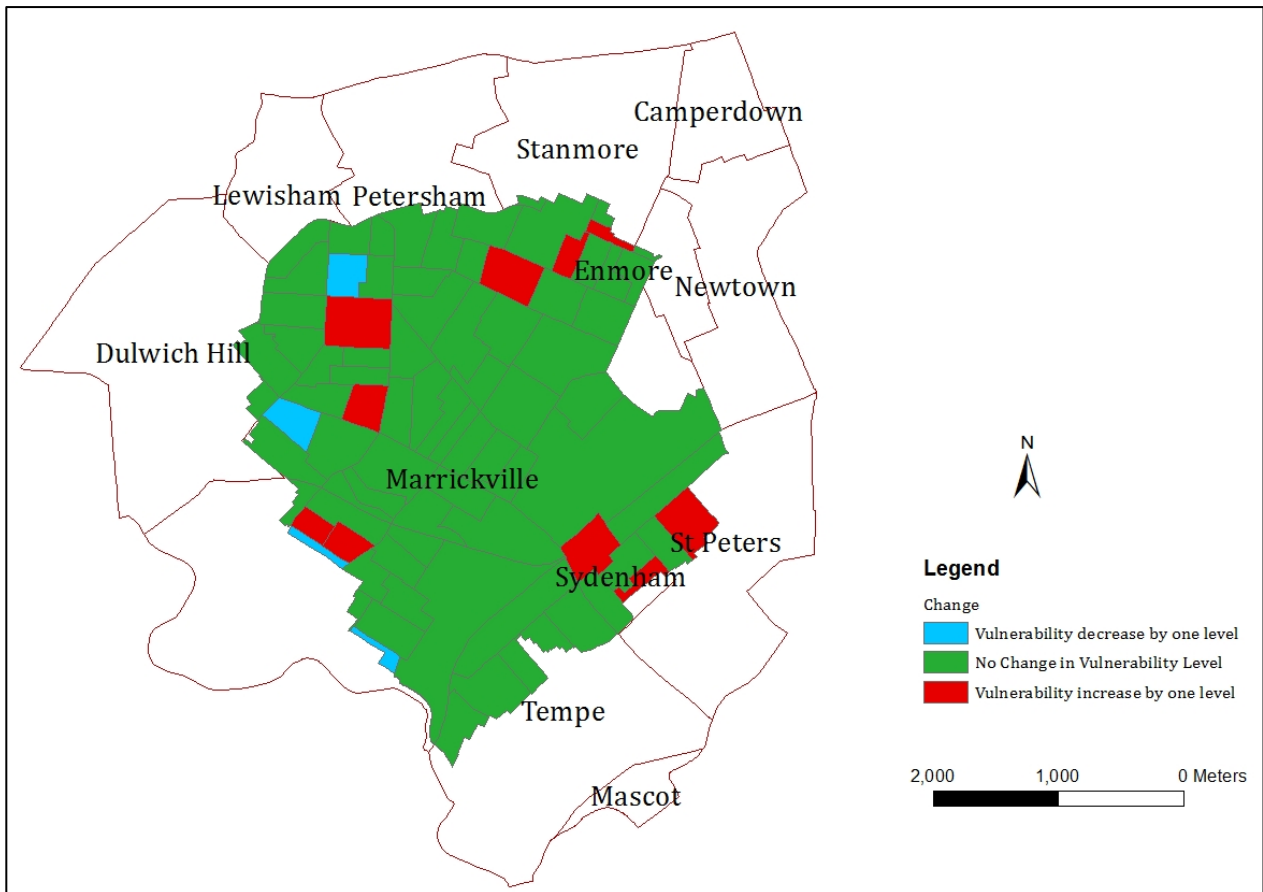


Figure 5-6: Change in level of Social Vulnerability

5.1.2 Flood Exposure Index

The standardised values (using Equation 3-1) of three selected flood exposure indicators (population density, building density and old building density) described in Section 4.4 are aggregated to construct exposure index F_E (Equation 3-2) by applying equal weights. The index values are then converted to a range of 1 to 10, yielding F_E as a proxy for vulnerability due to the built environment. Figure 5-4 shows the variation of F_E , discretised into five categories, within MSR. Several SA1s around Enmore, Lewisham, Dulwich Hill and Marrickville have high vulnerability, on account of high residential density. SA1s between Marrickville and Sydenham have very low vulnerability because of the predominantly industrial nature of the area. Figure 5-5 shows exposure index of MSR in the context of the wider inner west, and highlights around twenty SA1s with high or very high vulnerability in the Inner West, none of which is in MSR.

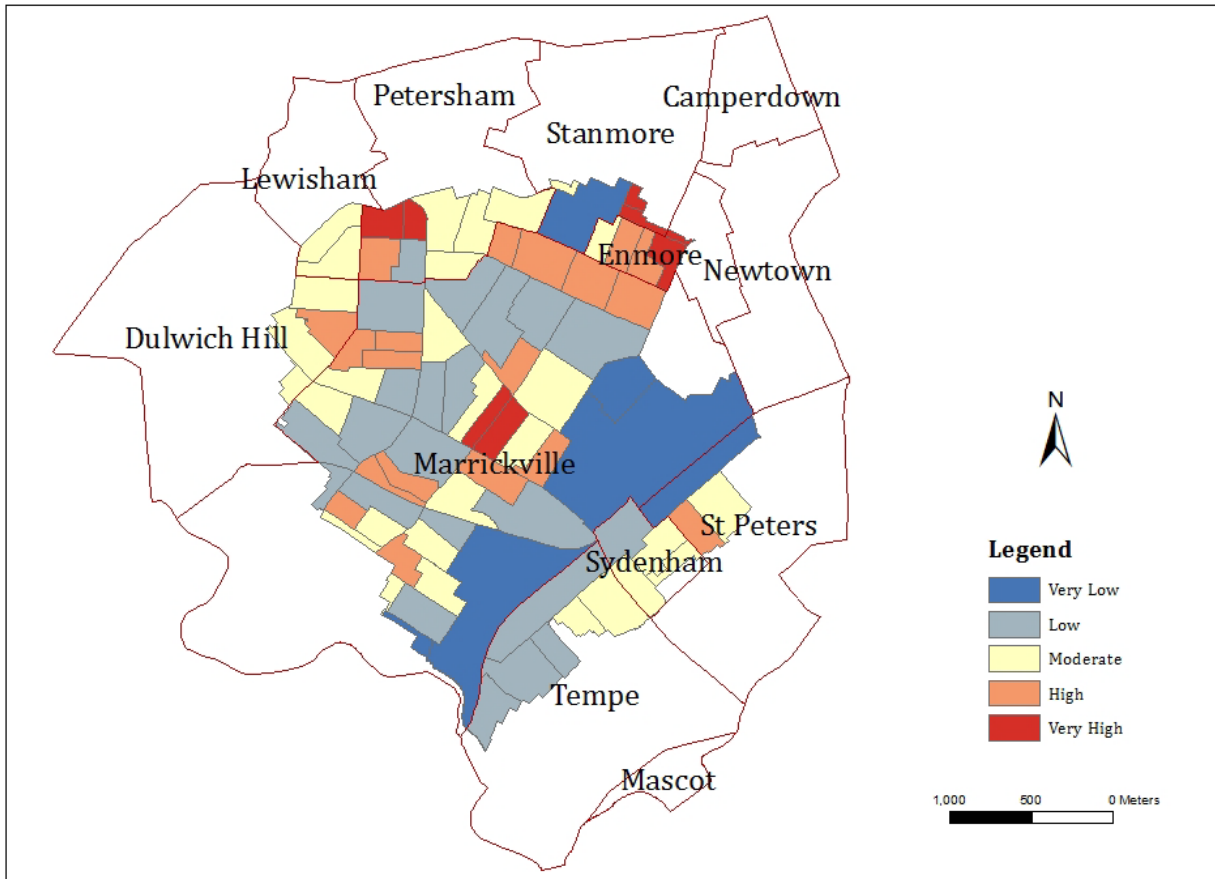


Figure 5-7: Exposure Index within Marrickville Valley

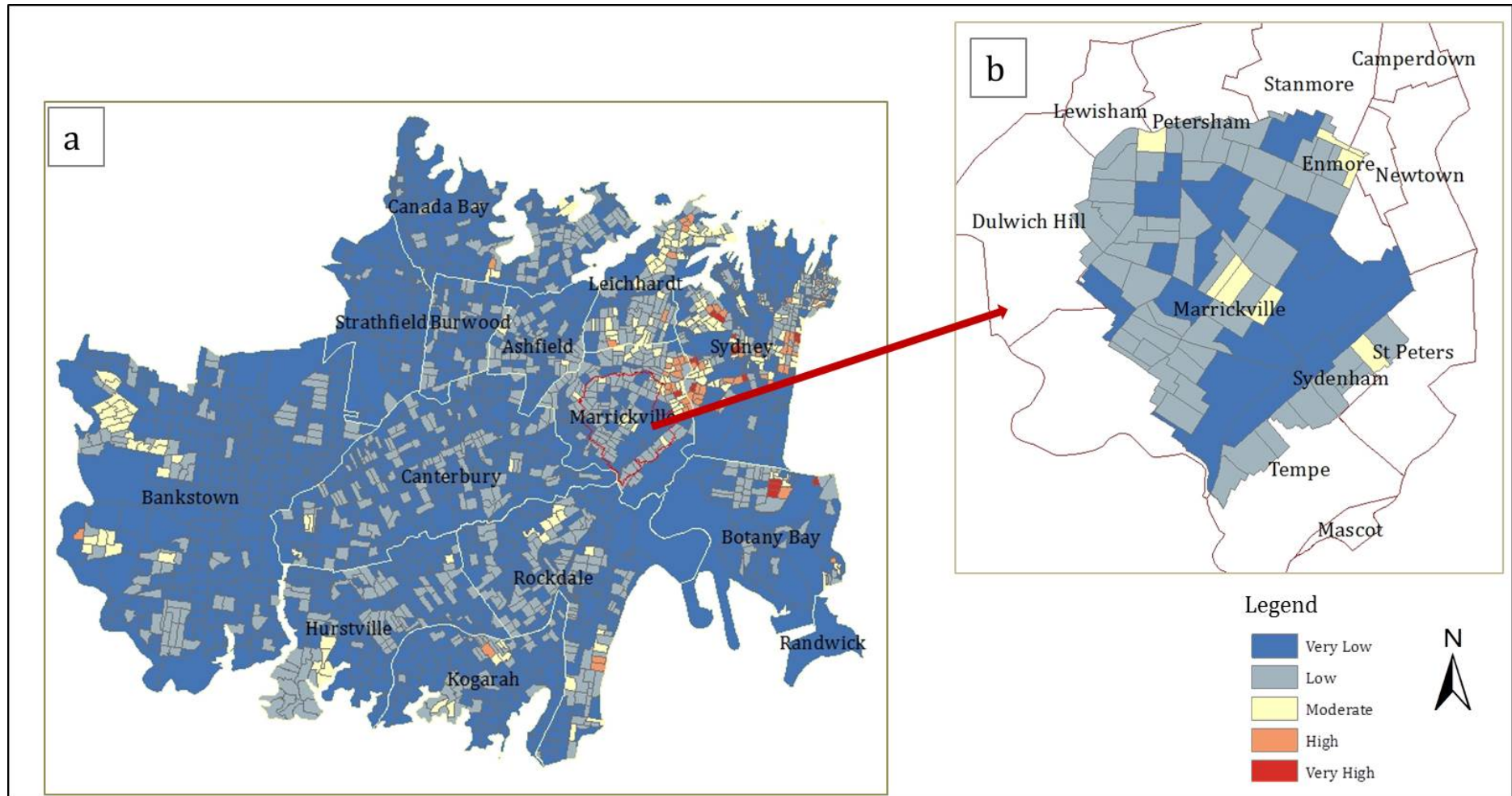


Figure 5-8: a) F_E of Marrickville Valley in comparison to its surrounding suburbs b) Zoom to Marrickville Valley

5.1.3 Flood Hazard

5.1.3.1 Hydrological Analysis

The Drains model is simulated with ensemble storms (storm pattern 1 to 10, discussed in Section 4.5.2) for different storm durations starting from 1 hour to 24 hours for the 1% AEP. The model is run over multiple periods to identify the critical duration producing the highest flow for the 1% AEP. The peak catchment flows of the study area at various durations for various storm patterns are shown in Table 5-2.

Table 5-3: Flows for the 1% Annual Exceedance Probability for ensemble storms

Storm Duration (Hour)	1% Peak Flow (m ³ /s)										
	Storm 1	Storm 2	Storm 3	Storm 4	Storm 5	Storm 6	Storm 7	Storm 8	Storm 9	Storm 10	Median
1	50.5	41.2	45.9	42.8	45.1	46.7	41.7	44.5	41.5	48.0	44.8
1.5	40.1	44.3	40.4	35.6	36.1	45.5	45.1	40.8	38.1	39.3	40.2
2	43.7	42.7	34.2	48.3	43.5	45.0	32.8	42.5	36.9	41.4	42.6
3	30.3	30.9	29.8	31.3	27.3	27.5	31.6	31.5	30.3	32.6	30.6
4.5	26.5	31.2	26.5	31.2	29.8	31.0	26.5	28.5	29.2	30.1	29.5
6	29.7	30.3	31.8	25.7	29.9	34.5	26.5	26.2	29.6	32.5	29.8
9	25.3	25.7	22.6	26.6	25.7	22.4	23.5	23.3	29.2	23.0	24.4
12	25.0	25.5	28.7	23.2	28.6	26.9	22.0	25.6	30.0	24.3	25.5
18	24.0	20.9	21.5	17.7	21.9	21.3	22.4	16.7	21.5	19.6	21.4
24	22.8	24.8	20.6	21.2	19.1	22.3	18.8	20.2	20.5	18.2	20.5

The maximum median peak flow (44.8 m³/s) occurs for 1-hour storm duration. This median peak flow closely matches the peak flow of storm pattern number 8 of that particular storm duration. Therefore, the temporal pattern number 8 of 1-hour duration rainfall, is taken as the design storm for 1% AEP and for this research. It will be referred to as the base condition or base scenario for this study. Further climate change impacts are analysed as variations on this base condition.

Figure 5-6 shows the temporal pattern of design storm for 1-hour duration storm for 1% AEP and how the temporal variation differs from the previous ARR 1987 temporal distribution used by Marrickville valley flood study. The average intensity of ARR 1987 is 33% higher than that of ARR 2016 which means that flood simulations were overestimated for the Marrickville Valley Flood Study.

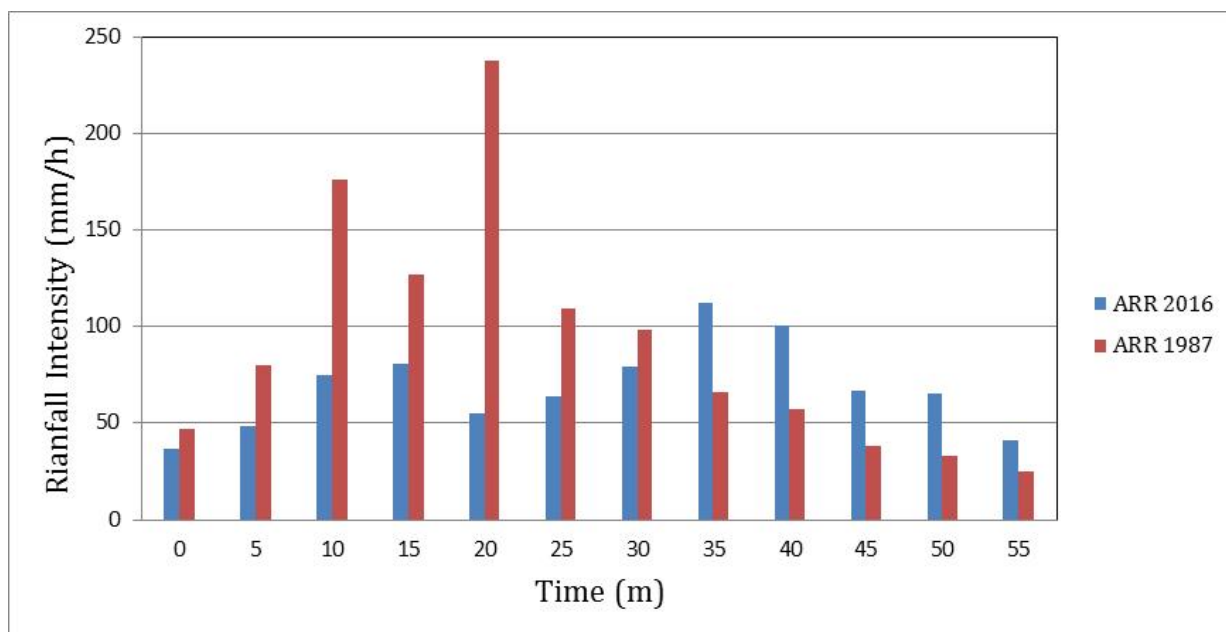


Figure 5-9: Comparison of rainfall intensities of ARR 1987 and ARR 2016 design storms for Marrickville valley

5.1.3.2 Hydraulic Analysis

The design runoff generated by the Drains model due to 1% AEP (runoff due to 1hr storm from pattern 8) are used next as an input in the TUFLOW hydraulic model to produce flooding results, in the form of flood depth, extent, water velocity and flood duration. In addition, flood depth and velocity are used to generate provisional flood hazard maps by following the NSW Floodplain Development Manual (Government, 2005). According to the manual, flood hazard is categorised into high or low hazard, defined as follows:

“High hazard: possible danger to personal safety; evacuation by truck difficult; able-bodied adults would have difficulty in wading to safety; potential for significant structural damage to buildings.

Low hazard: should it be necessary, truck could evacuate people and their possessions; able-bodied adults would have little difficulty in wading to safety.”

Accordingly, the data from Figure 5-7 extracted from the manual is used to generate the provisional hazard map for the MSR. Note that these categories are provisional because they do not reflect the effects of other factors such as flood readiness, damage, flood warning, flood duration, rate of rising of the flood, evacuation problems, effective flood access and type of built environment.

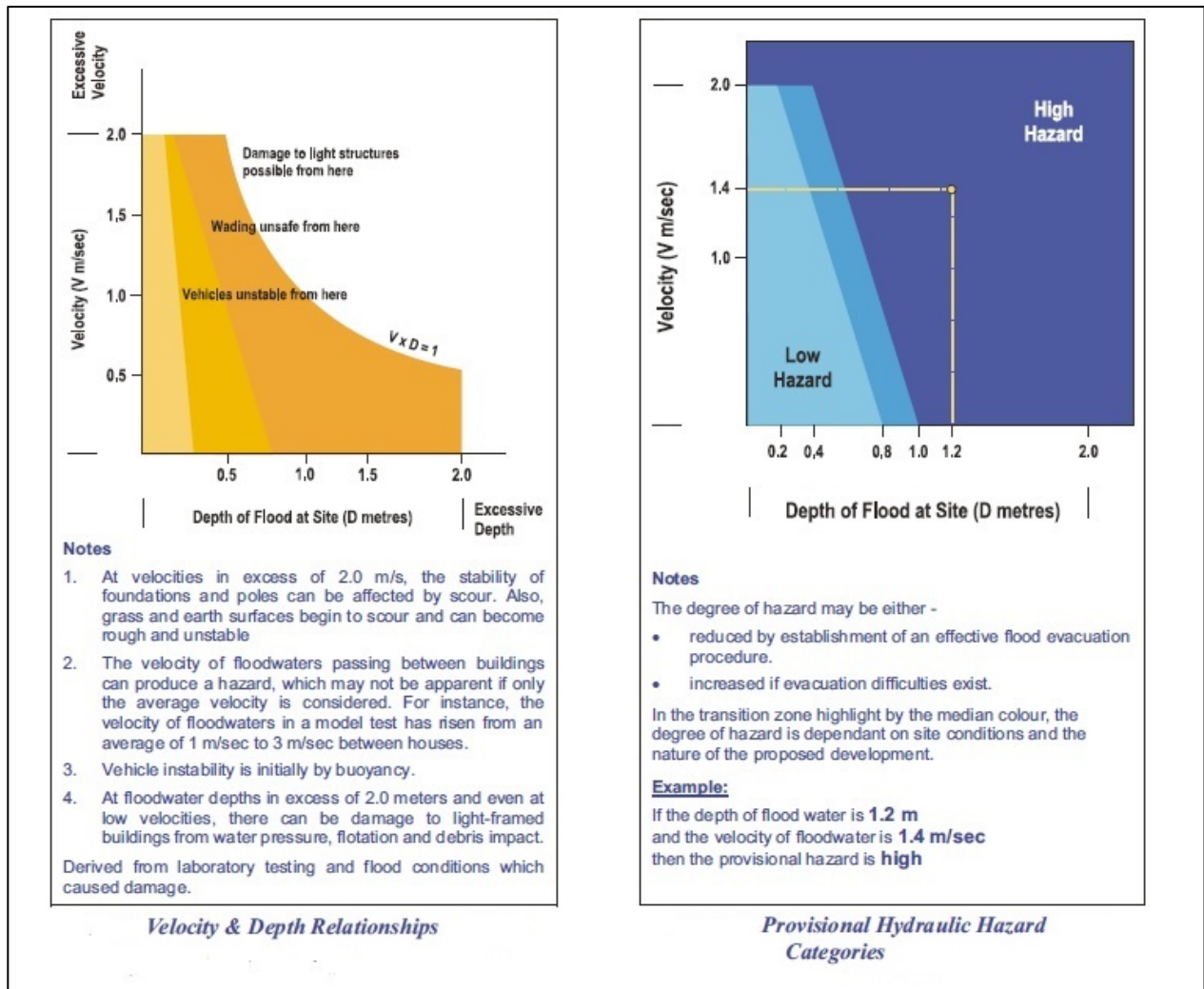


Figure 5-10: Provisional hazard categories (Source: NSW floodplain development manual)

Figure 5-8, Figure 5-9 and Figure 5-10 show the output from the TUFLOW model showing the variation of peak flood depth, peak velocity and flood duration, respectively, due to 1% AEP design flood event. A total of 17.6% of the MSR is flooded due to 1% AEP design flood event. Approximately 10% surface area of the MSR is under 0.1 to 1 meter of flood depth, with low flood velocity (≤ 0.4 m/s). A small surface area (0.6%) is highly flooded (depth > 1 meter) which mainly includes the Marrickville oval that acts as a retarding basin for temporary flood storage (see Table 5-3). It is mostly roads that fall under high flood velocity (≥ 2 m/s). The maximum flood duration due to 1% AEP for this region is 3 hours. Not surprisingly, the areas that are more deeply flooded (see Figure 5-8) are also found to be flooded for a longer duration (see Figure 5-10).

The provisional hazard map (Figure 5-11) for the MSR which represent the combined effect of flood depth and velocity is generated based on the data from Figure 5-7. Most of the MSR

(82.4%) does not experience flooding. Of the remaining part, most flooded areas (15.8% of MSR or 90% of flooded area) falls in a low-hazard category. The remaining part (1.8% of MSR or 10% of flooded area) is a high-hazard zone and includes the Marrickville oval and some roads towards the south of MSR.

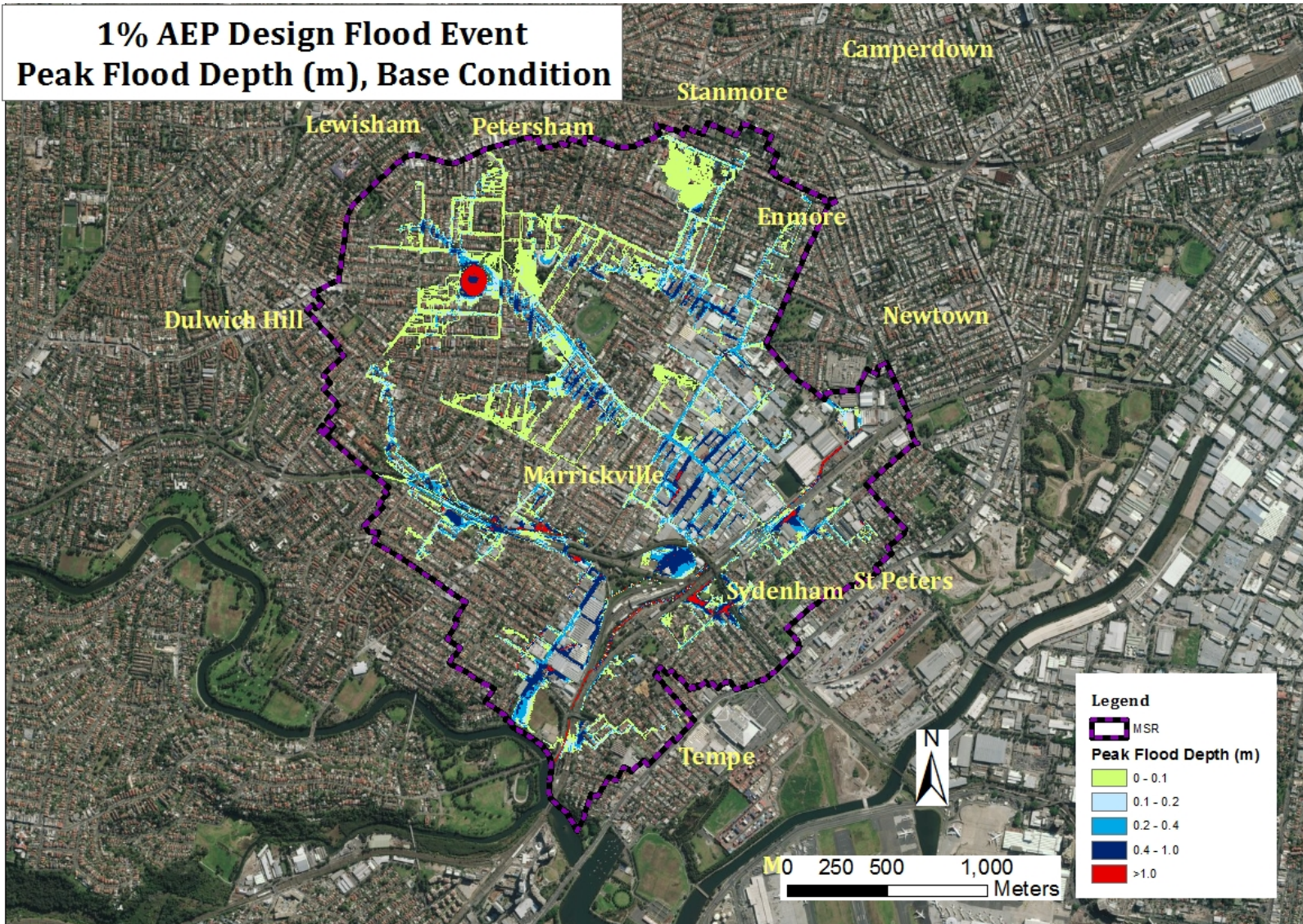


Figure 5-11: 1% AEP design flood event: Peak flood depth

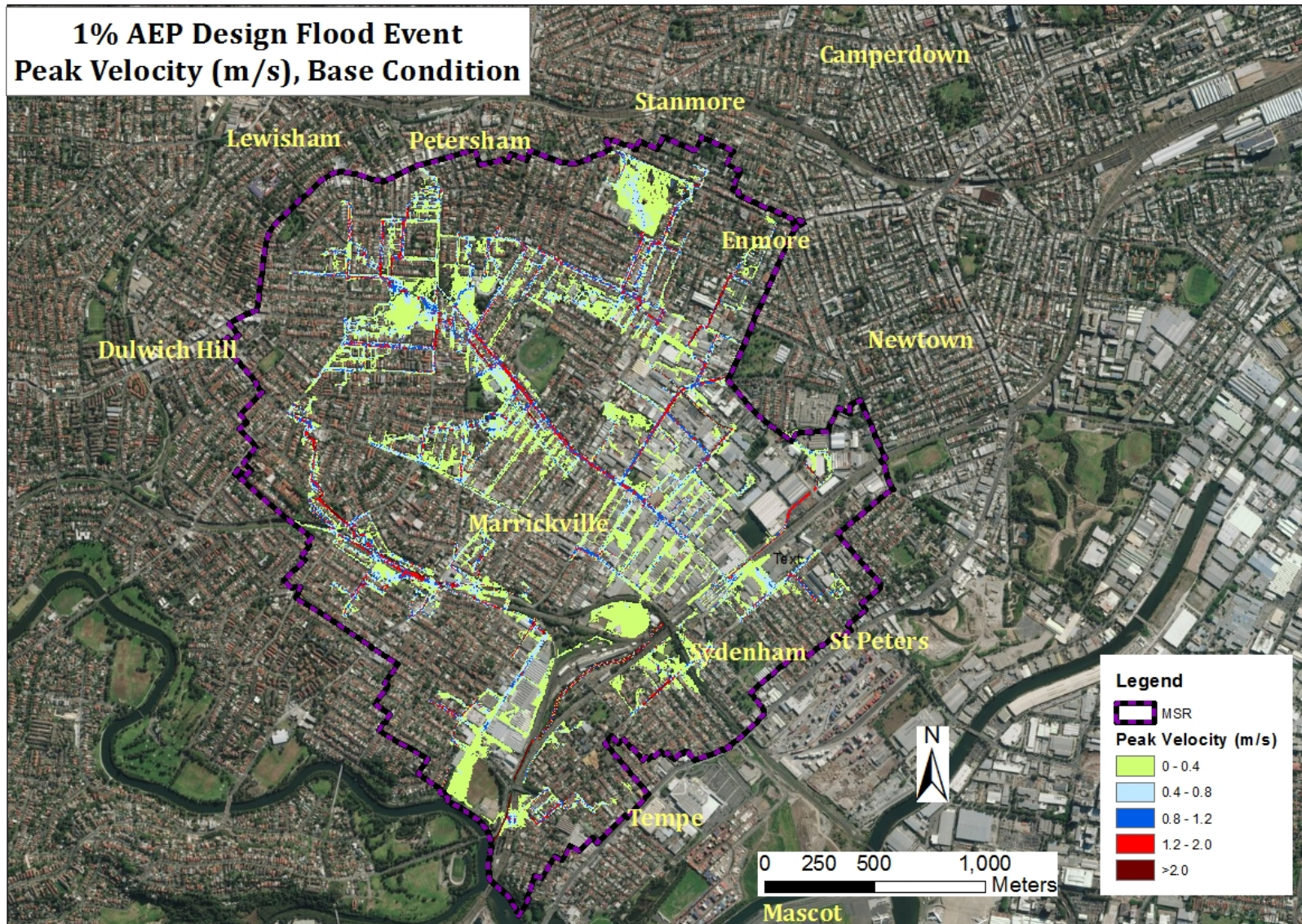


Figure 5-12: 1% AEP design flood event: Peak velocity vector

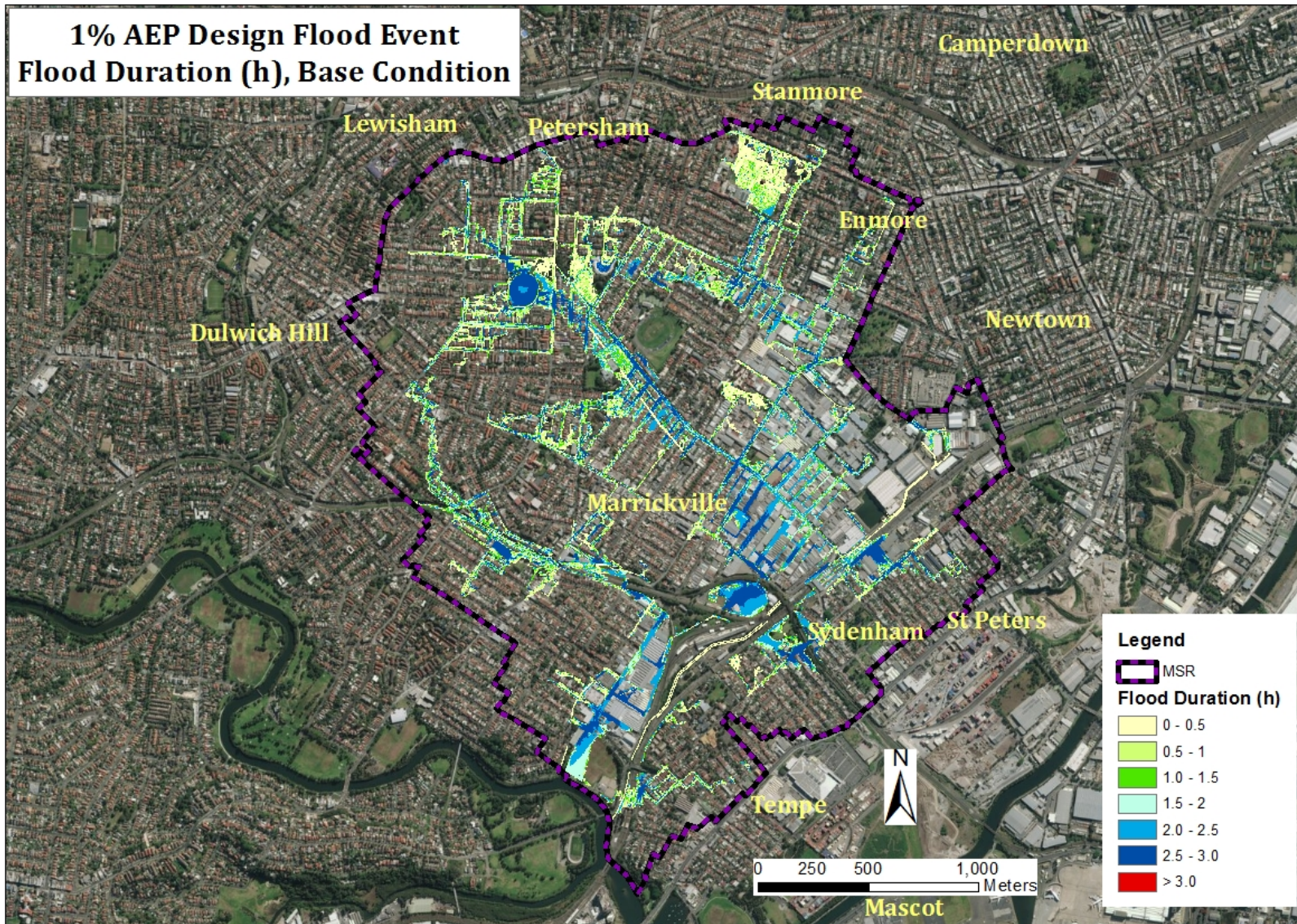


Figure 5-13: 1% AEP design flood event: Flood Duration

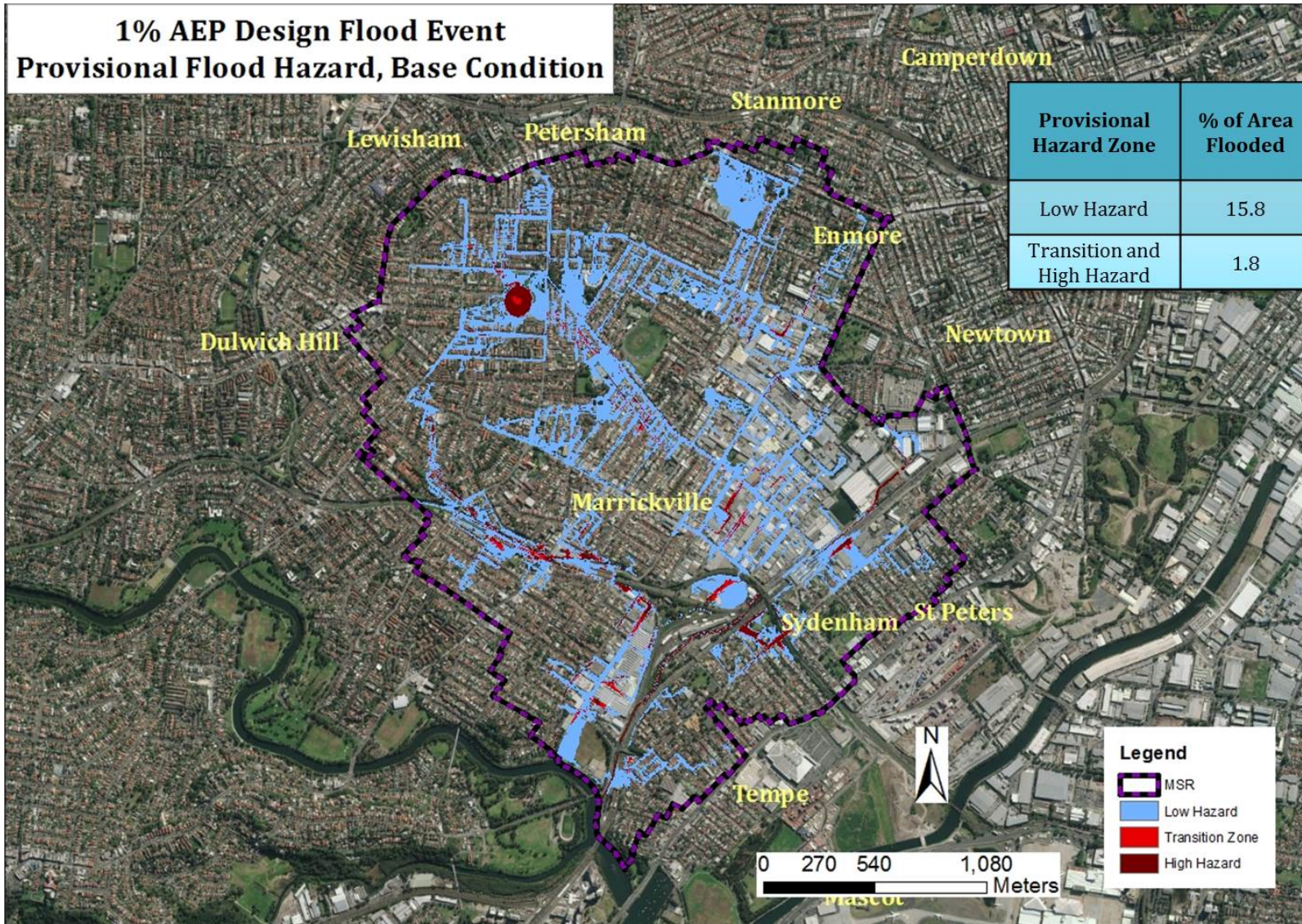


Figure 5-14: 1% AEP design flood event: Provisional Flood Hazard

Table 5-4: % of Area Flooded Under Different Flood Indicators (Base Condition)

Area Flooded Under Different Flood Depth Zone		Area Flooded Under Different Velocity Zone		Area Flooded Under different Flood Duration	
Flood Depth (m)	% of Area Flooded	Flood Velocity (m/s)	% of Area Flooded	Flood Duration (h)	% of Area Flooded
0 - 0.1	7.3	0 - 0.4	9.8	0 - 0.5	3.9
0.1 - 0.2	3.2	0.4 - 0.8	4.0	0.5 - 1	2.5
0.2 - 0.4	3.6	0.8 - 1.2	2.0	1 - 1.5	2.3
0.4 - 1	2.8	1.2 - 2.0	1.4	1.5 - 2	2.2
>1	0.6	>2	0.3	2 -2.5	2.8
-	-	-	-	2.5 - 3	3.8
-	-	-	-	> 3	0

5.1.3.3 Climate Change Impacts

Potential variations of flooding patterns in Marrickville due to future climate change are tested in this research by following the guidelines provided by ARR 2016 (Bates et al., 2016). The guidelines suggested testing the model by incorporating climate change projections of the study area for at least two different climate change scenarios (i.e. a low and a high emission scenario). Future rainfall projections are obtained from the “Climate Change in Australia” website, developed by the CSIRO’s Representative Climate Futures Framework. The changes in future rainfall intensity are derived by downscaling the results of a Global Circulation Model (GCM) for regional clusters of Australia (Figure 5-12). These projections are available for four Representative Concentration Pathways (RCPs) of future greenhouse gas and aerosol concentrations. Among the four RCPs, a low-emission scenario, RCP4.5 and a high-emission scenario RCP8.5 are used to test impacts of future climate change on flooding in Marrickville.

The Marrickville Study Region (MSR) is located in the East Coast Natural Resource Management Cluster (Figure 5-12). The projected changes in rainfall for the East Coast cluster relative to a 20-year (1986-2005) baseline are shown in Table 5-4.

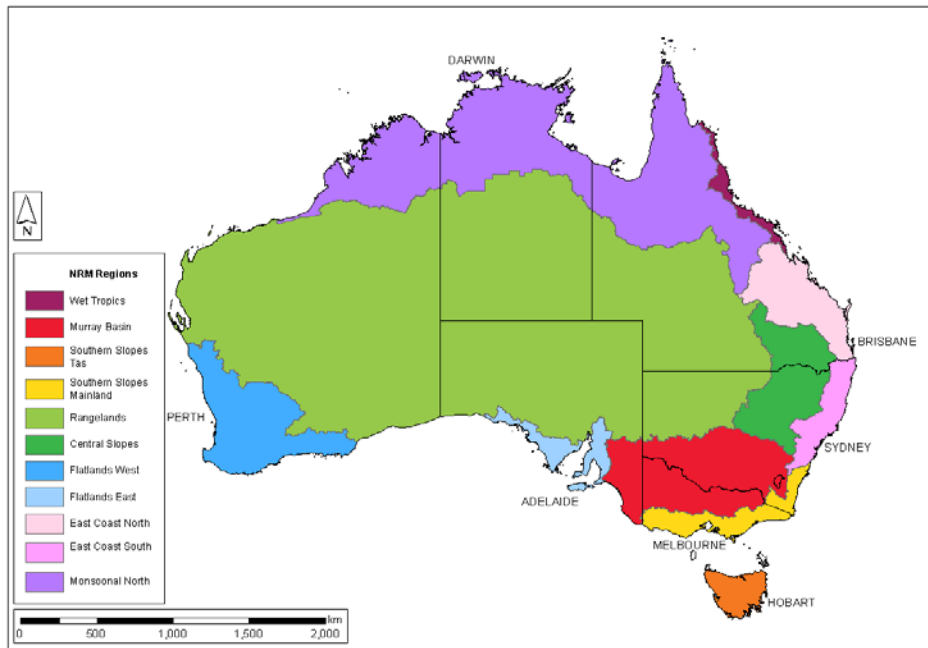


Figure 5-15: Locations of Natural Resource Management Clusters, source: Bates et al. (2016)

Table 5-5: Projected Rainfall Change for the Year 2060 and 2080 relative to the period 1986-2005

Represented concentration pathways (RCPs)	Year	
	2060	2080
RCP 4.5	+12%	+12%
RCP 8.5	+12%	+19%

Another factor that may affect the magnitude of flooding of MSR is the change in tailwater level due to sea level rise. This is mainly because the Cook River that flows through the Marrickville valley is connected to the Botany Bay coast (Figure 5-13). A rise in sea level coupled with tidal influence can act as a barrier reducing the runoff from the upper catchment. This phenomenon is known as change in tailwater level. In order to test its impact on MSR, this research used sea level rise projections for Botany Bay. These projections are obtained from the CoastAdapt tool (NCCARF, 2017). Developed by the National Climate Change Adaptation Research Facility (NCCARF), CoastAdapt provides access to sea level rise projections for different RCPs for all Australian coastal councils. Table 5-5 shows sea level rise projections for Botany Bay region relative to a historical average (1986 and 2005) for two different greenhouse gas emission scenarios.



Figure 5-16: Confluence of Cooks River

Table 5-6: Projected Sea Level Rise in meter for the Year 2060 and 2080 relative to 1986 - 2005

Represented concentration pathways (RCPs)	Year	
	2060	2080
RCP 4.5	0.3	0.42
RCP 8.5	0.36	0.56

5.1.3.4 Approach

In order to test climate change impacts on Marrickville flood predictions, four combinations of rainfall increase and tailwater increase, shown in Table 5-6, are modelled for estimating flood for the 1% AEP design event.

Table 5-7: Climate change scenarios

Combination	RCPs and projected year	% of RF increase	Sea Level rise Cooks River (m)
1	RCP 4.5 (2060)	12	0.3
2	RCP 4.5 (2080)	12	0.42
3	RCP 8.5 (2060)	19	0.36
4	RCP 8.5 (2080)	19	0.56

5.1.3.5 Climate change results

To implement each of the combinations of rainfall and tailwater rise conditions, firstly, the design input rainfall depth (1% AEP) is increased to the target percentage, and the corresponding runoff is generated from the Drains model. Then, simulations using the TUFLOW model are updated with the new runoff, while the tailwater level, a boundary condition in TUFLOW, is increased to the target values. Note that, the change in rainfall from base to climate change scenarios applies uniformly over the MSR. However, elements of topography and landuse might result in different effects in different SA1s. In addition relative vulnerability might change as a result of changes tailwater level which will affect some SA1s more than others.

Contours of peak flood depth, peak velocity, flood duration and provisional flood hazard map due to the more severe climate change scenario (RCP 8.5, 2080) are shown in Figure 5-14, Figure 5-16, Figure 5-18 and Figure 5-20, respectively. In addition, to better visualise the effect of climate change, contours of differences between base condition and climate change scenarios are also shown in these figures. Results for the other climate scenarios were found to differ from RCP 8.5, 2080, in values but not in overall patterns; therefore, for the sake of conciseness, output maps for the other climate change scenarios (RCP4.5-2060, RCP4.5-2080, and RCP8.5-2060) are shown in Appendix B but not in the main text. Finally, a comparison of the percentages of area flooded under different flood indicators due to the base and more severe CC scenario (RCP 8.5 - 2080) is shown in Table 5-8.

Under RCP 8.5, 2080, extent of flooding increases from 17.6% (base condition) to 19.37%. No significant differences are observed between the various RCP's for both the year 2060 and 2080, i.e. the percentages of flooding area are stable at around 19.3% (Table 5-8). Figure 5-15 reveals that an additional area of around 2% of MSR is flooded due to the influence of climate change, mostly in the vicinity of Cooks River and most likely due to the tailwater effect (sea level rise). In comparison to base condition, flooding depth increases by up to 0.2m and mostly within the area where flooding extent has increased (Figure 5-15). In addition, an increase in velocity by 0.2 m/s is seen in some areas (Figure 5-17). Nowhere in MSR is flood depth reduced, but velocity is projected to decline in around 2% of the MSR, under RCP 8.5, 2080.

In comparison to flooding extent, depth and velocity, the increase of flood duration due to the effect of climate change is noticeable. This is mainly due to sea level rise in the Cook River which slows down drainage of runoff water. The maximum flood duration is projected to increase to up to 7 hours, compared to 3 hours under the base condition (Figure 5-18). Even more significantly, more than 10.5% of MSR experiences a flood duration over 3 hours under climate change (see Figure 5-19). This may have significant implications for emergency services, flooding contingency plans and post-flooding recovery, which will be discussed later.

The provisional hazard zone due to the influence of CC reflects the combined change of flood depth and velocity (Figure 5-20). For most of the MSR, there is no change in hazard categories due to CC (Figure 5-21). The additional 2% of area which is flooded due to CC falls in the low-hazard category. The variation of the flooded area under different flood indicators and different provisional hazard zones for different climatic conditions is shown in Table 5-7 and Table 5-8.

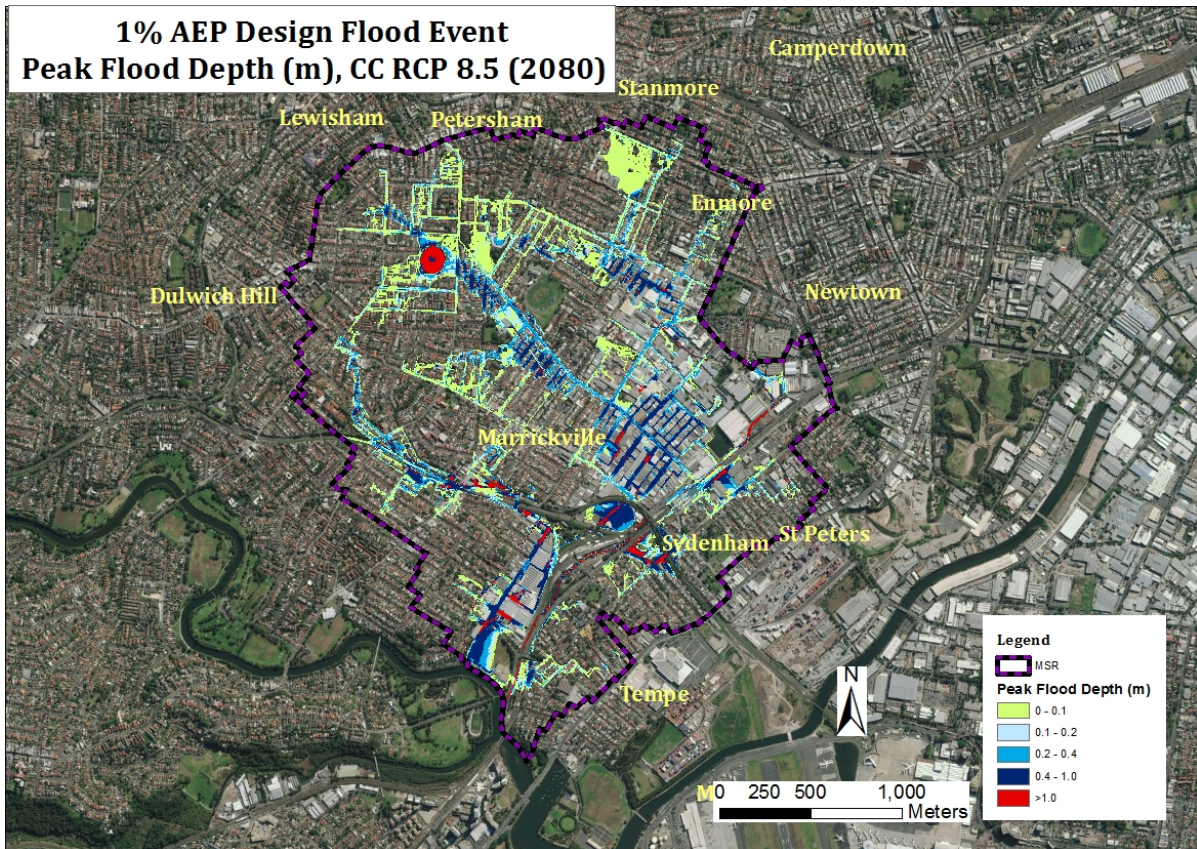


Figure 5-17: 1% AEP design flood event, Climate Change Scenario, RCP 8.5 (2080): Peak flood depth

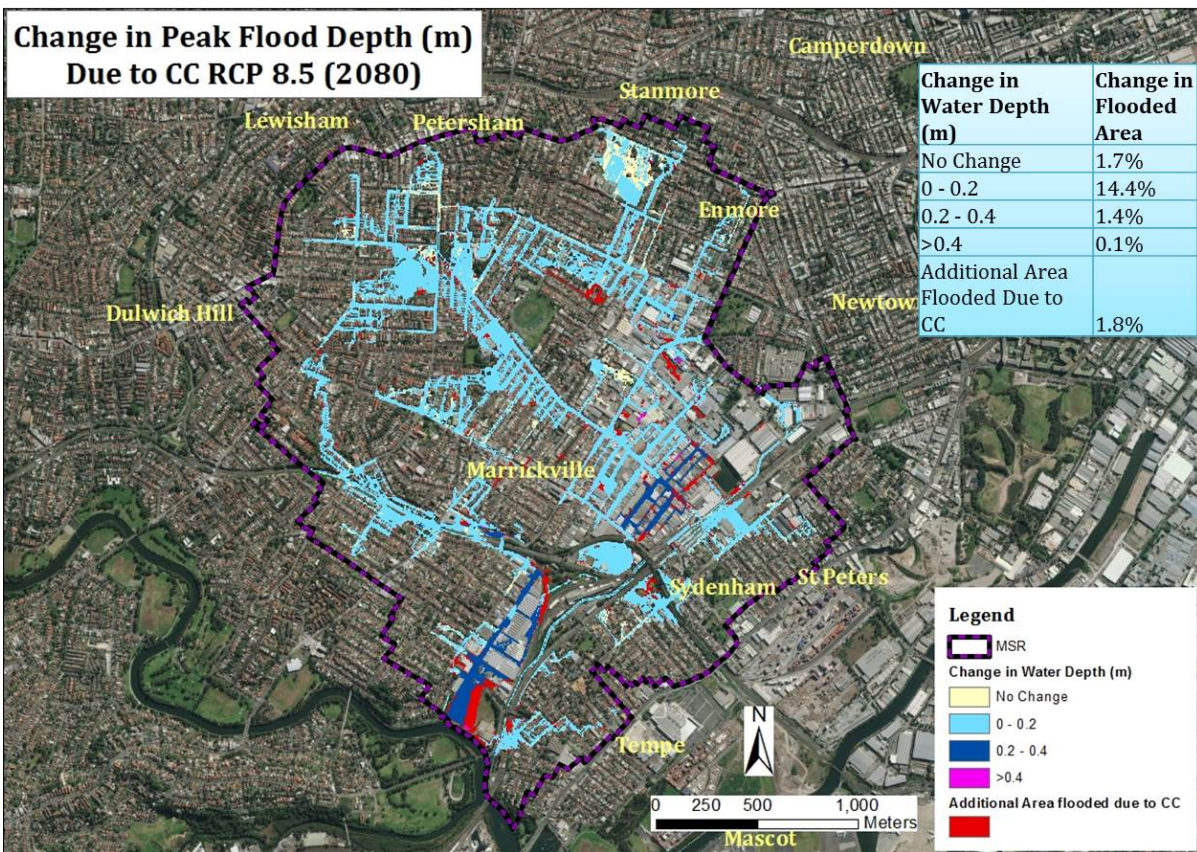


Figure 5-18: Change in flood depth due to CC in comparison to base condition

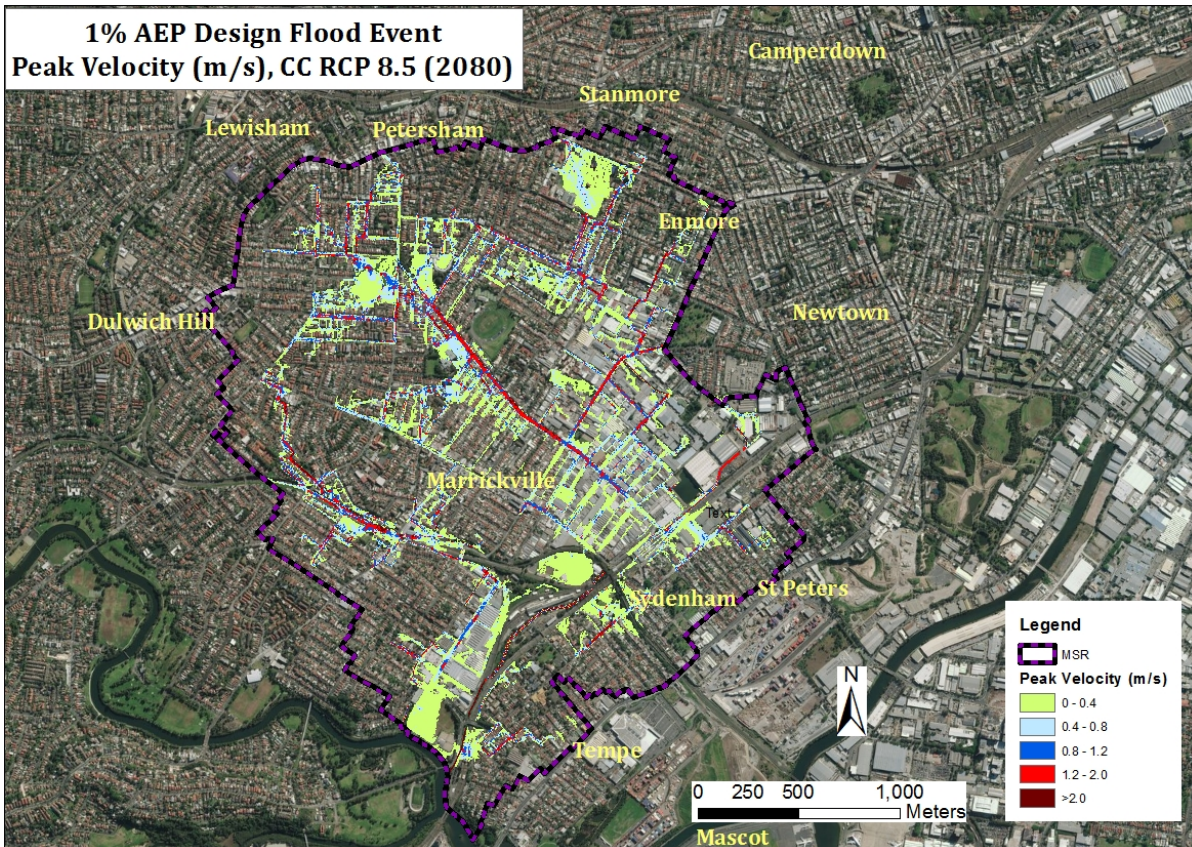


Figure 5-19: 1% AEP design flood event, Climate Change Scenario, RCP 8.5 (2080): Peak velocity vector

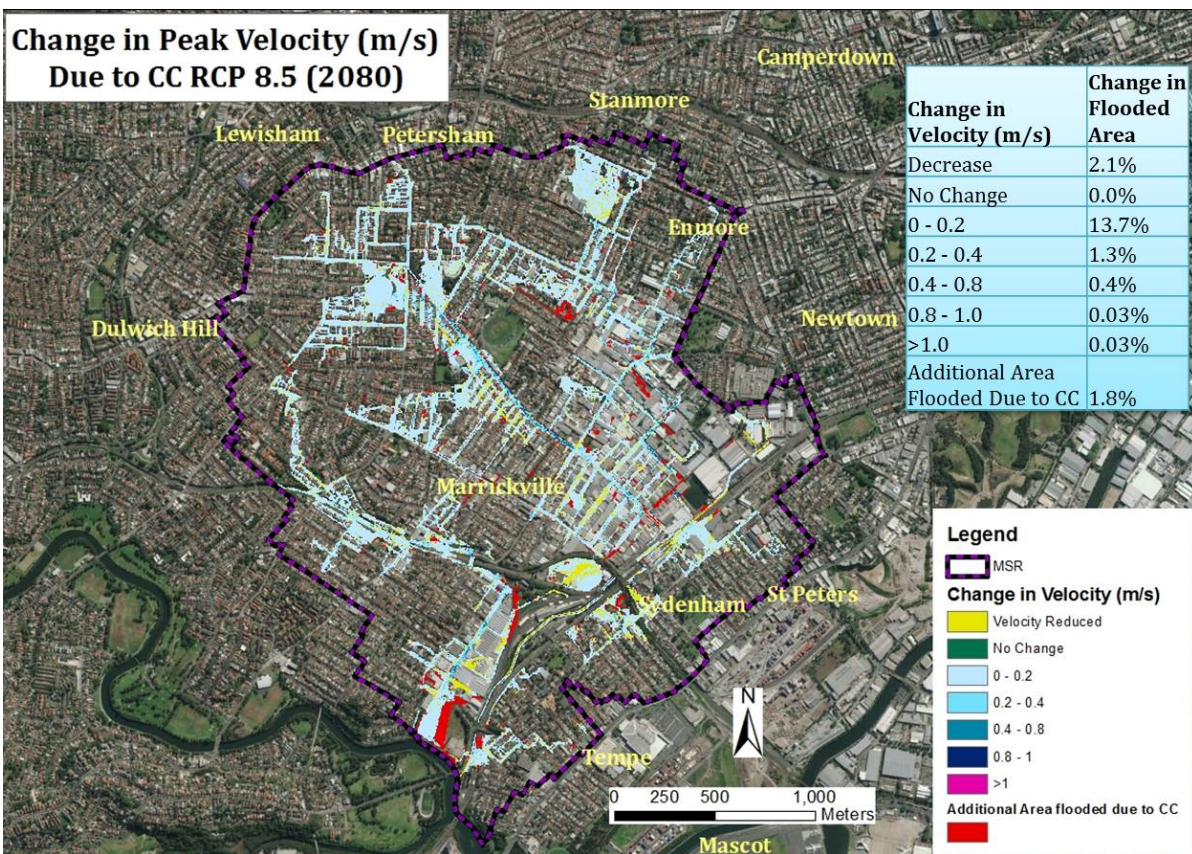


Figure 5-20: Change in flood velocity due to CC in comparison to base condition

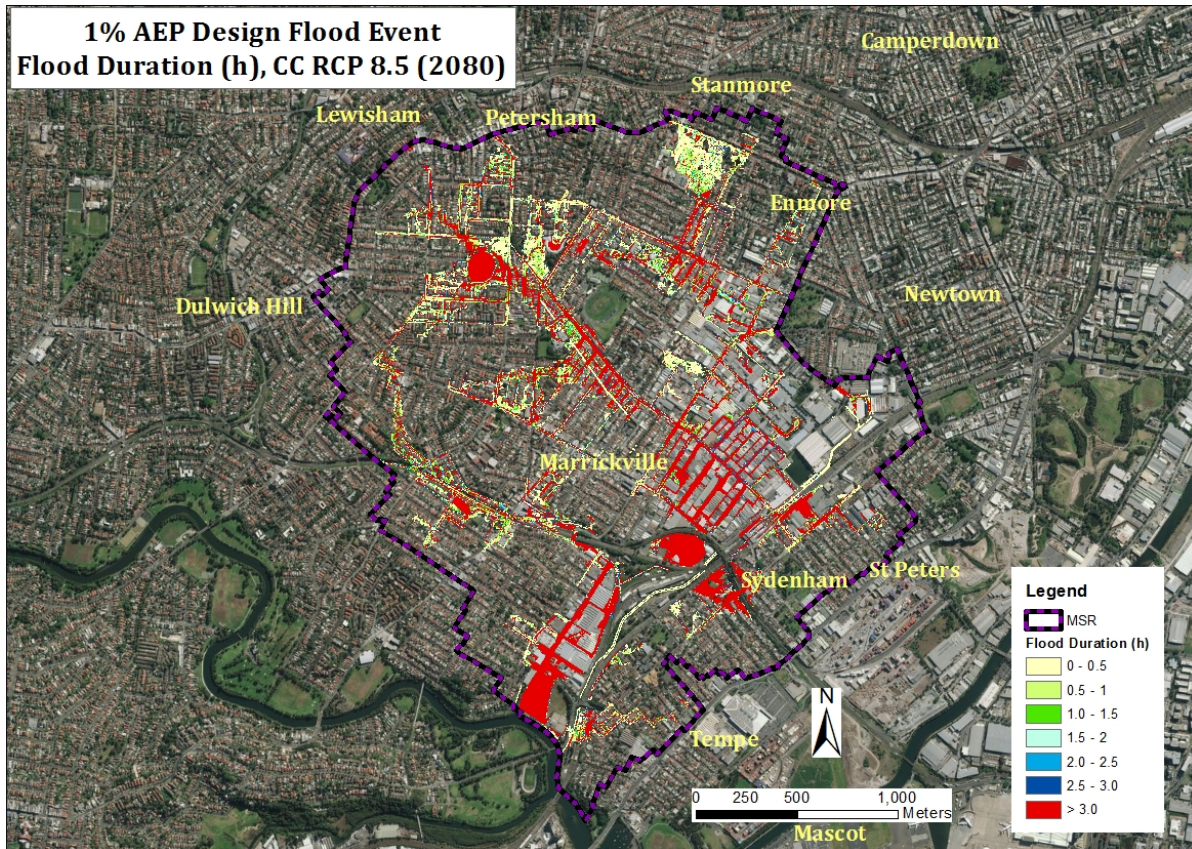


Figure 5-21: 1% AEP design flood event, Climate Change Scenario, RCP 8.5 (2080): Flood Duration

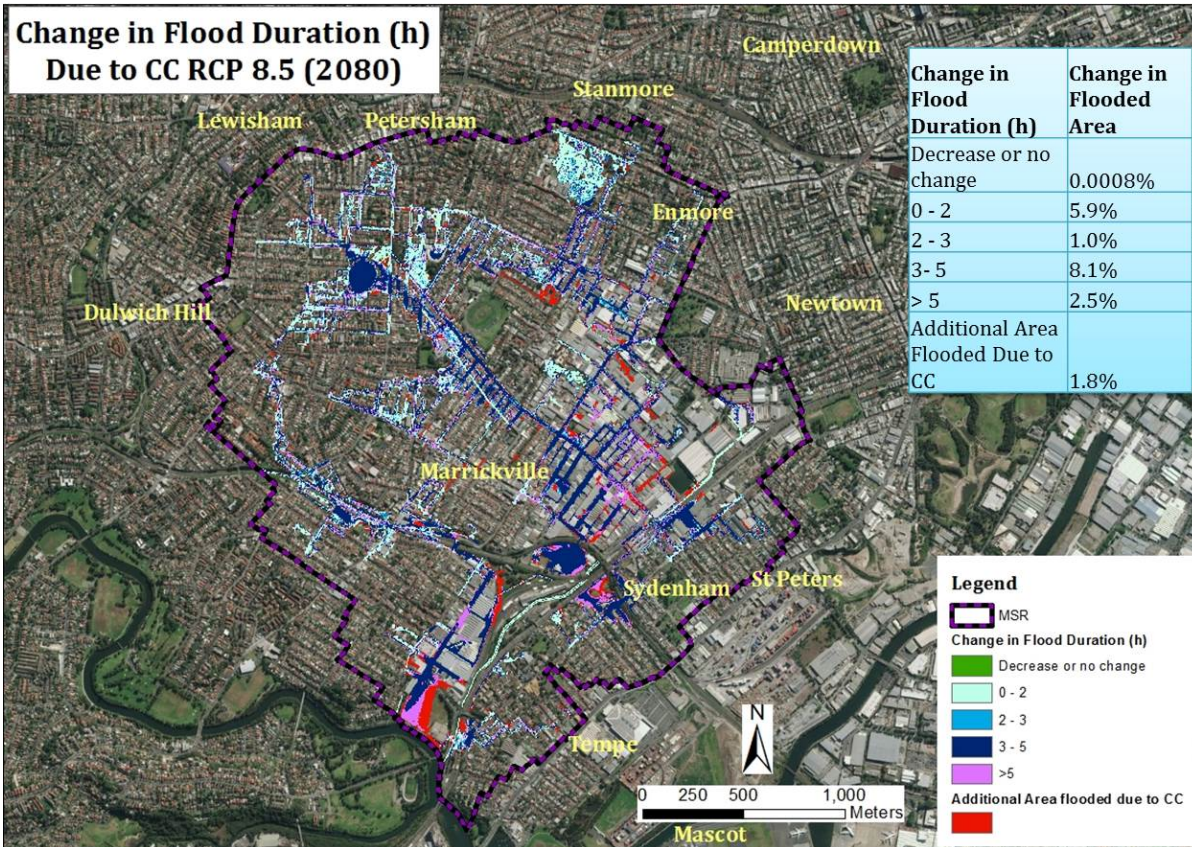


Figure 5-22: Change in flood duration due to CC in comparison to base condition

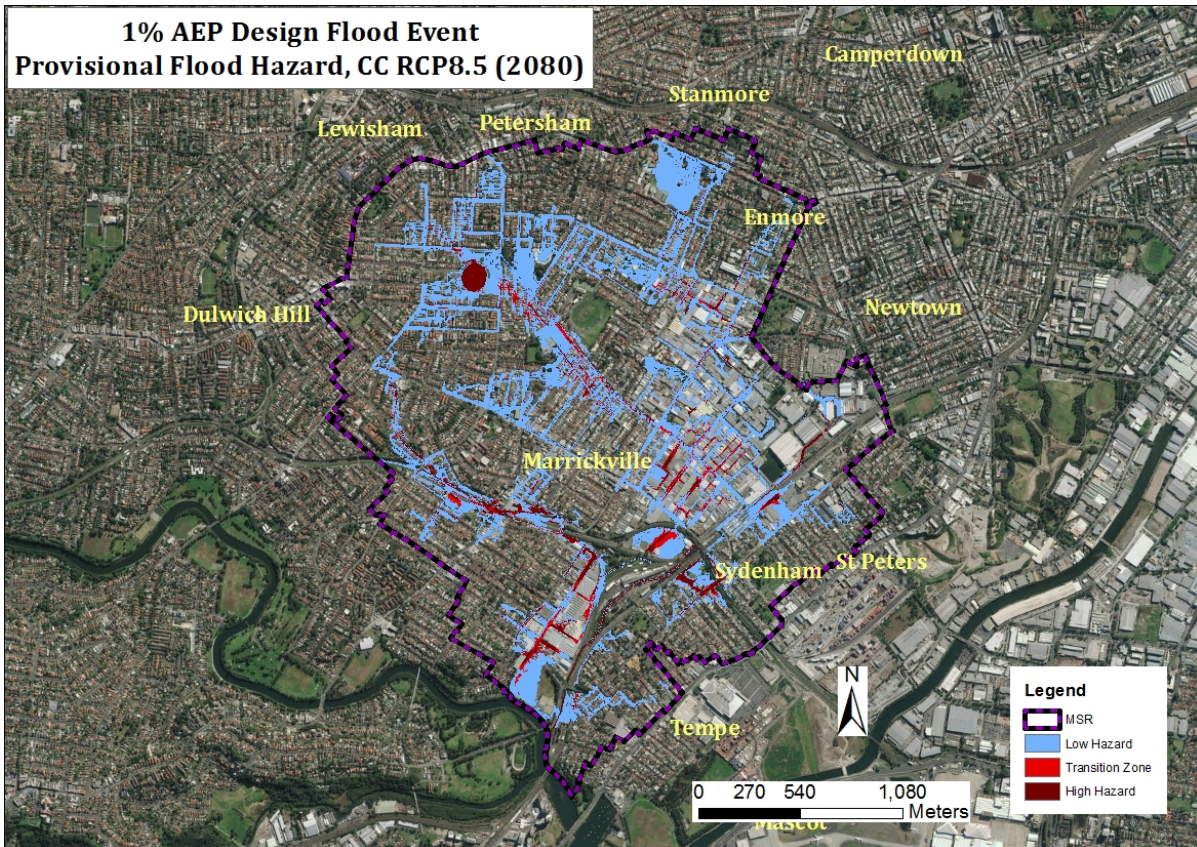


Figure 5-23: 1% AEP design flood event, CC Scenario, RCP8.5 (2080): Provisional Flood Hazard

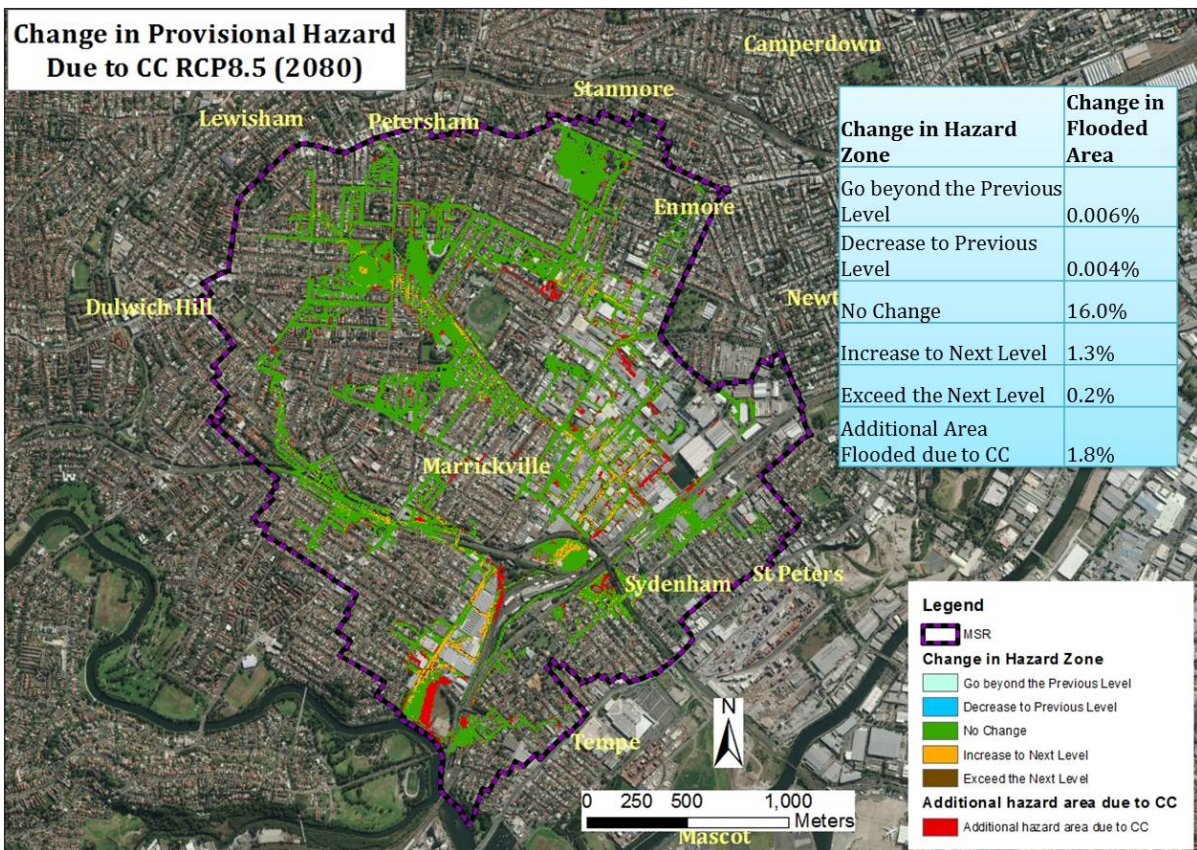


Figure 5-24: Change in provisional flood hazard zone due to CC in comparison to base condition

Table 5-8: Percentage of Area Flooded under Different Flood Indicators due to Base and RCP8.5 (2080)

Area Flooded Under Different Flood Depth Zone			Area Flooded Under Different Velocity Zone			Area Flooded Under different Flood Duration		
Flood Depth (m)	% of Area Flooded		Flood Velocity (m/s)	% of Area Flooded		Flood Duration (h)	% of Area Flooded	
	Base	CC		Base	CC		Base	CC
0 - 0.1	7.3	7.4	0 - 0.4	9.8	10.4	0 - 0.5	3.9	3.9
0.1 - 0.2	3.2	3.2	0.4 - 0.8	4.0	4.5	0.5 - 1	2.5	2.2
0.2 - 0.4	3.6	3.9	0.8 - 1.2	2.0	2.3	1 - 1.5	2.3	1.2
0.4 - 1	2.8	4.0	1.2 - 2.0	1.4	1.8	1.5 - 2	2.2	0.7
>1	0.6	0.9	>2	0.3	0.5	2 - 2.5	2.8	0.5
-	-	-	-	-	-	2.5 - 3	3.8	1.2
-	-	-	-	-	-	> 3	0	9.6

Table 5-9: Percentage of Area Flooded Under Different Flood Hazard Zone due to Base and RCP8.5 (2080)

Scenario	Area Flooded as a % of Total MSR Area	Low Hazard Zone as % of Total MSR Area	Transition and High Hazard Zone as % of Total MSR Area
Base	17.55	15.77 (90)	1.78 (10)
RCP 4.5 (2060)	19.30	16.41 (85)	2.88 (15)
RCP 4.5 (2080)	19.34	16.43 (85)	2.91 (15)
RCP 8.5 (2060)	19.31	16.41 (85)	2.90 (15)
RCP 8.5 (2080)	19.37	16.42 (85)	2.94 (15)

*The value inside the bracket indicates Low/High Hazard Zone as a % of total flooded area

5.1.3.6 Flood Hazard Index

The four flood hazard indicators, described in Section 4.5.3, are extracted from the TUFLOW model results for the base case and the different climate change scenarios. Results for each indicator along with provisional hazard categories for the base and climate change scenarios have already been discussed in Section 5.1.3.2 and Section 5.1.3.5. It is worth mentioning that flood results discussed so far, are based on fine spatial resolution (3-meter grid size). On the other hand, the flood hazard index (F_H) to be built is based on the combined effect of these four indicators, upscaled to the SA1 resolution, by averaging all grid values that fall within a given SA1. MSR includes a total of 84 SA1s, 80 of which are found to be flooded under base and all four climate scenarios. Indicators are then standardised (Equation 3-1) and later aggregated (Equation 3-2) to construct F_H using equal weights. The F_H index is calculated and normalised to a scale between 1 and 10, where 1 represents the lowest vulnerability and 10 the highest. For the presentation of the result, F_H is then further classified into the following five categories by subdividing the index value into five equal intervals.

- i. Very Low
- ii. Low
- iii. Moderate
- iv. High
- v. Very High

Note that the 4 SA1s which are not flooded are automatically allocated to the category of Very Low F_H . The variation of F_H due to 1% AEP design event is shown in Figure 5-23. Among the 84 flooded SA1s, 34 fall into categories of high to very high vulnerability. The outcome is consistent with findings from Section 5.1.3.2. As an example, results from the Marrickville oval which is located within the SA1 identified as number 1 in Figure 5-23 can be compared with the results discussed in Section 5.1.3.2 (Figure 5-8, Figure 5-9 and Figure 5-10). These figures show that in most of the flooded part of this SA1, flood depth is higher than 1 meter, and duration of flood is between 2.5 and 3 hours. These values are close to the maximum values for the base condition. Though the average flood velocity in this SA1 seems low (mainly varies between 0 and 0.4 m/s), this range of velocity exists over approximately 60% of the total flooded area. On the other hand, 49% area of this SA1 is

flooded, a proportion close to the maximum of 56%. The comparatively high magnitudes of the combined effects of these four indicators make this SA1 potentially exposed to significant flooding hazard. A similar reasoning can be applied to SA1s marked as 2 and 3 in Figure 5-23.

F_H due to CC scenario is developed based on the results discussed in Section 5.1.3.5. Unsurprisingly, the F_H 's due to the base and climate change condition are found to be very highly correlated (Figure 5-22). For this reason, only 7 SA1's are identified (marked with a red dot in Figure 5-24) where the hazard increases to the next higher level. This does not necessarily mean that vulnerability of other SA1s hasn't increased, just not severely enough to move to the next hazard category. In fact, Section 5.1.3.5 shows that the magnitude of all four indicators have increased, relative to the base case, to different extents and at different locations of MSR (and not just those seven SA1s). The relative vulnerabilities of the other SA1's are affected by climate change but not to the extent of changing their hazard index relative to the base case. Therefore, while the flood hazard can be a good representation of flood vulnerability of the MSR, it may not be the best proxy for assessing the impacts of CC.

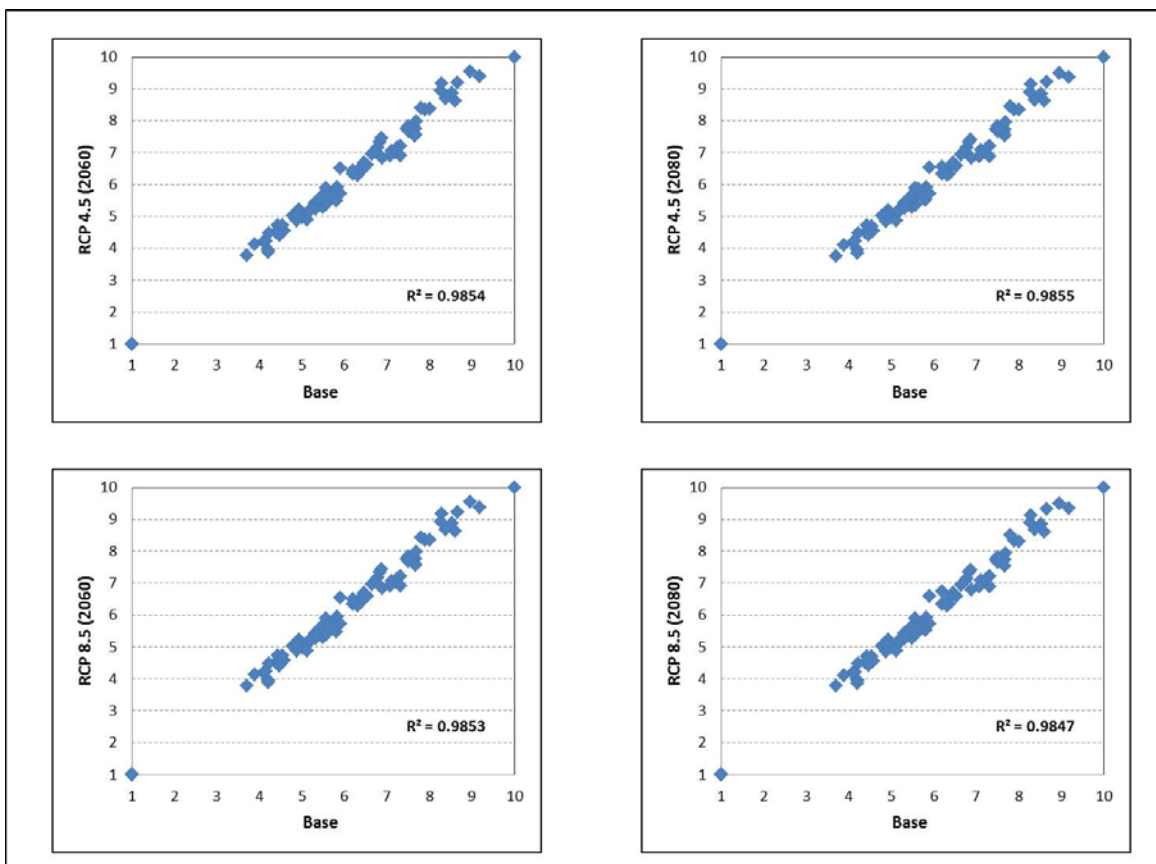


Figure 5-25: Correlation of flood hazard index between base condition Vs different climate change scenarios

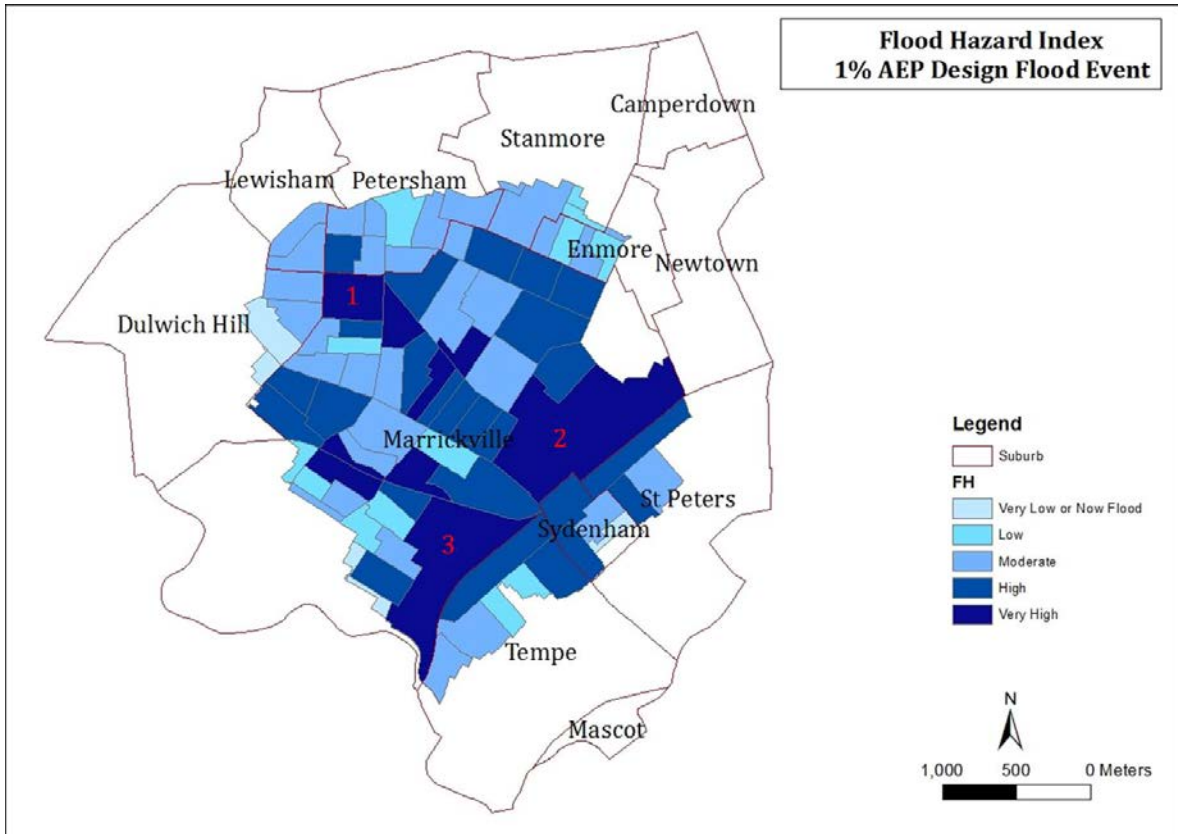


Figure 5-26: Flood Hazard Index: 1% AEP design flood event

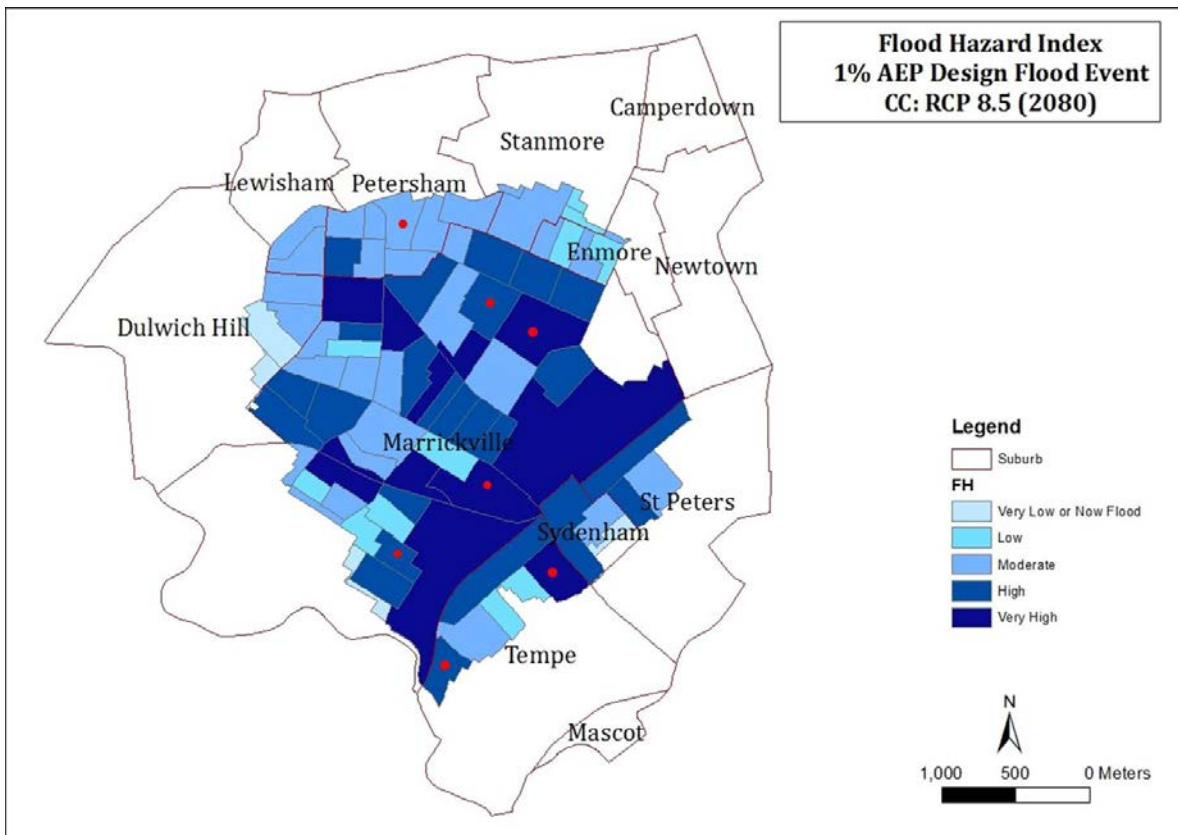


Figure 5-27: Flood Hazard Index: RCP 8.5 (2080)

5.1.3.7 Sector-specific flood hazard index (SF_H)

The MSR is mostly residential, albeit industrial and commercial activities are also present (see Section 4.1.3). The SA1's in the MSR are either single or mixed land use (Figure 4-5). With the methodology presented here, it is possible to analyse the vulnerability to flooding of specific land uses. This can provide sector-specific flooding information to local authorities. To illustrate this, the following two sectors specific flood hazard (SF_H) indices are determined:

- i. Residential flood hazard index (RF_H)
- ii. Industrial flood hazard index (IF_H)

The analyses are conducted by considering flood hazard indicators within a given land use type. For any area other than residential or industrial area, the value of the indicators is set to zero. The difference between the F_H and SF_H (RF_H or IF_H) is that the SF_H only shows the variation of vulnerability due to flood hazard within a specific land use type. The SA1 labelled as 1 (Figure 5-23) falls into the Very High hazard zone, while in the case of RF_H (Figure 5-25), this area falls into High hazard zone. A large portion of this particular SA1 contains a green area (Marrickville oval) that is highly flooded due to 1% AEP; however this area does not affect the construction of RF_H because it is not residential.

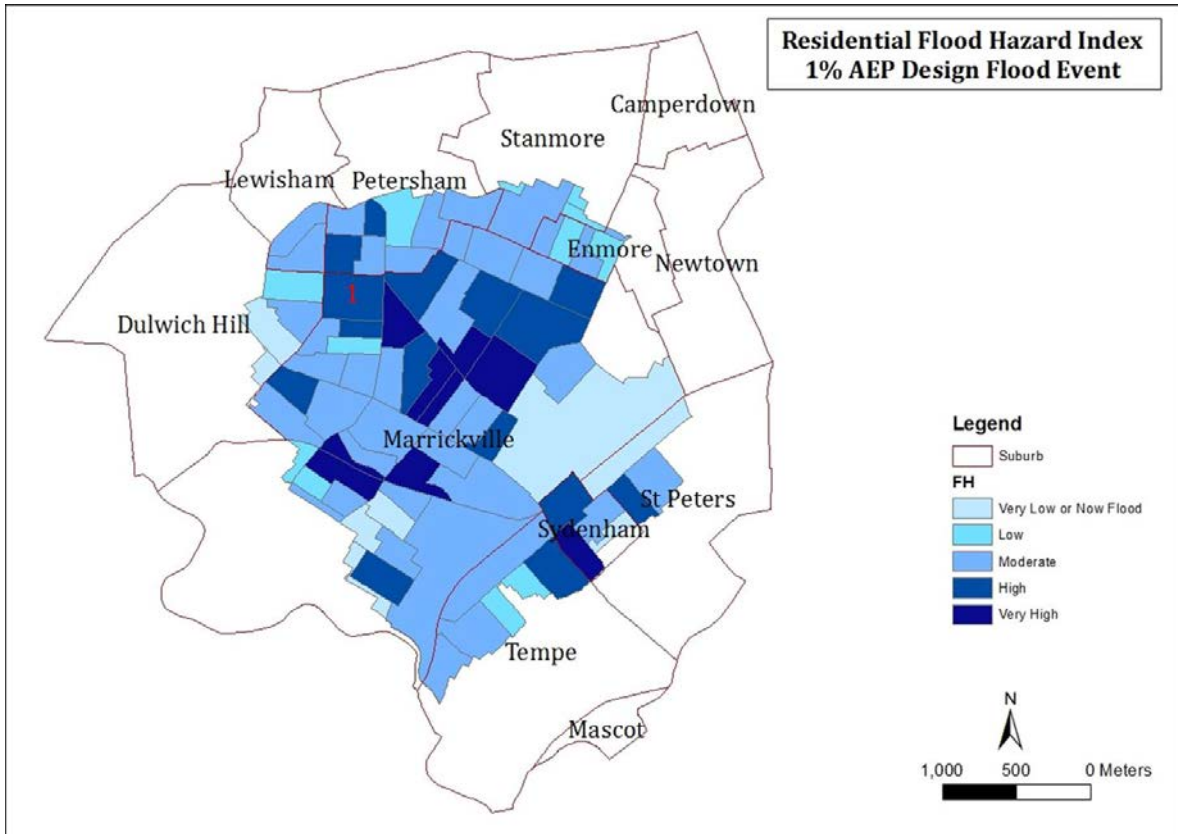


Figure 5-28: Residential flood hazard index for 1% AEP design event

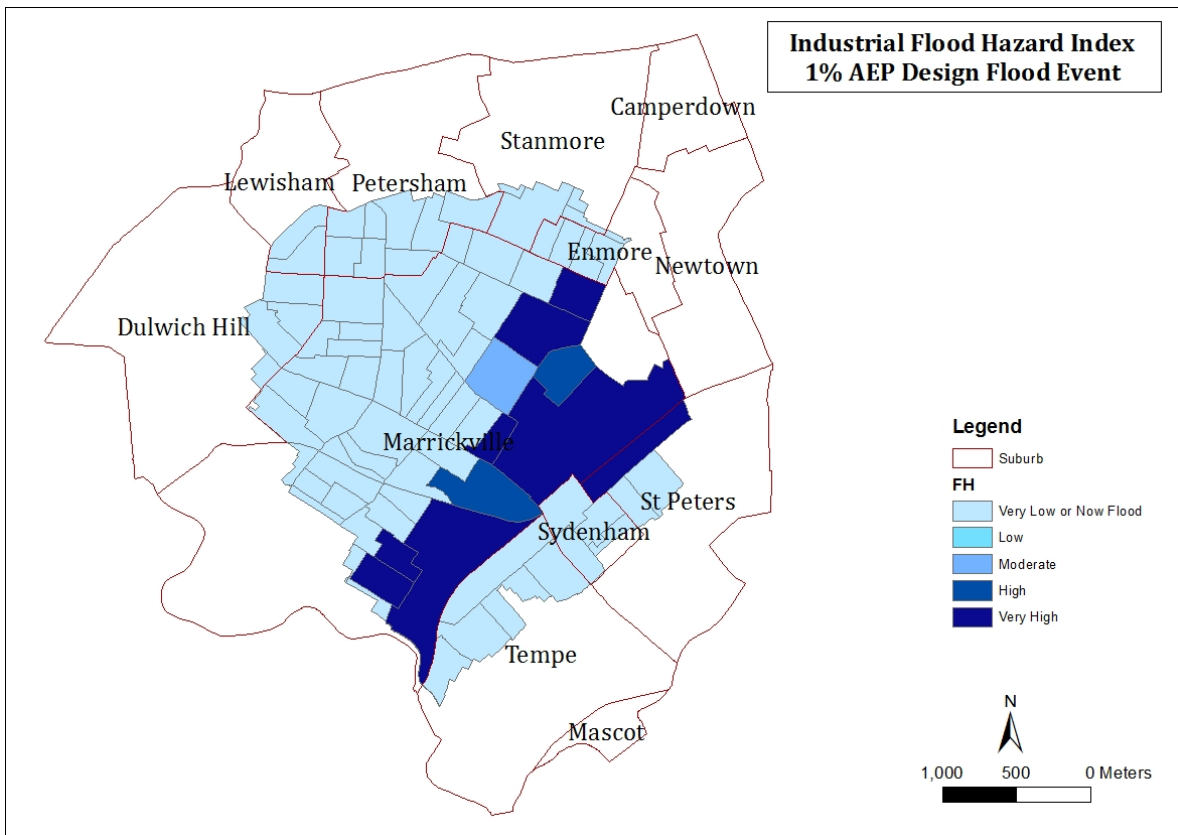


Figure 5-29: Industrial flood hazard index for 1% AEP design event

5.1.4 Flood Social Vulnerability Index (FSVI)

No correlations were found between SoVI, F_E and F_H (Figure 5-27). Hence, constructing FSVI by combining the three indices can provide useful information. FSVI is constructed using multiplicative and additive aggregation for the different scenarios outlined in Table 4-4 (see Figure 5-28 and Figure 5-29).

Only the SA1's with high indices value are magnified in multiplicative aggregation as High/Very High FSVI category, i.e. if any of the three indices have a low score then the FSVI becomes low/very low. That is why the percentages of high and very high categories of FSVI are much lower in this approach than those obtained using additive aggregation (see Figure 5-30). Considering all combinations of weights, with additive aggregation, the percentage of high/very high categories of FSVI varies from 15 to 27 percent, whereas with multiplicative aggregation, the range varies from 0.5 to 7 percent (Figure 5-31).

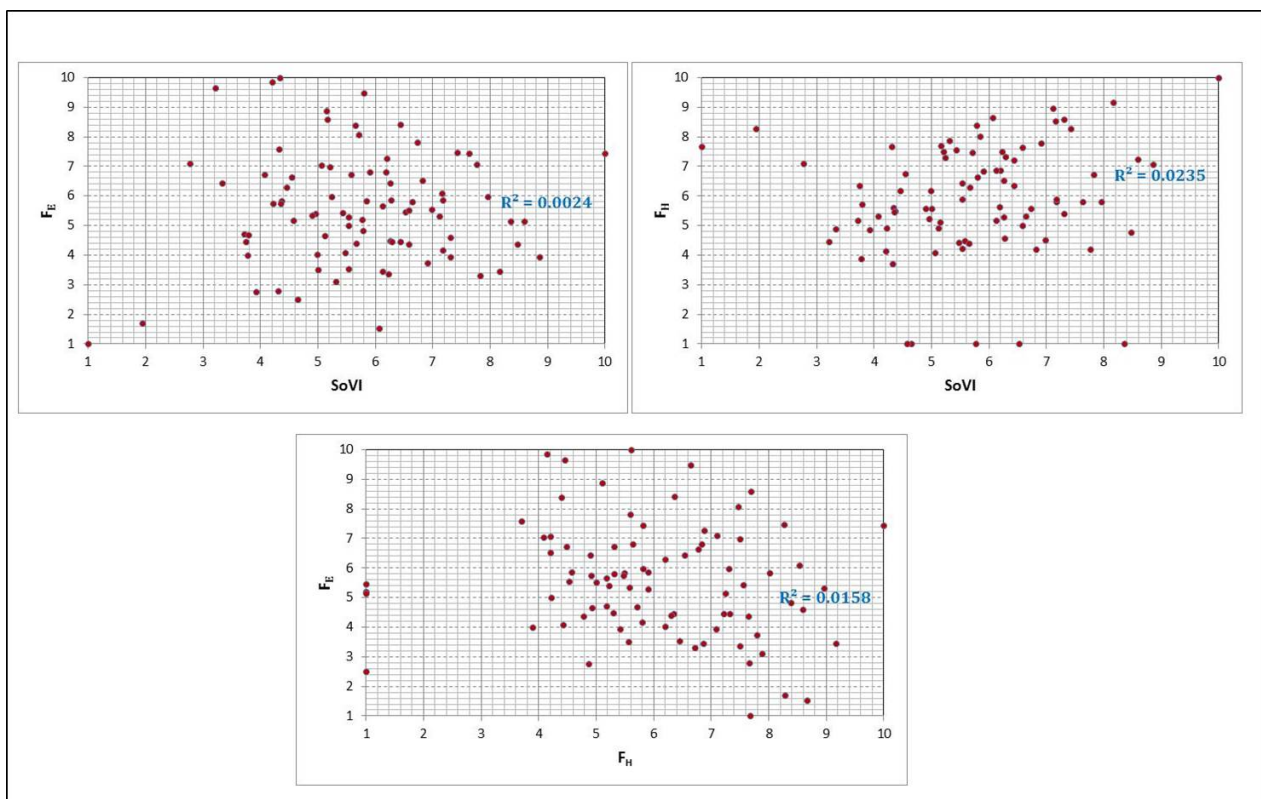


Figure 5-30: Correlation between different indices

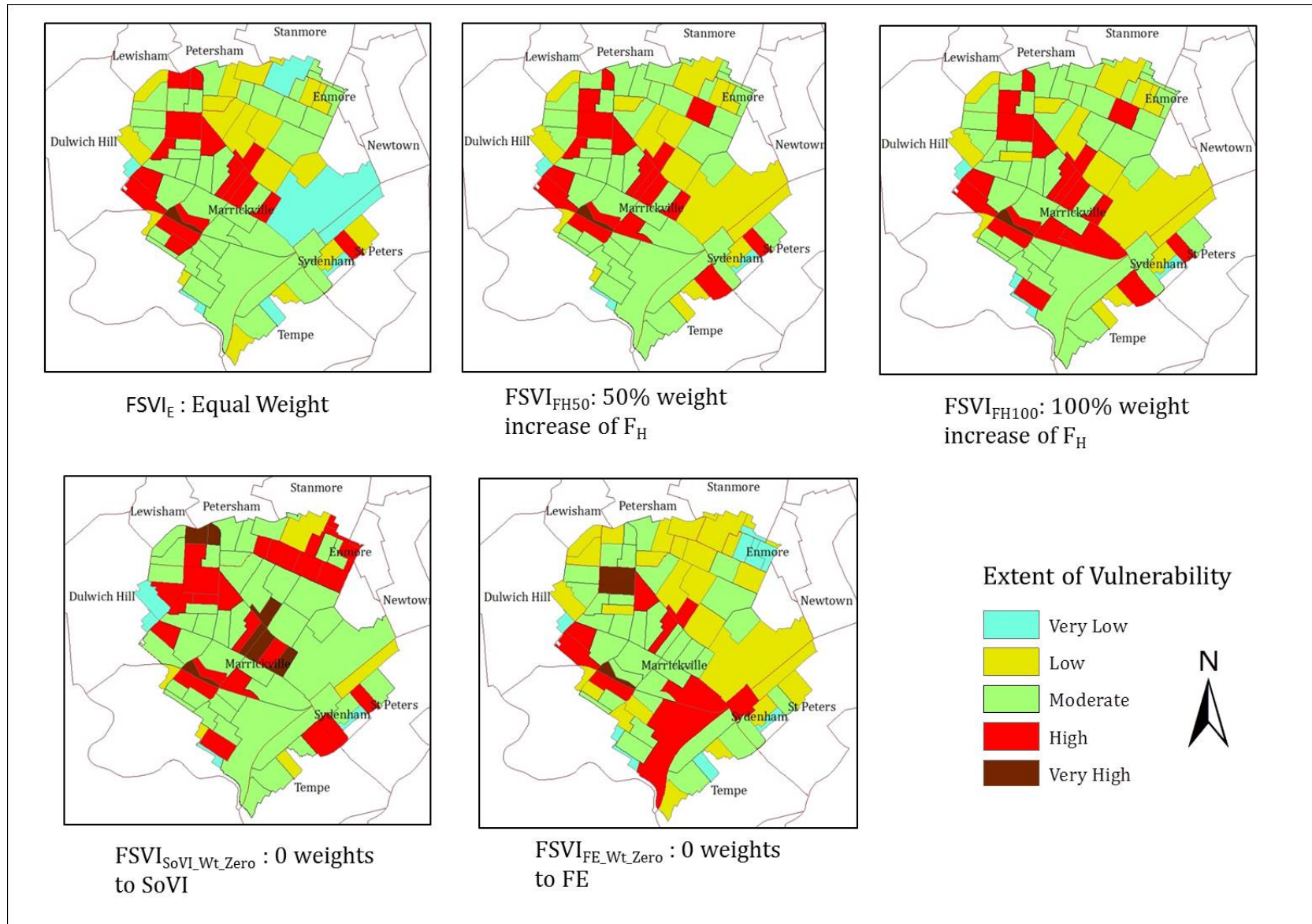


Figure 5-31: Flood Social Vulnerability Index for different weight combination: additive aggregation

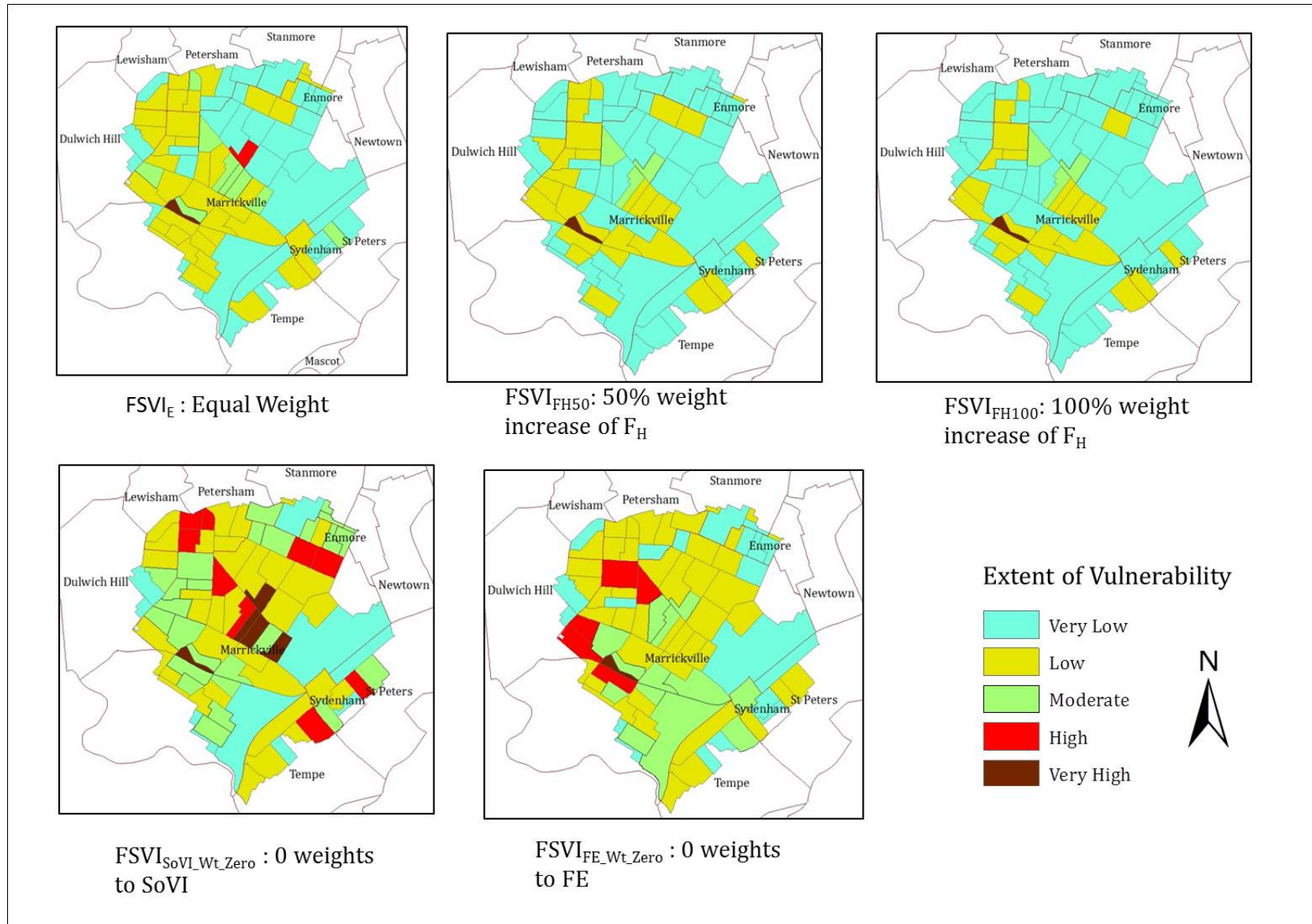


Figure 5-32: Flood Social Vulnerability Index for different weight combination: multiplicative aggregation

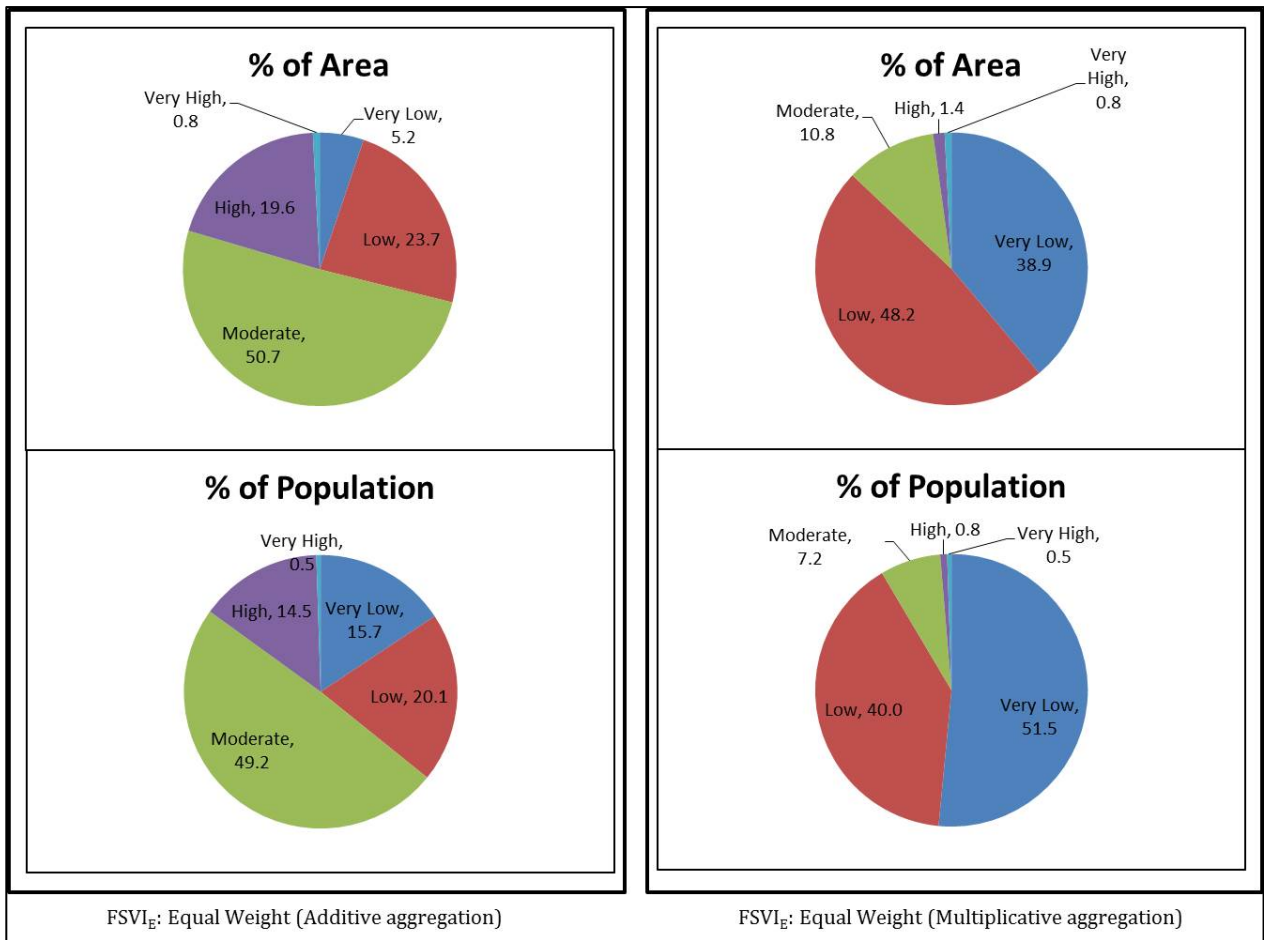


Figure 5-33: Percentage of area and population exposed under each categories of F_H

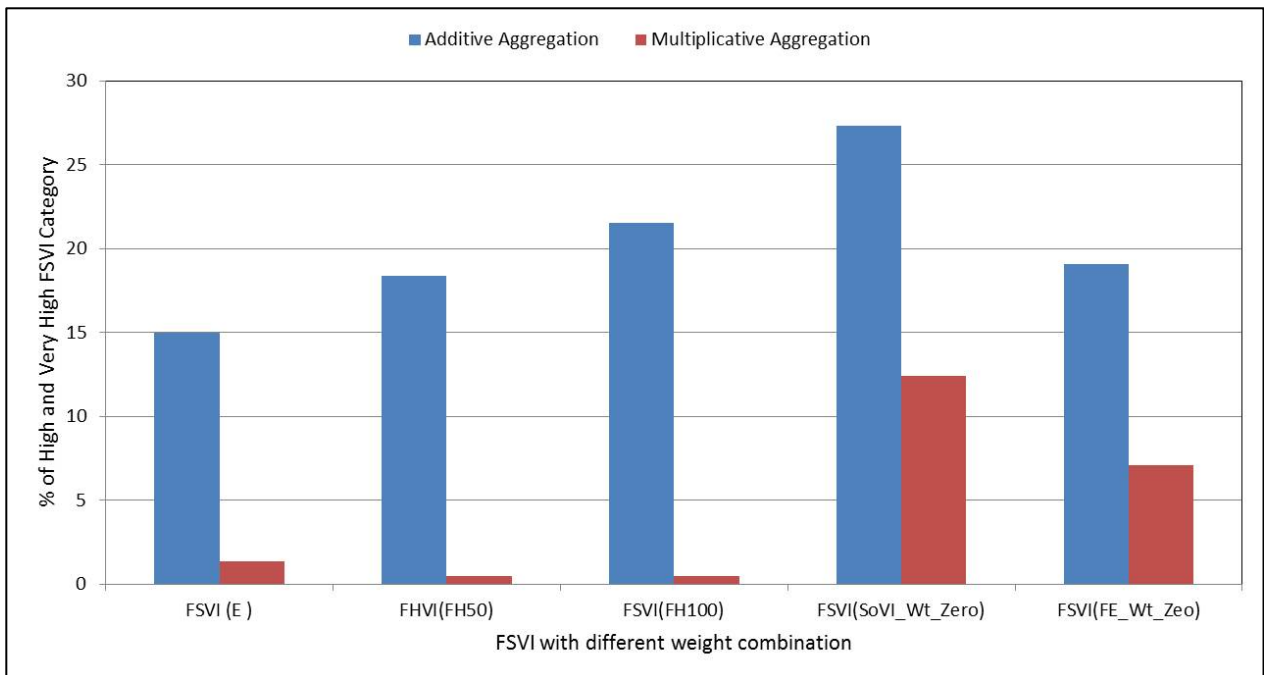


Figure 5-34: percentage of high/very high categories of FSVI with different weight combination

To gain an understanding of the reasons behind the vulnerability classification obtained, four SA1's (A₁, A₂, A₃ and A₄ shown in Figure 5-32) with different FSVI categories (low, medium, high and very high, respectively) are selected from the results (additive aggregation with equal weights) to check how different indices contribute to the FSVI. The individual indicator/component score producing of F_H, F_E and SoVI are shown in Table 5-9. All selected SA1s have High or Very High F_H, indicating physical susceptibility to flooding. A₁ has high population density, and high buildings density, a relatively large proportion of which is old building stock. This leads to a high value of F_E. The area also has relatively high scores for the components of social vulnerability. High/Very High index values of every component leads to a Very High value of FSVI for A₁. A₂ is also highly physically susceptible to flooding, but in A₂, the densities of population, buildings and old buildings are comparatively low and SoVI is one level lower. That is why the FSVI of the SA1 becomes one level lower than A₁. On the other hand, area A₃ is located in a largely industrial zone with no old buildings, and only a small proportion of residential properties. This leads to low F_E and SoVI and, therefore, despite high F_H, low overall vulnerability FSVI. Among the four SA1s, the vulnerability level of A₄ is moderate, with high social vulnerability but low exposure index.

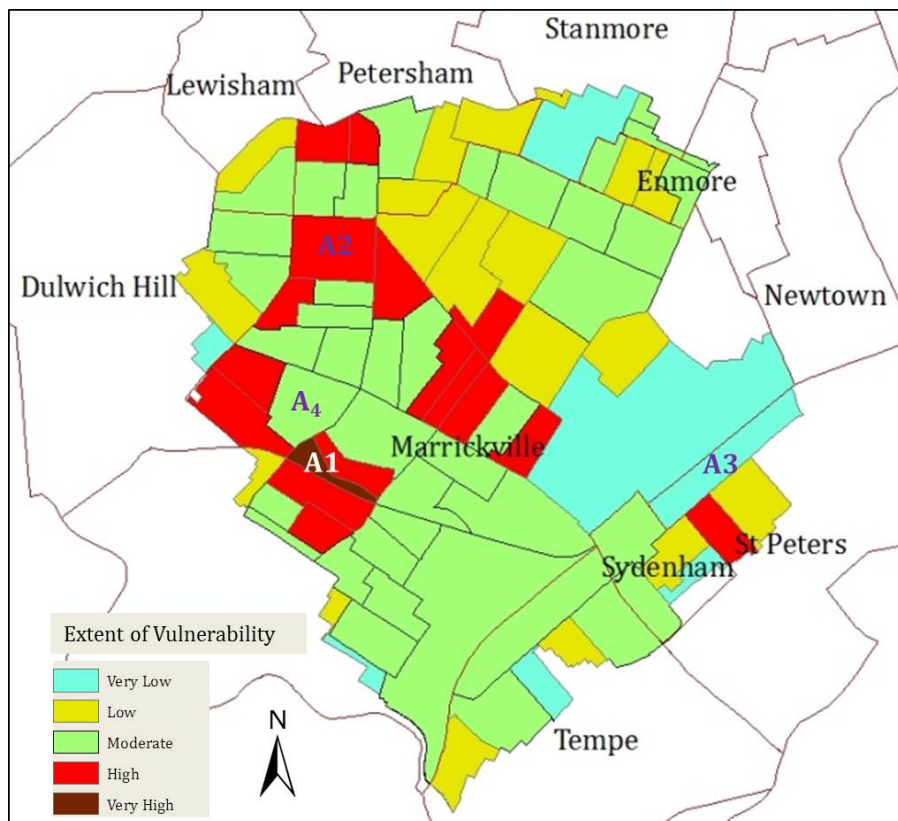


Figure 5-35: FSVI_E: Equal Weight (additive aggregation) with four selected SA1s

Table 5-10: Comparison of indicators/component score between four selected SA1s

Indices	FSVI Category Indicators	A ₁ (Residential)		A ₂ (Residential & parkland)		A ₃ (Industrial)		A ₄ (Residential)	
		VH		H		L		M	
Flood Hazard Index	Mean Flood Depth (m)	0.31	VH	0.37	VH	0.35	H	0.12	H
	% of Flooded Area	0.56		0.49		0.16		0.04	
	Flood Duration (h)	1.53		1.62		1.99		1.51	
	Flood Velocity (m/s)	0.78		0.45		0.38		1.10	
Flood Exposure Index	Population density/sq km	7954	H	3395	L	57	VL	5149	L
	Building density/sq km	1525		1039		97		1418	
	Old building density/sq km	449		64		0		73	
Social Vulnerability Index (major indicators under each component*)	C1 (DWL_5, DWL_2FAM, DWL_1PPL)	5.8	VH	6.9	H	1.0	VL	7.6	H
	C2 (NON_CIT, HH_INCNIL, REC_MIG)	9.0		4.1		1.5		4.0	
	C3 (HH_LRNT, FAM_SPAR, FAM_UNEMP)	8.9		6.2		4.6		5.4	
	C4 (PPL_AGE, MED_AGE, CHLD_AGE)	5.0		6.8		3.4		4.7	
	C5 (EDU_YR11, EDU_CERT)	8.9		8.2		1.0		5.6	

*The full explanation of indicators are given at Table 4-2

5.2 Feedback from Inner-West Council

This research project has been done in collaboration with the Inner-West Council where the Marrickville Study Region (MSR) is located. At the beginning of the project, a meeting was conducted at the Council's Office to discuss the project brief (27th July 2016). The Council provided a set off data required for the simulation of flood model. After a first round of analyses were completed, another meeting was organised (24th August 2017) at the Council's Office attended by, in addition to the researchers (the author and his supervisor, Abbas El-Zein), the following Council staff:

1. Coordinator of Asset Planning
2. Development and Planning Engineer
3. Engineering Design and Planning Engineer

The researchers presented the project's objectives, methodology and outcomes followed by extensive discussions and responses by stakeholders. Feedback from the meeting was used to refine the analyses and findings. The meeting lasted approximately 90 minutes. A summary of the feedback received from Council's stakeholders is as follows:

- The council staff saw a good potential for the findings of the research project to inform existing Council's flood management process. The study findings were considered especially useful for the flood emergency response services. In particular, combining geophysical, built-environment and social vulnerability provide information not usually available to emergency services and help them develop better contingency plans.
- The Flood Hazard Index (F_H) was constructed using flood depth, areal extent and flood duration. Council staff advised that the incorporation of flood velocity in F_H is important. Note that the inclusion of velocity is in agreement with the methodology used to develop flood hazard zoning maps in the New South Wales Flood Plain Manual of Australia. The F_H was hence modified accordingly. (Only the final F_H , i.e., including velocity, has been presented in the thesis.)
- One of the limitations of the social vulnerability index, noted by stakeholders, is that it is based on household survey data by the Australian Bureau of Statistics, which does not capture the vulnerability of employees of workplaces located in Marrickville. Different kind of data will would be required to develop a map of

workplace vulnerability, including, amongst others, number of employees, firms assets and resources, and the adequacy of emergency procedures in place at the firms. This was beyond the scope of this thesis.

- Following a discussion between researchers and stakeholders, it was agreed that no particular weighting scheme can be identified for the constructing the FSVI. Hence, it was deemed that using equal weight for all indicators is a sound approach, provided the qualitative nature of the exercise is kept in mind when interpreting the results. On the other hand, stakeholders were interested in finding out how vulnerability varies within MSR when flood hazard is integrated either with social vulnerability or the exposure, but not both. In addition, the effect of allocating higher relative weight to hazard index was of interest. This is why FSVI is also constructed with different weight combinations (see Table 4-4).

5.3 Discussion

Planning for urban flooding has been traditionally based on geophysical assessment of flooding patterns at city scale (Muis et al., 2015; Jongman et al., 2015; Wu et al., 2002). However, the literature on vulnerability and environmental risk emphasises that impacts of extreme weather events are experienced differently by different segments of the population, depending on socio-economic and institutional factors (Jongman et al., 2015; Cutter et al., 2013; Zahran et al., 2008). Several attempts at combining socio-economic and geophysical elements of flooding have been attempted in the literature (Garbutt et al., 2015; Tavares et al., 2015; Koks et al., 2015), including construction of composite indices (Connor and Hiroki, 2005; Zachos et al., 2016; Balica et al., 2009). However, very few attempts have been made at building such indices at local scale, i.e., using fine-scaled municipal data and aiming to compare units within one municipality rather than between different municipalities. Hence, the modalities and usefulness of such an exercise remains an open question.

This thesis has proposed a new flooding index termed as Flood Social Vulnerability Index (FSVI) based on a combination of hydrological modelling, built-environment and socio-economic indicators, at the lowest statistical unit available. It was hypothesised that the index is particularly suitable for application at local scale in ways that may assist local government in developing adaptation measures. The index was applied to the Marrickville

Study Region (MSR), in Sydney's inner west. The thesis aimed to answer three research questions:

1. Does an index combining geophysical and socio-economic elements of flood risk provide useful information on vulnerable groups, over and above that found in more conventional flood studies?
2. How does the spatial pattern of flooding in the Marrickville valley change under various scenarios of climate change and what kind of adaptation measures are most likely to reduce vulnerability to flooding under climate change?
3. How likely are vulnerability assessments, such as the one conducted here, to contribute to municipal planning for flooding?

These questions will now be discussed based on findings from the project.

5.3.1 Usefulness of Combined Indices

The three components of the combined index proposed in this research were found to be poorly correlated when applied to the Marrickville Study Region (MSR), hence lending support to the hypothesis that such an index may yield additional information, not provided by its individual components. The possibility of a strong correlation between the three components arises from the fact that the economically and/or politically disenfranchised often occupy environmentally marginal land and are hence more exposed to the impacts of pollution and extreme weather events (Adger, 2006; Hewitt, 1983). However, this is not always the case, as Cutter et al. (2000) argued that the most vulnerable places from the biophysical viewpoint do not always overlap with the most vulnerable populations. In the case of MSR studied here, no consistent pattern relating the three components of risk was found, with some areas of MSR identified as susceptible to flooding scoring low social vulnerability, while other socially-vulnerable areas were found to be at low risk of flooding.

The study results identified that the FSVI exhibit significant spatial variation within MSR especially in relation to its hazard and social vulnerability components. This is aligned with previous research on social vulnerability which is often used as a tool for the mitigation of floods (e.g. Cutter et al., 2003; Holand et al., 2011; Tavares et al., 2015; Koks et al., 2015).

Flood studies conducted by local government in Australia typically develop geophysical flood models to estimate flood characteristics (extent, depth, velocity) and convert them into estimates of potential flood damage in monetary terms (e.g. Cornelius, 2012; GRAY,

2011; Reid et al., 2014). This information is then used to determine flood mitigation options through cost-benefit analyses in which hard protection measures such as levee banks, improved stormwater management systems are favoured. The findings of this thesis suggest that more effective flood adaptation measures may be achieved, compared to those typically generated by the current approaches, which often preclude consideration of social vulnerability and built-environment characteristics from flood mitigation decision making.

Combining information about the physical characteristics of flood with local-scale data on social vulnerability and built environment allow flood mitigation efforts to be targeted at the most vulnerable segments of the population (Cutter et al., 2003) and brings to the portfolio of flood adaptation actions a set of targeted, non-infrastructure measures that are often low-cost. Examples include increasing flood awareness amongst migrants, new residents and/or those with low levels of education and minor retrofitting to waterproof old buildings (Koks et al., 2015).

The data can further be used by emergency services to predict the recovery capacity of various localities and flood evacuation plans can hence be tailored and prioritised, targeting those with low mobility and low access to resources. Cutter et al. (2003) suggested that resource prioritisation for flood mitigation may be vulnerable to politics of vested interests. Data, such as those developed in this thesis, can help in providing an objective basis to discussions between stakeholders attempting to develop collective action on flooding. This was, indeed, confirmed by Council stakeholders feedback as stated earlier.

5.3.2 Vulnerability to Flooding under Climate Change in Marrickville

While identifying flood vulnerability under climate change, two different greenhouse gas emission scenarios (low and high emission scenario RCP4.5 & RCP8.5) for the years 2060 and 2080 were used to predict future physical characteristics of floods in MSR. On the other hand, any future projections of demographic and socioeconomic changes in MSR, were bound to suffer from a high level of uncertainty. Therefore, the aim of the thesis was to predict the effects of climate change on vulnerability to flooding in MSR, under current socio-economic, demographic and built-environment conditions. One drawback of this approach is that urban expansion, which has been identified as an important driver of future flood risk in a number of climate change studies, is not taken into account here (Zhu et al., 2007; Muis et al., 2015). Note that the approach adopted here has been followed in

several other studies in the literature wherein future flood risk is predicted without considering urban expansion (e.g. Zhou, 2014; Berggren et al., 2011; Ashley et al., 2005; Schreider et al., 2000).

Two sources of change, under each climate change scenario, were injected in the analysis: a) change in rainfall which can affect water flow in MSR and b) change in sea levels which can affect the run-off during floods. Note that the change in rainfall as a result of climate change is applied uniformly across MSR, a limitation of the spatial resolution of global circulation models. As a result, the flood hazard index F_H under climate change scenarios was found to be highly spatially correlated to its values under base conditions.

Flood duration is a significant aspect of floods, also considered as a critical factor in determining the expected level of damage of properties. The longer the flood duration, the higher the damage (Soetanto and Proverbs, 2004; Kelman and Spence, 2004). In coastal areas, long-term inundation may also occur due to the sea level rise (Poulter and Halpin, 2008). During the last few decades, the average annual flood duration along the U.S. East Coast has been increasing due to sea level rise (Ezer and Atkinson, 2014). In this research, flood simulations incorporating climate change scenarios showed a noticeable increase in the duration of the floods, but only limited change in other flood hazard indicators such as flood depth and velocity (see Table 5-7). The increase in flood duration is due to sea level rise which slows down discharges by urban drainage system of MSR into the Cooks River. Longer flood durations can lead to higher dependency on emergency services, higher costs of emergency and longer recovery times for the community. Another implication of this finding is that, if the bottleneck to drainage occurs downstream, increasing the drainage capacity through infrastructural change plan may not address the problem and resources may be better directed at improvement of flood warning and better access to flood-affected communities. This is clearly an open question which deserves more research. Significantly, the NSW Flood Plain Manual (FPM) categorises flood hazards based on flood depth and velocity, but not flood duration. This was reflected in the analyses conducted here when, under both base and climate change conditions, the MSR was categorised as low-flood-hazard area (85% of the total flooded area low hazard due to CC which was 90% under base condition), despite the increase in flood duration under climate change. The findings in this season suggests that there may be a case for revising this categorisation in order to include flood duration.

5.3.3 Vulnerability Assessment in Policy Making

The purpose of vulnerability assessments is to inform decision-makers, raise awareness of impacts of climate change and monitor adaptation policy (Schröter et al., 2005; Patt et al., 2012). Most of the vulnerability research are conducted at regional or national level (Tonmoy et al., 2014). The indicator-based flood social vulnerability assessment was conducted in this study at a local scale. However, a question remains as whether, and how, such studies can lead into local government policy for flood mitigation? Though this new methodology of vulnerability assessment was found to be useful by council stakeholders (see Section 5.2), the potential of this tool as part of an adaptation policy for local government is still an open question. This is because conversion of scientific information to policy and accomplishment is a not an easy task. According to Wolf et al. (2011), “a lack of correspondence between vulnerability theory and action indicates weak links between analyses and decision making”. In some cases local councils are liable for building and executing policy but these are constrained by the regulatory environments at regional and national levels (Eisenack et al., 2014). However, globally policy interest in vulnerability assessment has increased and implementation of climate change impacts as an adaptation policy has become a priority for many city and regions (Tonmoy et al., 2018; Carmin et al., 2012; Measham et al., 2011; Füssel, 2007; Adger et al., 2005; Adger et al., 2003). The state of New South Wales (NSW) in Australia requires councils to develop their own sea level rise planning and to adopt their own place specific sea level rise projections. For example, the Shoalhaven City Council requires every development application to consider flood risk including flooding projections under climate change (Council, 2014).

The NSW Flood Plain Manual (FPM) recommends that any flood mitigation measure consider in addition to cost-benefit criteria, considerations of social feasibility and impacts. However, significantly, no mention is made specifically of socio-economically differentiated impacts and vulnerabilities. This manual is prepared to assist the local government in formulating flood management plans through the flood risk management process. The first step of this process is to formulate a Floodplain Risk Management Committee whose objective is to assist the Council in the development and implementation of a flood plain risk management plan. For example, there is a Flood Management Advisory Committee (FMAC) exists for Inner West local government area (MSR is located within this local government area). As far as the Inner West Council are concerned as stated earlier,

consulted stakeholders believed that the vulnerability assessments conducted here can be useful for flood planning in Marrickville Study Region. A key actor in developing policy at the Council is FMAC which helps develop and implement flood risk management plans. This is a discussion forum which includes technical, social, economic and environmental matters and whose recommendations are usually adopted by the council. Hence, the adoption and dissemination of the study's findings by this committee would be the most effective route by which the study may have an impact in actual flood policy. Whether such an adoption will take place in the future remains to be seen.

5.3.4 Future Research

Calibration and Validation of Flood Model

There is further scope for validating results obtained from this research. Currently, no historical water level or flow data are available for the study area. As a result, the flood model that has been received from the Council is calibrated based on available information such as expert knowledge amongst council Engineers on flooding, previous studies and community questionnaires. The model would hence benefit from more rigorous based on detailed water level or flood data.

Assisting in Development of Finer Scale Flood Mitigation Policies

Qualitative research at a household level within the highly vulnerable parts of the study areas can be conducted in order to develop a better understanding of how residents experienced previous flood events. This would help in qualitatively validating the vulnerability maps developed in this research. It would also help identify needs of, and adaptation strategies developed by, residents, hence informing adaptation policy. On the other hand, the methodology proposed here can be extended to develop a Social Vulnerability Index for the workplace, taking into account patterns of vulnerability specific to workplace environments.

Assessing Impacts of Changing Socioeconomic Profile and Ageing Built Environment of FSV

Socioeconomic profile (e.g. increasing ageing population) and built environment conditions (e.g. older houses and infrastructure systems) are expected to change in the future. Further research exploring the impacts of these changing conditions on FSV can be beneficial. It could assist policymakers in better allocating resources for infrastructure development and maintenance projects.

A. Appendix A

Table A-1

Component	Factor Loading for each component before rotation				
	1	2	3	4	5
Number of houses with weekly rent over the median household rent within the study region	-.808	-.106	-.245	.096	.019
Number of non-citizens	-.765	.435	-.263	.031	.047
Number of dwelling owned outright or being purchased	.746	-.098	-.252	-.443	-.047
Number of couple families with more than 2 dependent children	.682	.179	-.151	.185	.112
Number of recent migrants (previous 8 months)	-.640	.274	-.229	-.095	.236
Number of dwellings occupied by 5 individuals or more	.622	.450	-.198	.126	.069
Number of people whose highest level of education is Certificate Level (Certificate 1, 2, 3 or 4)	.598	-.287	.107	-.013	.304
Number of people with low speaking proficiency in English	.082	.829	.045	.096	-.186
Number of people with weekly negative or nil income	-.135	.707	-.376	-.258	.124
Number of unemployed families	-.152	.601	.270	.182	.117
Number of people who never went to school	.312	.569	.147	.169	-.329
Number of household with 2 or more families	.476	.527	-.184	.034	-.075
Number of households with negative or nil income	-.451	.475	-.230	-.163	.238
Number of houses with weekly rent below \$150	-.032	.251	.821	.050	.056
Number of dwellings occupied by single individuals	-.514	-.173	.650	-.014	.046
Number of dwellings owned with mortgage	.463	-.343	-.500	.256	.082
Number of children below 5 years of age	.390	.000	-.144	.642	-.089
Number of people over 65 years of age	.479	.013	.436	-.553	-.138
Number of people between 35 and 39 years	-.413	-.470	-.097	.515	-.160
Number of single-parent families with children under 15	.167	.356	.429	.475	.097
Number of people whose highest level of education is year 11	.325	-.039	.172	.126	.731

Table A-2

Indicators	Factor Loading for each component after rotation				
	1	2	3	4	5
Number of dwellings occupied by 5 individuals or more	.773	-.073	-.016	-.066	.206
Number of household with 2 or more families	.726	.027	.024	-.128	.009
Number of dwellings occupied by single individuals	-.655	.008	.533	-.035	-.057
Number of people with low speaking proficiency in English	.630	.317	.427	-.088	-.231
Number of couple families with more than 2 dependent children	.623	-.277	-.092	.007	.305
Number of people who never went to school	.605	-.074	.377	-.057	-.250
Number of non-citizens	-.118	.843	.108	.211	-.257
Number of households with negative or nil income	.034	.747	.051	-.064	-.004
Number of recent migrants (previous 8 months)	-.205	.743	.010	.079	-.034
Number of people with weekly negative or nil income	.430	.706	-.043	-.228	-.058
Number of houses with weekly rent over the median household rent within the study region	-.491	.542	-.098	.372	-.227
Number of houses with weekly rent below \$150	-.110	-.136	.812	-.218	.071
Number of single-parent families with children under 15	.290	-.118	.633	.209	.178
Number of unemployed families	.236	.340	.575	.020	.029
Number of dwellings owned with mortgage	.267	-.319	-.562	.316	.255
Number of dwelling owned outright or being purchased	.407	-.381	-.500	-.500	.137
Number of people over 65 years of age	.082	-.415	.126	-.741	-.012
Number of people between 35 and 39 years	-.418	-.100	-.080	.685	-.177
Number of children below 5 years of age	.436	-.334	.010	.531	.096
Number of people whose highest level of education is year 11	.057	-.077	.125	-.022	.814
Number of people whose highest level of education is Certificate Level (Certificate 1, 2, 3 or 4)	.116	-.483	-.132	-.144	.508

B. Appendix B

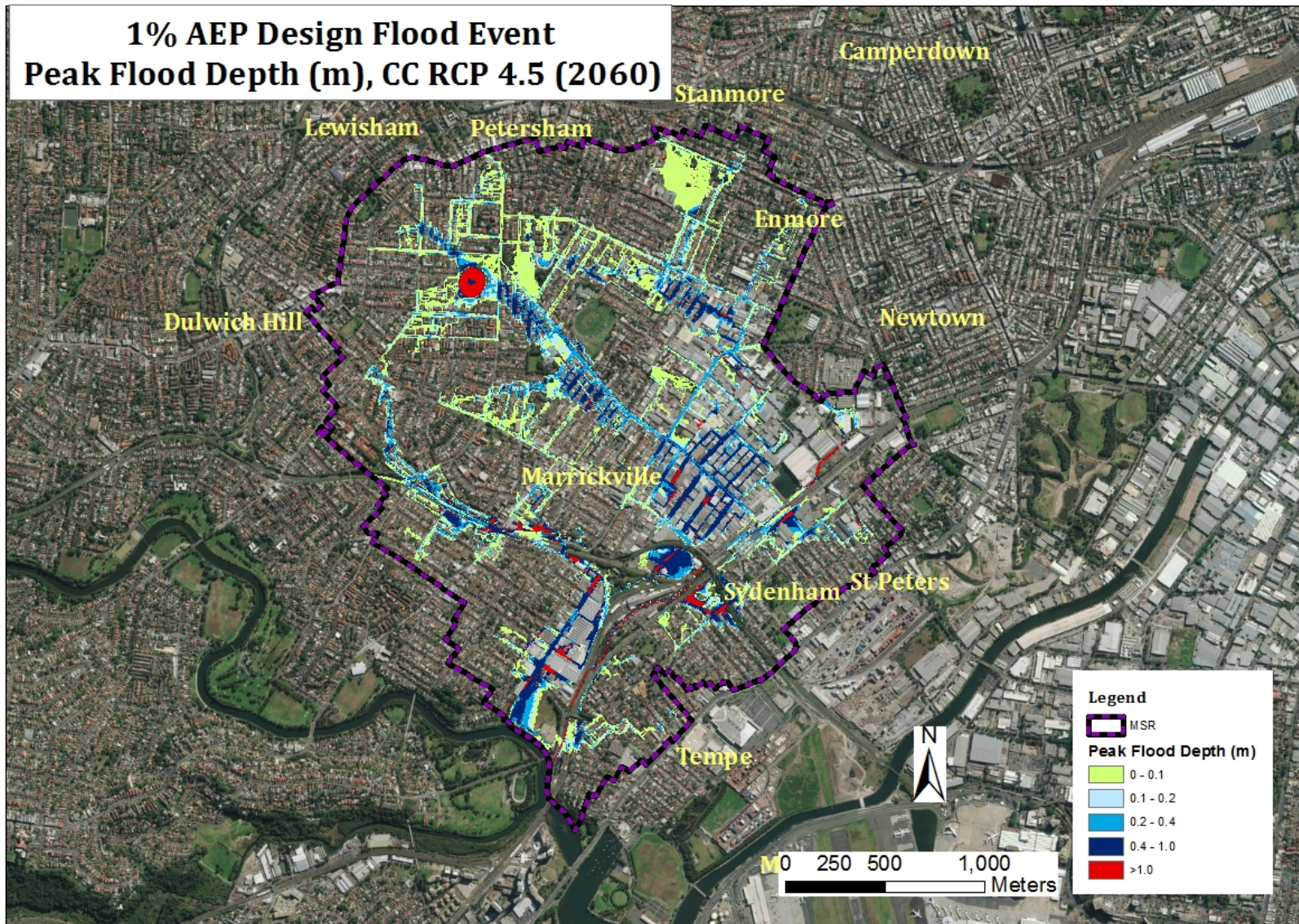


Figure B-1: 1% AEP design flood event, Climate Change Scenario, RCP 4.5 (2060): Peak flood depth

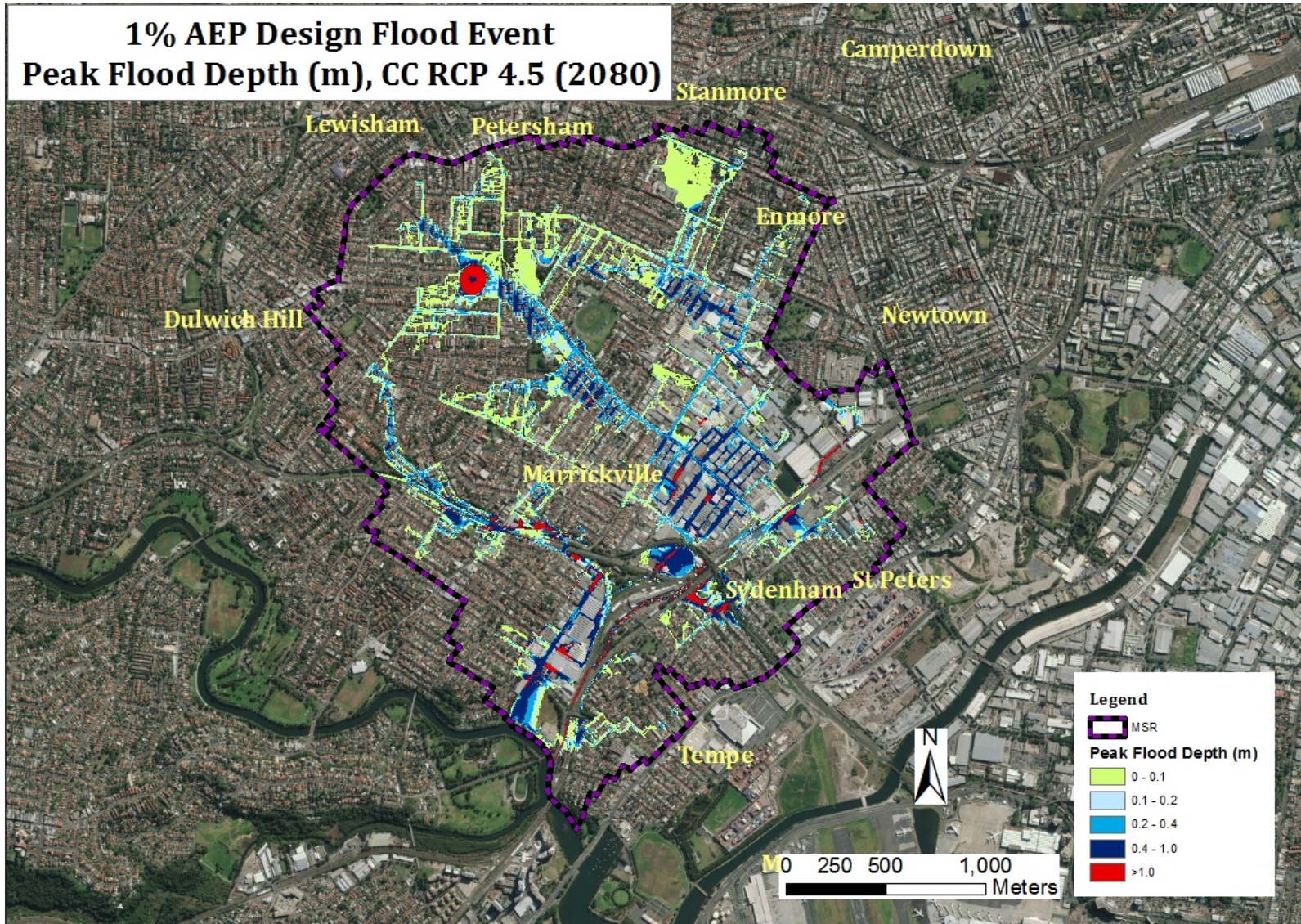


Figure B-2: 1% AEP design flood event, Climate Change Scenario, RCP 4.5 (2080): Peak flood depth

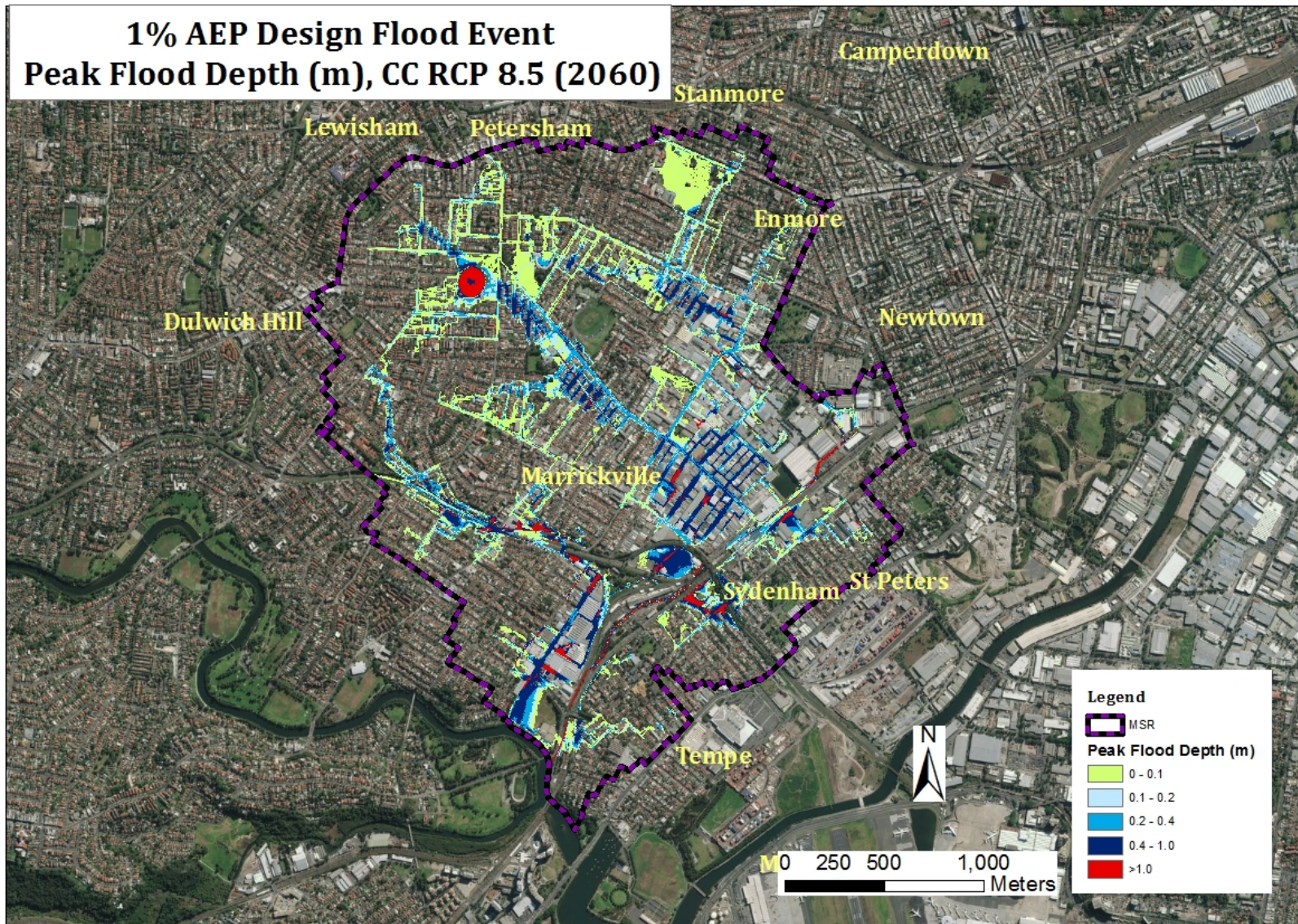


Figure B-3: 1% AEP design flood event, Climate Change Scenario, RCP 8.5 (2060): Peak flood depth

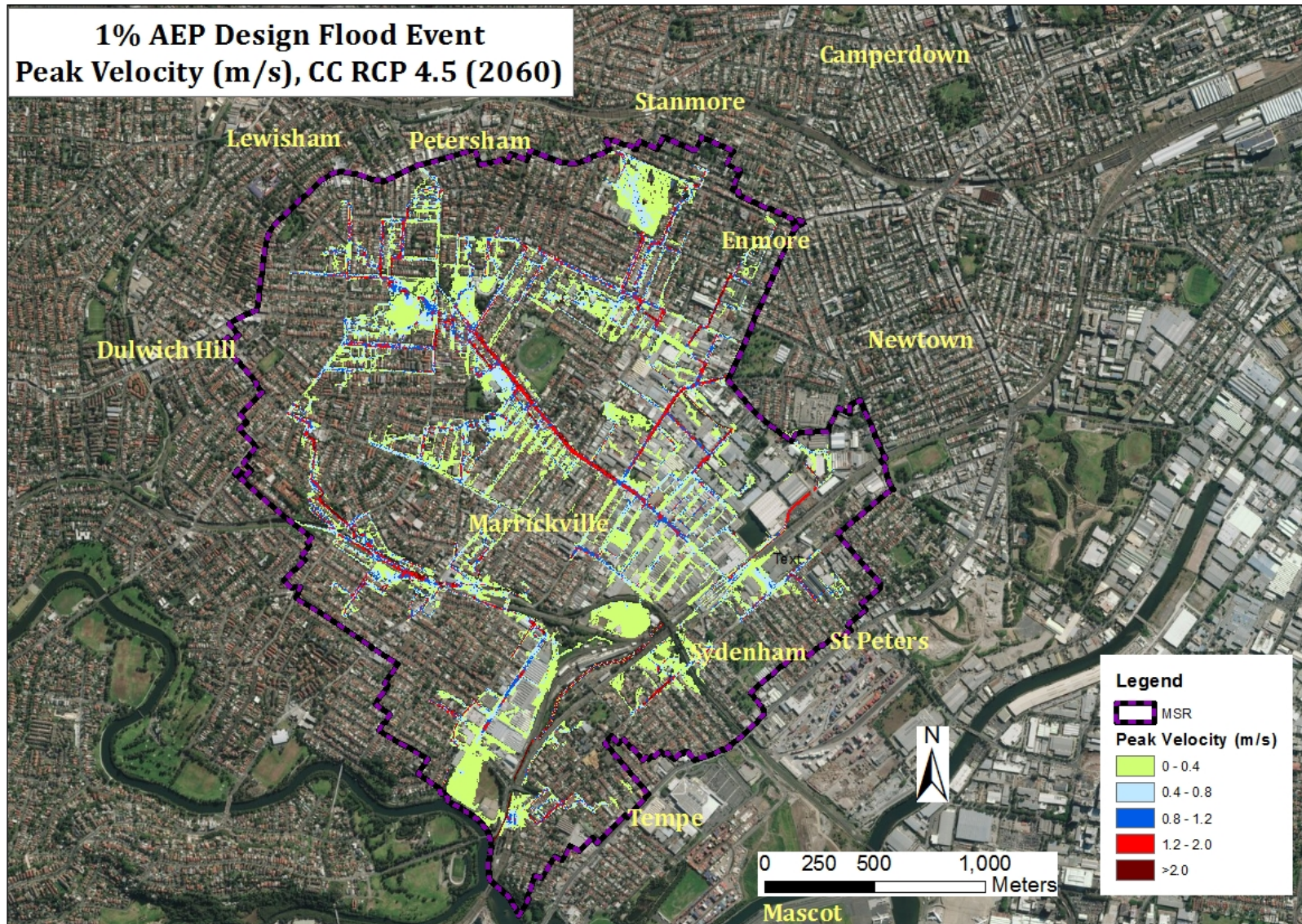


Figure B-4: 1% AEP design flood event, Climate Change Scenario, RCP 4.5 (2060): Peak velocity vector

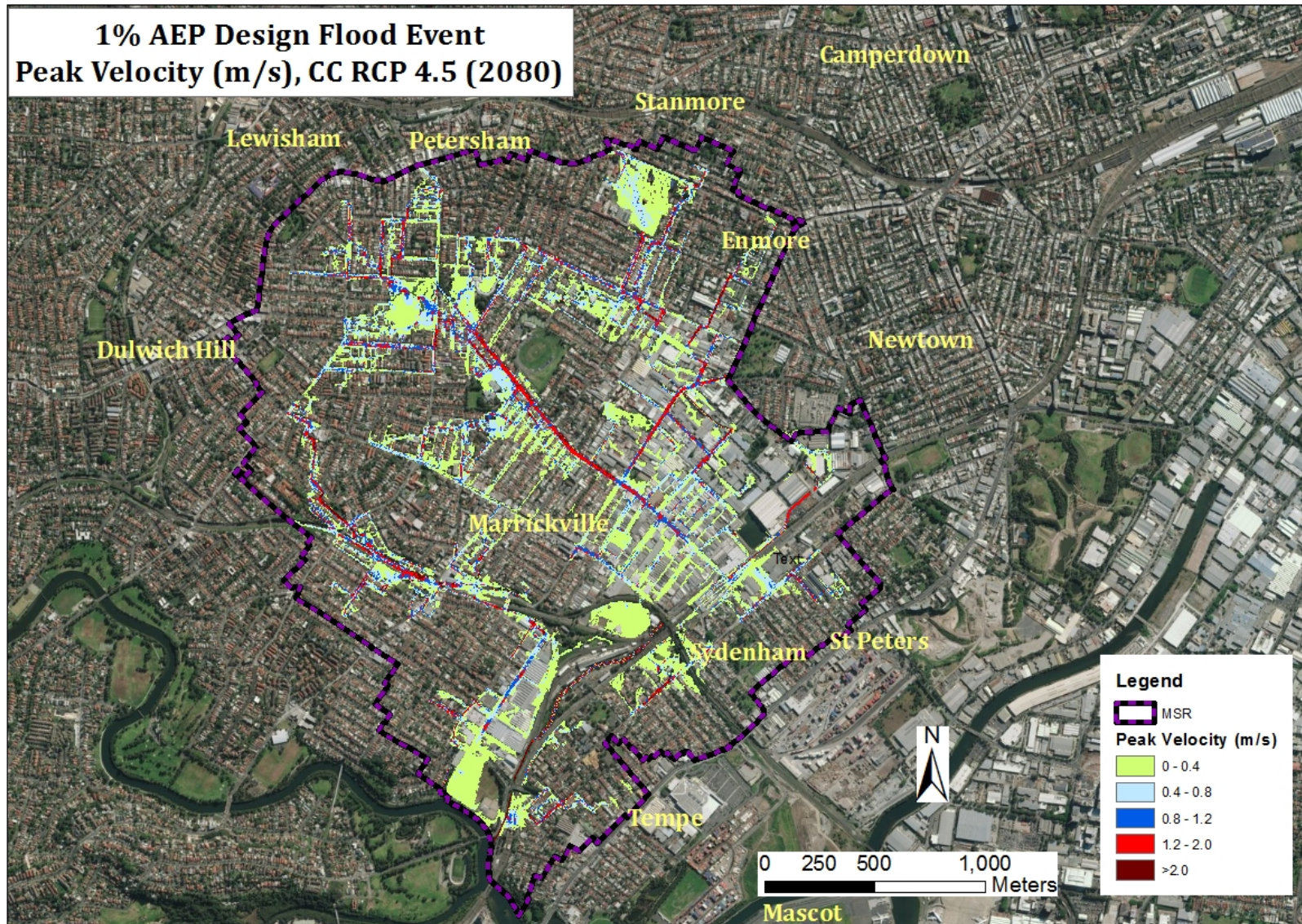


Figure B-5: 1% AEP design flood event, Climate Change Scenario, RCP 4.5 (2080): Peak velocity vector

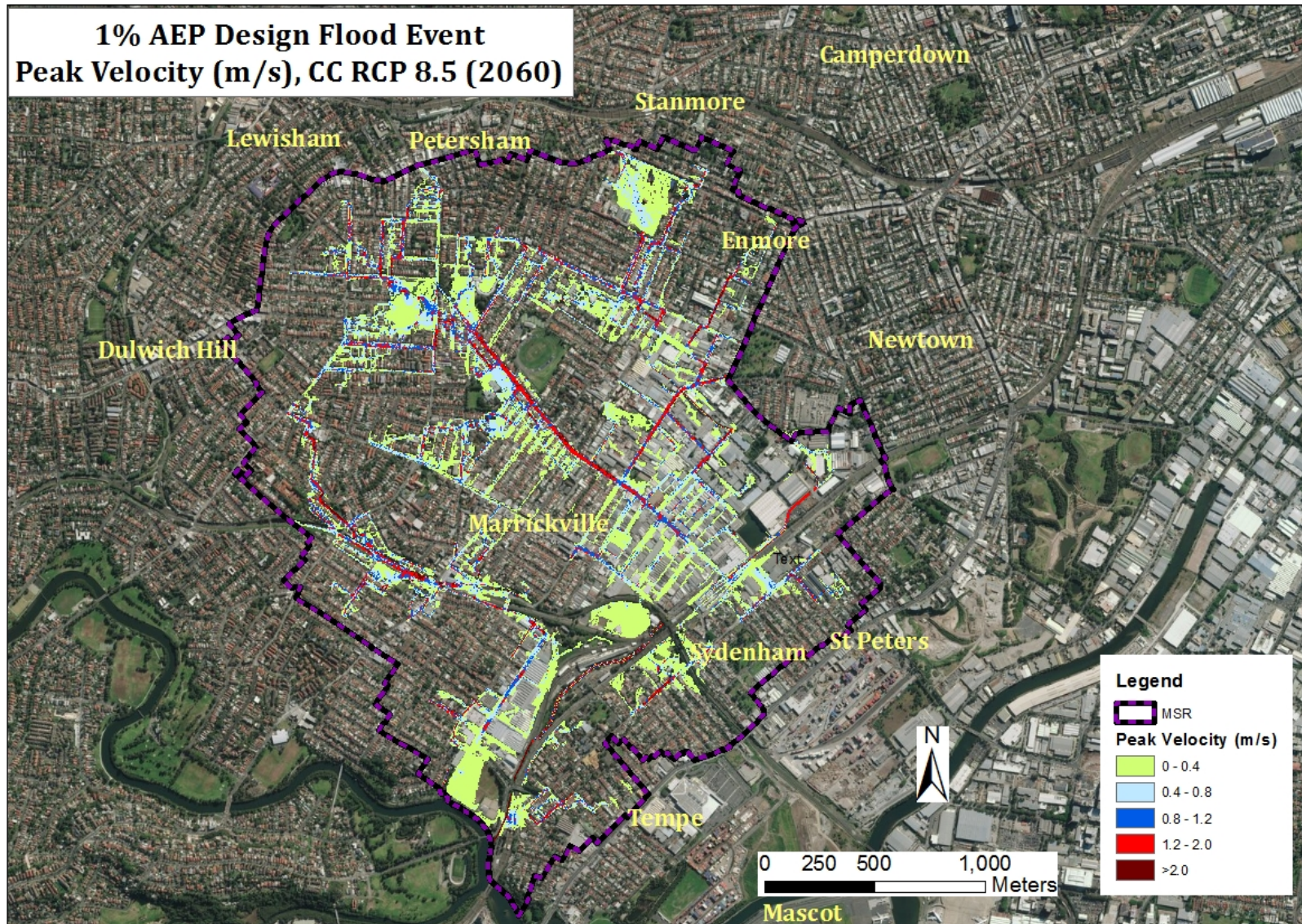


Figure B-6: 1% AEP design flood event, Climate Change Scenario, RCP 8.5 (2060): Peak velocity vector

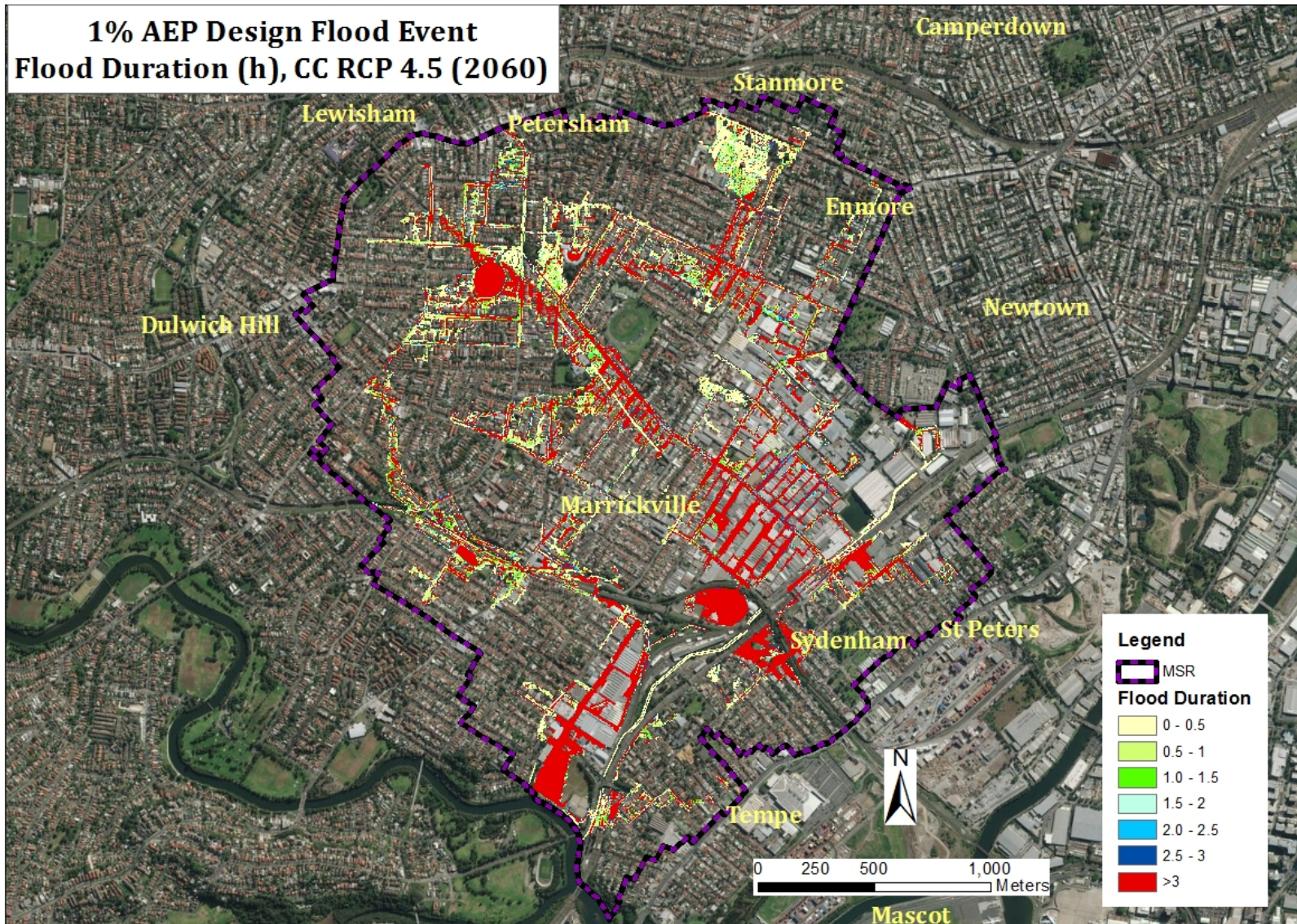


Figure B-7: 1% AEP design flood event, Climate Change Scenario, RCP 4.5 (2060): Flood Duration

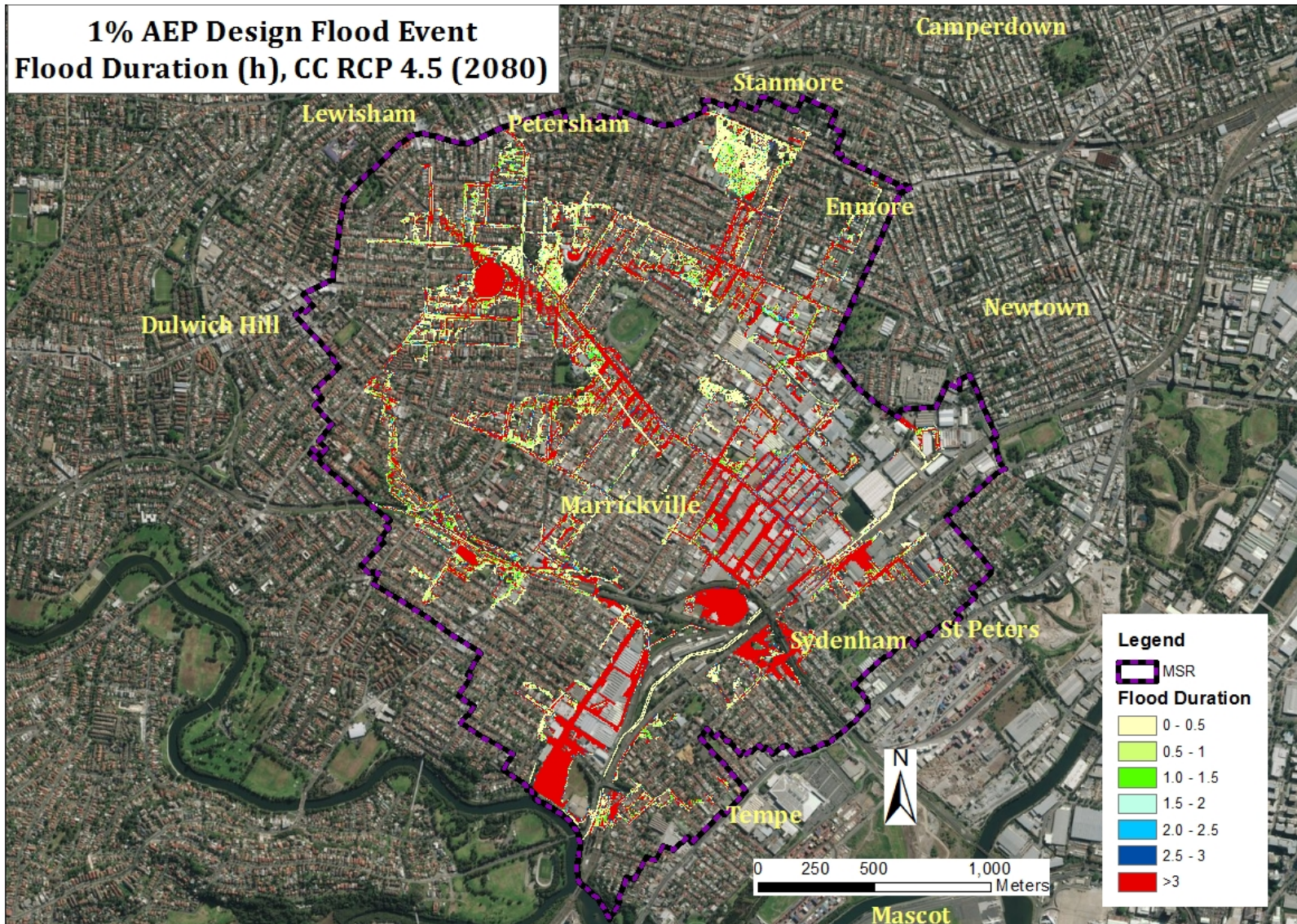


Figure B-8: 1% AEP design flood event, Climate Change Scenario, RCP 4.5 (2080): Flood Duration

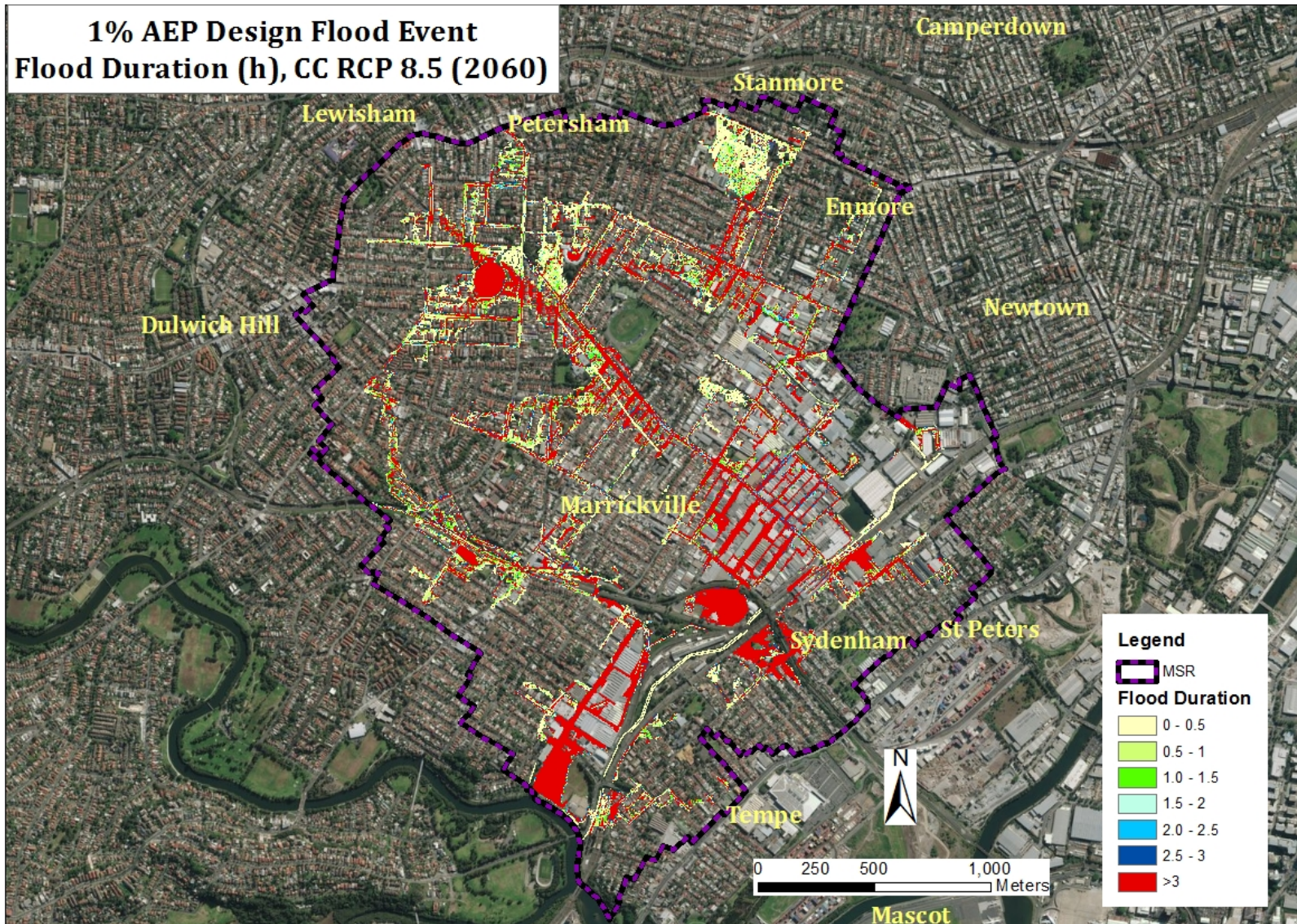


Figure B-9: 1% AEP design flood event, Climate Change Scenario, RCP 8.5 (2060): Flood Duration

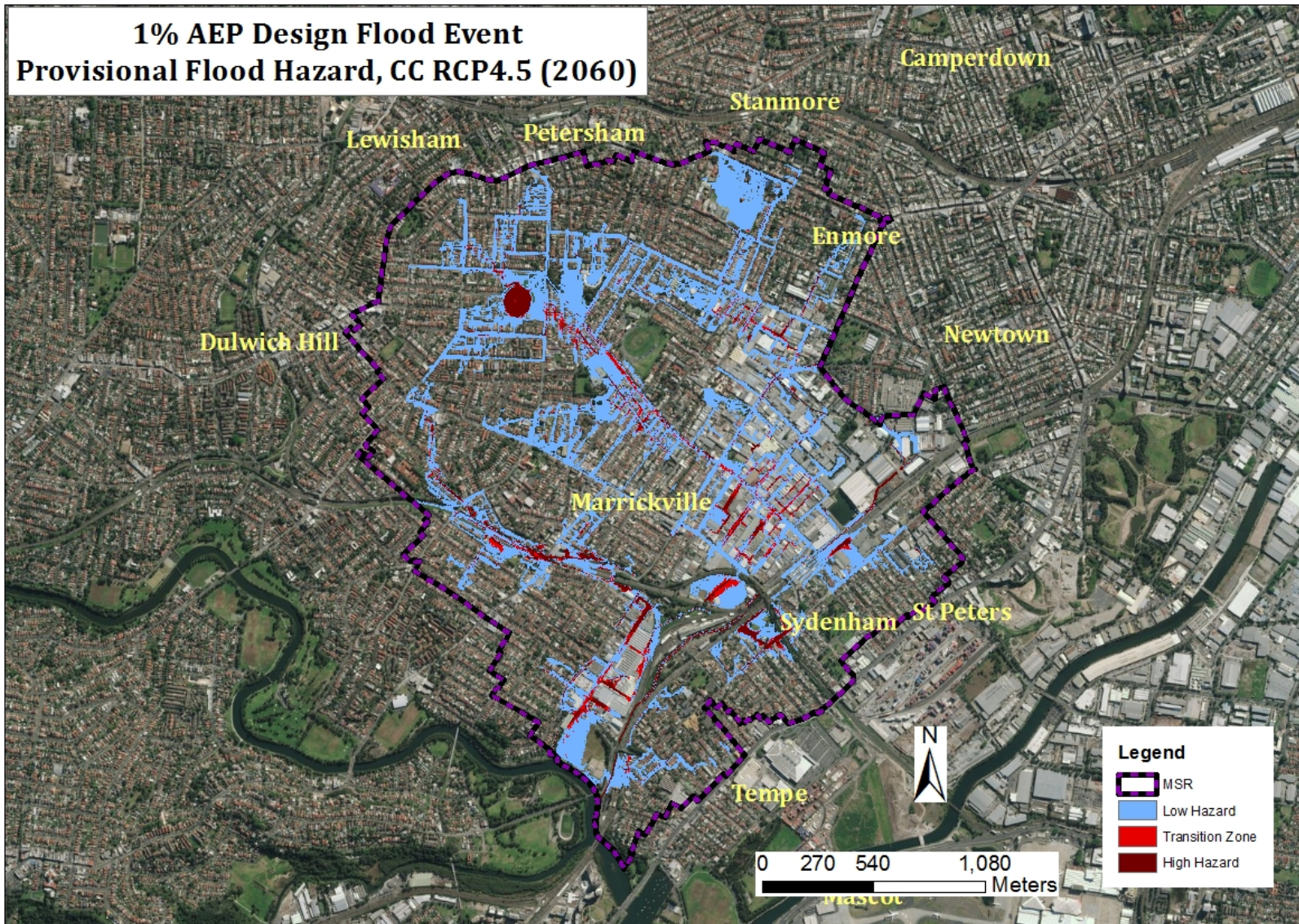


Figure B-10: 1% AEP design flood event, CC Scenario, RCP4.5 (2060): Provisional Flood Hazard

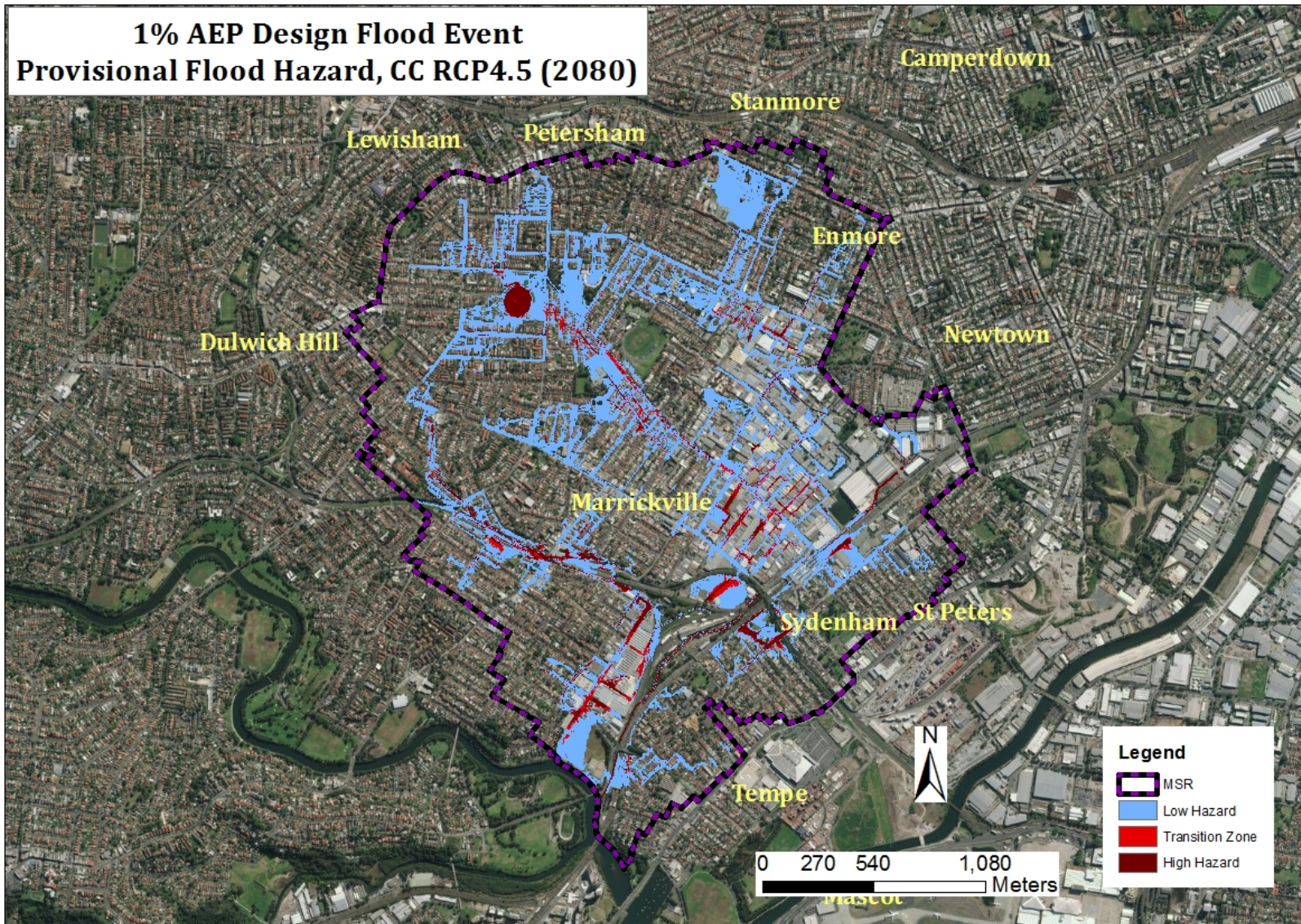


Figure B-11: 1% AEP design flood event, CC Scenario, RCP4.5 (2080): Provisional Flood Hazard

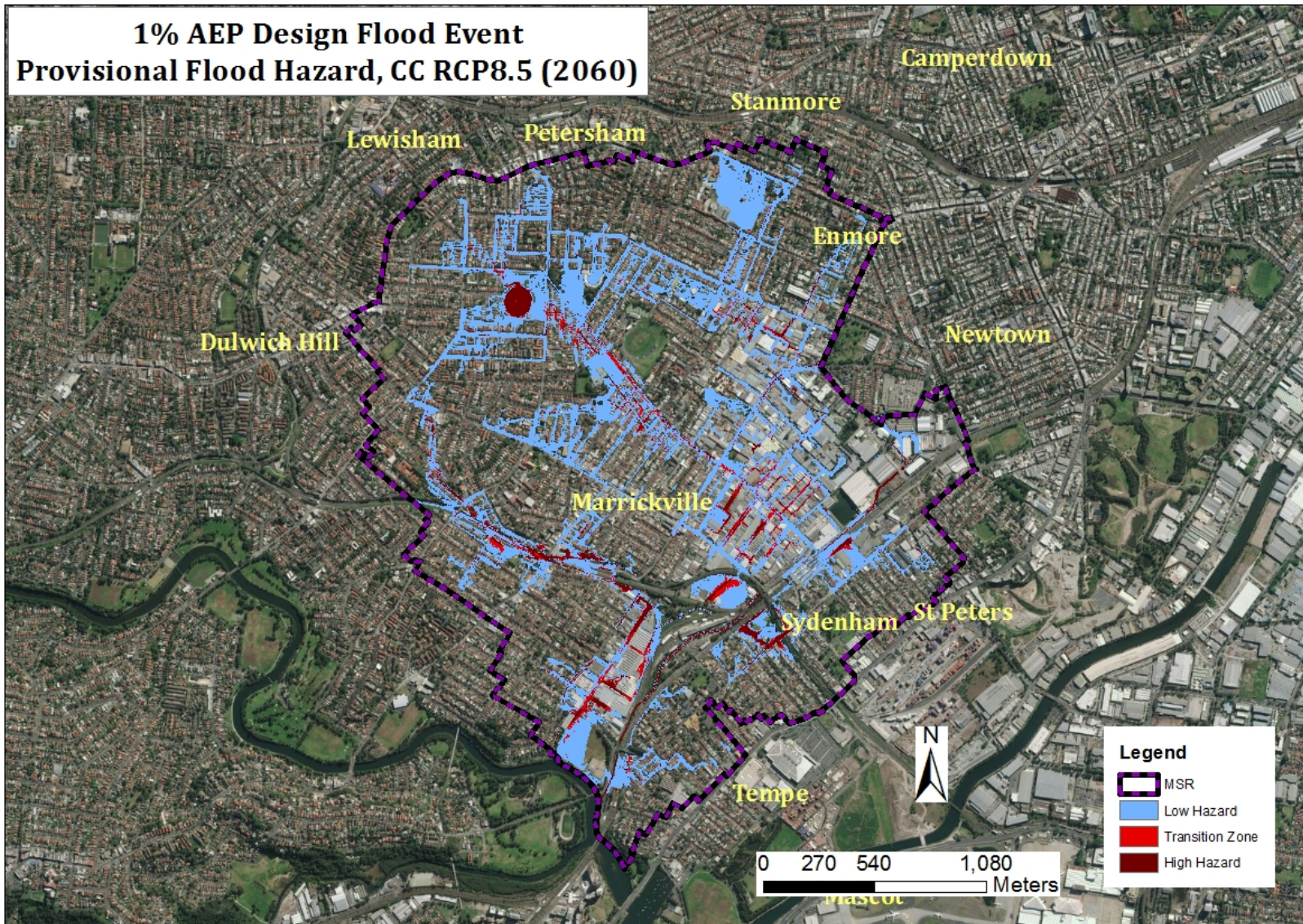


Figure B-12: 1% AEP design flood event, CC Scenario, RCP8.5 (2060): Provisional Flood Hazard

References

- Adger, W. N. 2006. Vulnerability. *Global environmental change*, 16, 268-281.
- Adger, W. N., Arnell, N. W. & Tompkins, E. L. 2005. Successful adaptation to climate change across scales. *Global environmental change*, 15, 77-86.
- Adger, W. N., Huq, S., Brown, K., Conway, D. & Hulme, M. 2003. Adaptation to climate change in the developing world. *Progress in development studies*, 3, 179-195.
- Alwang, J., Siegel, P. B. & Jorgensen, S. L. 2001. Vulnerability: a view from different disciplines. Social protection discussion paper series.
- Apel, H., Thielen, A. H., Merz, B. & Blöschl, G. 2004. Flood risk assessment and associated uncertainty. *Natural Hazards and Earth System Science*, 4, 295-308.
- Ashley, R. M., Balmforth, D. J., Saul, A. J. & Blanskby, J. 2005. Flooding in the future—predicting climate change, risks and responses in urban areas. *Water Science and Technology*, 52, 265-273.
- Babister, M., Retallick, M., Loveridge, M., Testoni, I. & Podger, S. 2016. Temporal patterns, Book 2 in in Australian Rainfall and Runoff - A Guide to Flood Estimation, Commonwealth of Australia
- Balica, S., Douben, N. & Wright, N. 2009. Flood vulnerability indices at varying spatial scales. *Water science and technology*, 60, 2571-2580.
- Balica, S., Wright, N. G. & Van Der Meulen, F. 2012. A flood vulnerability index for coastal cities and its use in assessing climate change impacts. *Natural hazards*, 64, 73-105.
- Bates, B., Mcluckie, D., Westra, S., Johnson, F., Green, J., Mummery, J. & Abbs, D. 2016. Climate change considerations, Book 1 in Australian Rainfall and Runoff - A Guide to Flood Estimation, Commonwealth of Australia
- Berggren, K., Olofsson, M., Viklander, M., Svensson, G. & Gustafsson, A.-M. 2011. Hydraulic impacts on urban drainage systems due to changes in rainfall caused by climatic change. *Journal of Hydrologic Engineering*, 17, 92-98.
- Blaikie, P., Cannon, T., Davis, I. & Wisner, B. 2014. *At risk: natural hazards, people's vulnerability and disasters*, Routledge.
- Bmt-Wbm 2016. TUFLOW user manual.
- Borden, K. A., Schmidlein, M. C., Emrich, C. T., Piegorsch, W. W. & Cutter, S. L. 2007. Vulnerability of US cities to environmental hazards. *Journal of Homeland Security and Emergency Management*, 4, 1-21.
- Brody, S. D., Kang, J. E. & Bernhardt, S. 2010. Identifying factors influencing flood mitigation at the local level in Texas and Florida: the role of organizational capacity. *Natural hazards*, 52, 167-184.

- Bruni, G., Reinoso, R., Van De Giesen, N., Clemens, F. & Ten Veldhuis, J. 2015. On the sensitivity of urban hydrodynamic modelling to rainfall spatial and temporal resolution. *Hydrology and Earth System Sciences*, 19, 691.
- Burton, I. 1993. *The environment as hazard*, Guilford Press.
- Carmin, J., Anguelovski, I. & Roberts, D. 2012. Urban climate adaptation in the global south: planning in an emerging policy domain. *Journal of Planning Education and Research*, 32, 18-32.
- Cattell, R. B. 1966. The scree test for the number of factors. *Multivariate behavioral research*, 1, 245-276.
- Chang, S. E. 2003. Evaluating disaster mitigations: methodology for urban infrastructure systems. *Natural Hazards Review*, 4, 186-196.
- Chang, T.-J., Wang, C.-H. & Chen, A. S. 2015. A novel approach to model dynamic flow interactions between storm sewer system and overland surface for different land covers in urban areas. *Journal of Hydrology*, 524, 662-679.
- Charlesworth, S. 2010. A review of the adaptation and mitigation of global climate change using sustainable drainage in cities. *Journal of Water and Climate Change*, 1, 165-180.
- Chau, K., Wu, C. & Li, Y. 2005. Comparison of several flood forecasting models in Yangtze River. *Journal of Hydrologic Engineering*, 10, 485-491.
- Cloke, H. & Pappenberger, F. 2009. Ensemble flood forecasting: a review. *Journal of Hydrology*, 375, 613-626.
- Coastadapt. n.d. *What is climate change?* [Online]. Available: <https://coastadapt.com.au/learn-about-climate-change> [Accessed 21/05/2018].
- Connor, R. & Hiroki, K. 2005. Development of a method for assessing flood vulnerability. *Water science and technology*, 51, 61-67.
- Cornelius, S. 2012. EXPERIENCE AND TECHNIQUES IN MODELLING URBAN STORMWATER NETWORKS AND OVERLAND FLOW PATHS.
- Council, S. C. 2014. Chapter G9: Development on flood prone Land, Shoalhaven development control plan 2014.
- Crichton, D. 2002. UK and global insurance responses to flood hazard. *Water International*, 27, 119-131.
- Cutter, S., Emrich, C., Morath, D. & Dunning, C. 2013. Integrating social vulnerability into federal flood risk management planning. *Journal of Flood Risk Management*, 6, 332-344.
- Cutter, S. L., Boruff, B. J. & Shirley, W. L. 2003. Social vulnerability to environmental hazards. *Social science quarterly*, 84, 242-261.

- Cutter, S. L., Mitchell, J. T. & Scott, M. S. 2000. Revealing the vulnerability of people and places: a case study of Georgetown County, South Carolina. *Annals of the association of American Geographers*, 90, 713-737.
- Dang, N. M., Babel, M. S. & Luong, H. T. 2011. Evaluation of food risk parameters in the day river flood diversion area, Red River delta, Vietnam. *Natural hazards*, 56, 169-194.
- Domingo, N. S., Refsgaard, A., Mark, O. & Paludan, B. 2010. Flood analysis in mixed-urban areas reflecting interactions with the complete water cycle through coupled hydrologic-hydraulic modelling. *Water Science and Technology*, 62, 1386-1392.
- Dwyer, A., Zoppou, C., Nielsen, O., Day, S. & Roberts, S. 2004. *Quantifying Social Vulnerability: A methodology for identifying those at risk to natural hazards*, Citeseer.
- Ebert, U. & Welsch, H. 2004. Meaningful environmental indices: a social choice approach. *Journal of Environmental Economics and Management*, 47, 270-283.
- Eisenack, K., Moser, S. C., Hoffmann, E., Klein, R. J., Oberlack, C., Pechan, A., Rotter, M. & Termeer, C. J. 2014. Explaining and overcoming barriers to climate change adaptation. *Nature Climate Change*, 4, 867.
- El-Zein, A. & Tonmoy, F. N. 2015. Assessment of vulnerability to climate change using a multi-criteria outranking approach with application to heat stress in Sydney. *Ecological Indicators*, 48, 207-217.
- El-Zein, A. & Tonmoy, F. N. 2017. Nonlinearity, fuzziness and incommensurability in indicator-based assessments of vulnerability to climate change: A new mathematical framework. *Ecological Indicators*, 82, 82-93.
- Ezer, T. & Atkinson, L. P. 2014. Accelerated flooding along the US East Coast: on the impact of sea - level rise, tides, storms, the Gulf Stream, and the North Atlantic oscillations. *Earth's Future*, 2, 362-382.
- Fatemi, F., Ardalan, A., Aguirre, B., Mansouri, N. & Mohammadfam, I. 2017. Social vulnerability indicators in disasters: Findings from a systematic review. *International journal of disaster risk reduction*, 22, 219-227.
- Fatichi, S., Vivoni, E. R., Ogden, F. L., Ivanov, V. Y., Mirus, B., Gochis, D., Downer, C. W., Camporese, M., Davison, J. H. & Ebel, B. 2016. An overview of current applications, challenges, and future trends in distributed process-based models in hydrology. *Journal of Hydrology*, 537, 45-60.
- Fekete, A. 2009. Validation of a social vulnerability index in context to river-floods in Germany. *Natural Hazards and Earth System Sciences*, 9, 393-403.
- Fekete, A. 2010. *Assessment of Social Vulnerability River Floods in Germany*, Citeseer.
- Fernandez, P., Mourato, S., Moreira, M. & Pereira, L. 2016. A new approach for computing a flood vulnerability index using cluster analysis. *Physics and Chemistry of the Earth, Parts A/B/C*, 94, 47-55.

Field, A. 2009. *Discovering statistics using SPSS:(and sex and drugs and rock 'n'roll). Introducing statistical methods.* London: Sage.

Floodsite. n.d. *Integrated flood risk analysis and management methodologies* [Online]. Available: http://www.floodsite.net/html/cd_task17-19/overall_project.html [Accessed 21/05/2018].

Frigerio, I. & De Amicis, M. 2016. Mapping social vulnerability to natural hazards in Italy: A suitable tool for risk mitigation strategies. *Environmental Science & Policy*, 63, 187-196.

Füssel, H.-M. 2007. Adaptation planning for climate change: concepts, assessment approaches, and key lessons. *Sustainability science*, 2, 265-275.

Garbutt, K., Ellul, C. & Fujiyama, T. 2015. Mapping social vulnerability to flood hazard in Norfolk, England. *Environmental Hazards*, 14, 156-186.

Geoscienceaustralia. n.d. *Risk and Impact* [Online]. Available: <http://www.ga.gov.au/scientific-topics/hazards/risk-and-impact> [Accessed 21/05/2018].

Gharbi, M., Soualmia, A., Dartus, D. & Masbernat, L. 2016. Comparison of 1D and 2D hydraulic models for floods simulation on the Medjerda River in Tunisia. *J. Mater. Environ. Sci*, 7, 3017-3026.

Gilbert, P. H., Isenberg, J., Baecher, G. B., Papay, L. T., Spielvogel, L. G., Woodard, J. B. & Badolato, E. V. 2003. Infrastructure issues for cities—Countering terrorist threat. *Journal of infrastructure systems*, 9, 44-54.

Gilles, D., Young, N., Schroeder, H., Piotrowski, J. & Chang, Y.-J. 2012. Inundation mapping initiatives of the Iowa Flood Center: Statewide coverage and detailed urban flooding analysis. *Water*, 4, 85-106.

Government, N. 2005. *Floodplain development manual, the management of flood liable land.*

Gray, S. 2011. *Marrickville valley flood study, Final draft report.* Sydney, NSW: Marrickville Council.

Green, J., Johnson, F., Beesley, C. & The, C. 2016. *Design Rainfall, Book 2 in Australian Rainfall and Runoff - A Guide to Flood Estimation, Commonwealth of Australia*

Gupta, R. P. 2018. *Digital Elevation Model. Remote Sensing Geology.* Springer.

Hallegatte, S., Green, C., Nicholls, R. J. & Corfee-Morlot, J. 2013. Future flood losses in major coastal cities. *Nature climate change*, 3, 802.

Hewitt, K. 1983. The idea of calamity in a technocratic age. *Interpretation of Calamity: From the Viewpoint of Human Ecology.* Allen & Unwin, Boston, 3-32.

Holand, I. S., Lujala, P. & Rød, J. K. 2011. Social vulnerability assessment for Norway: a quantitative approach. *Norsk Geografisk Tidsskrift-Norwegian Journal of Geography*, 65, 1-17.

- Hsu, M.-H., Chen, S. H. & Chang, T.-J. 2000. Inundation simulation for urban drainage basin with storm sewer system. *Journal of Hydrology*, 234, 21-37.
- Hunt, A. & Watkiss, P. 2011. Climate change impacts and adaptation in cities: a review of the literature. *Climatic Change*, 104, 13-49.
- Hunter, N., Bates, P., Neelz, S., Pender, G., Villanueva, I., Wright, N., Liang, D., Falconer, R. A., Lin, B. & Waller, S. Benchmarking 2D hydraulic models for urban flood simulations. Proceedings of the institution of civil engineers: water management, 2008. Thomas Telford (ICE publishing), 13-30.
- Huong, H. & Pathirana, A. 2013. Urbanization and climate change impacts on future urban flooding in Can Tho city, Vietnam. *Hydrology and Earth System Sciences*, 17, 379-394.
- Ippcc 2014a. *Climate change 2014: synthesis report. Contribution of Working Groups I, II and III to the fifth assessment report of the Intergovernmental Panel on Climate Change [Core Writing Team, R.K. Pachauri and L.A. Meyer (eds.)]. IPCC, Geneva, Switzerland, 151 pp., IPCC.*
- Johnson, P. 2013. *Comparison of direct rainfall and lumped-conceptual rainfall runoff routing methods in tropical North Queensland—a case study of Low Drain, Mount Low, Townsville.* University of Southern Queensland.
- Jongman, B., Winsemius, H. C., Aerts, J. C., De Perez, E. C., Van Aalst, M. K., Kron, W. & Ward, P. J. 2015. Declining vulnerability to river floods and the global benefits of adaptation. *Proceedings of the National Academy of Sciences*, 112, E2271-E2280.
- Kaiser, H. F. 1960. The application of electronic computers to factor analysis. *Educational and psychological measurement*, 20, 141-151.
- Kaiser, H. F. 1970. A second generation little jiffy. *Psychometrika*, 35, 401-415.
- Karim, F., Petheram, C., Marvanek, S., Ticehurst, C., Wallace, J. & Gouweleeuw, B. The use of hydrodynamic modelling and remote sensing to estimate floodplain inundation and flood discharge in a large tropical catchment. Proceedings of MODSIM2011: The 19th International Congress on Modelling and Simulation, Perth, Australia, 2011.
- Każmierczak, A. & Cavan, G. 2011. Surface water flooding risk to urban communities: Analysis of vulnerability, hazard and exposure. *Landscape and Urban Planning*, 103, 185-197.
- Kelman, I. & Spence, R. 2004. An overview of flood actions on buildings. *Engineering Geology*, 73, 297-309.
- Koks, E. E., Jongman, B., Husby, T. G. & Botzen, W. J. 2015. Combining hazard, exposure and social vulnerability to provide lessons for flood risk management. *Environmental Science & Policy*, 47, 42-52.
- König, A., Sægrov, S. & Schilling, W. 2002. Damage assessment for urban flooding. *Global Solutions for Urban Drainage*.

- Koop, S. H. & Van Leeuwen, C. J. 2017. The challenges of water, waste and climate change in cities. *Environment, development and sustainability*, 19, 385-418.
- Leandro, J., Chen, A. S., Djordjević, S. & Savić, D. A. 2009. Comparison of 1D/1D and 1D/2D coupled (sewer/surface) hydraulic models for urban flood simulation. *Journal of hydraulic engineering*, 135, 495-504.
- Leandro, J., Schumann, A. & Pfister, A. 2016. A step towards considering the spatial heterogeneity of urban key features in urban hydrology flood modelling. *Journal of Hydrology*, 535, 356-365.
- Lindley, S. J., Handley, J. F., Theuray, N., Peet, E. & Mcevoy, D. 2006. Adaptation strategies for climate change in the urban environment: assessing climate change related risk in UK urban areas. *Journal of Risk Research*, 9, 543-568.
- Liu, J., Hertel, T. W., Diffenbaugh, N. S., Delgado, M. S. & Ashfaq, M. 2015. Future property damage from flooding: sensitivities to economy and climate change. *Climatic Change*, 132, 741-749.
- Mark, O. & Djordjevic, S. While waiting for the next flood in your city. 7th international Conference on Hydroinformatics, Nice, France, 2006.
- Mark, O., Weesakul, S., Apirumanekul, C., Aroonnet, S. B. & Djordjević, S. 2004. Potential and limitations of 1D modelling of urban flooding. *Journal of Hydrology*, 299, 284-299.
- Mcgrane, S. J. 2016. Impacts of urbanisation on hydrological and water quality dynamics, and urban water management: a review. *Hydrological Sciences Journal*, 61, 2295-2311.
- Measham, T. G., Preston, B. L., Smith, T. F., Brooke, C., Gorddard, R., Withycombe, G. & Morrison, C. 2011. Adapting to climate change through local municipal planning: barriers and challenges. *Mitigation and adaptation strategies for global change*, 16, 889-909.
- Mikeurban. n.d. *Integrated urban water modelling* [Online]. Available: <https://www.mikepoweredbydhi.com/products/mike-urban> [Accessed 21/05/2018].
- Mileti, D. 1999. *Disasters by design: A reassessment of natural hazards in the United States*, Joseph Henry Press.
- Miller, J. D. & Hutchins, M. 2017. The impacts of urbanisation and climate change on urban flooding and urban water quality: A review of the evidence concerning the United Kingdom. *Journal of Hydrology: Regional Studies*, 12, 345-362.
- Morrow, B. H. 1999. Identifying and mapping community vulnerability. *Disasters*, 23, 1-18.
- Muis, S., Güneralp, B., Jongman, B., Aerts, J. C. & Ward, P. J. 2015. Flood risk and adaptation strategies under climate change and urban expansion: A probabilistic analysis using global data. *Science of the Total Environment*, 538, 445-457.
- Muller, M. 2007. Adapting to climate change water management for urban resilience. *Environment and Urbanization*, 19, 99-113.

- Nccarf. 2017. *Sea-level rise and future climate information for coastal councils* [Online]. Available: <https://coastadapt.com.au/about-coastadapt> [Accessed 4/10/2017].
- O'brien, P. W. & Mileti, D. S. 1992. Citizen participation in emergency response following the Loma Prieta earthquake. *International Journal of Mass Emergencies and Disasters*, 10, 71-89.
- O'loughlin, G. & Stack, B. 2014. Drains users manual. *A manual on the Drains program for urban stormwater drainage system design and analysis*. Sydney: Watercom Pty Ltd.
- O'sullivan, C., Mulgan, G., Ali, R. & Norman, W. 2009. Sinking and swimming: Understanding Britain's unmet needs. *Young Foundation*.
- Overton, I. C. 2005. Modelling floodplain inundation on a regulated river: integrating GIS, remote sensing and hydrological models. *River Research and Applications*, 21, 991-1001.
- Parfomak, P. W. Vulnerability of concentrated critical infrastructure: Background and policy options. 2005. Library of congress Washington DC Congressional research Service.
- Patro, S., Chatterjee, C., Mohanty, S., Singh, R. & Raghuwanshi, N. 2009. Flood inundation modeling using MIKE FLOOD and remote sensing data. *Journal of the Indian Society of Remote Sensing*, 37, 107-118.
- Patt, A. G., Schröter, D., De La Vega-Leiner, A. C. & Klein, R. J. 2012. Vulnerability research and assessment to support adaptation and mitigation: common themes from the diversity of approaches. *Assessing vulnerability to global environmental change*. Routledge.
- Paul, M. J. & Meyer, J. L. 2001. Streams in the urban landscape. *Annual review of Ecology and Systematics*, 32, 333-365.
- Petersen, O., Rasmussen, E. B., Enggrob, H. & Rungø, M. 2002. Modelling of Flood Events Using Dynamically Linked 1-D and 2-D Models. *DHI Water & Environment*.
- Phillips, B., Yu, S., Thompson, G. & De Silva, N. 1D and 2D Modelling of Urban Drainage Systems using XP-SWMM and TUFLOW. 10th International Conference on Urban Drainage, 2005. Citeseer, 21-26.
- Pilgrim, D. H. 1987. Australian rainfall and runoff- A guide to flood estimation, Institute of Engineers, Australia.
- Pink, B. 2011. Socio-economic indexes for areas (SEIFA). *Technical paper*.
- Plate, E. J. 2002. Flood risk and flood management. *Journal of Hydrology*, 267, 2-11.
- Poulter, B. & Halpin, P. N. 2008. Raster modelling of coastal flooding from sea - level rise. *International Journal of Geographical Information Science*, 22, 167-182.
- Pulido, L. 2000. Rethinking environmental racism: White privilege and urban development in Southern California. *Annals of the Association of American Geographers*, 90, 12-40.
- Qudm 2013. Queensland Urban Drainage Manual. Third ed.: Department of Energy and Water Supply.

- Rauch, W., Bertrand-Krajewski, J.-L., Krebs, P., Mark, O., Schilling, W., Schütze, M. & Vanrolleghem, P. A. 2002. Deterministic modelling of integrated urban drainage systems. *Water science and technology*, 45, 81-94.
- Reid, A., Maratea, E., Kilaparty, B. & Fang, T. 2014. Floodplain risk management plan, Alexandra canal floodplain risk management study and plan, prepared for City of Sydney. Sydney, NSW.
- Rygel, L., O'sullivan, D. & Yarnal, B. 2006. A method for constructing a social vulnerability index: an application to hurricane storm surges in a developed country. *Mitigation and adaptation strategies for global change*, 11, 741-764.
- Sarewitz, D., Pielke, R. & Keykhah, M. 2003. Vulnerability and risk: some thoughts from a political and policy perspective. *Risk analysis*, 23, 805-810.
- Schanze, J. 2006. Flood risk management—a basic framework. *Flood risk management: hazards, vulnerability and mitigation measures*, 1-20.
- Schmidtlein, M. C., Deutsch, R. C., Piegorsch, W. W. & Cutter, S. L. 2008. A sensitivity analysis of the social vulnerability index. *Risk Analysis*, 28, 1099-1114.
- Schmitt, T. G., Thomas, M. & Ettrich, N. 2004. Analysis and modeling of flooding in urban drainage systems. *Journal of Hydrology*, 299, 300-311.
- Schreider, S. Y., Smith, D. & Jakeman, A. 2000. Climate change impacts on urban flooding. *Climatic Change*, 47, 91-115.
- Schröter, D., Polsky, C. & Patt, A. G. 2005. Assessing vulnerabilities to the effects of global change: an eight step approach. *Mitigation and Adaptation Strategies for Global Change*, 10, 573-595.
- Soetanto, R. & Proverbs, D. G. 2004. Impact of flood characteristics on damage caused to UK domestic properties: the perceptions of building surveyors. *Structural Survey*, 22, 95-104.
- Solangaarachchi, D., Griffin, A. L. & Doherty, M. D. 2012. Social vulnerability in the context of bushfire risk at the urban-bush interface in Sydney: a case study of the Blue Mountains and Ku-ring-gai local council areas. *Natural Hazards*, 64, 1873-1898.
- Sole, A., Giosa, L., Nolè, L., Medina, V. & Bateman, A. 2008. Flood risk modelling with LiDAR technology. *Flood Recovery, Innovation and Response*, 118, 127.
- Tapsell, S. M., Penning-Rowsell, E. C., Tunstall, S. M. & Wilson, T. L. 2002. Vulnerability to flooding: health and social dimensions. *Philosophical Transactions of the Royal Society of London A: Mathematical, Physical and Engineering Sciences*, 360, 1511-1525.
- Tavares, A. O., Dos Santos, P. P., Freire, P., Fortunato, A. B., Rilo, A. & Sá, L. 2015. Flooding hazard in the Tagus estuarine area: The challenge of scale in vulnerability assessments. *Environmental Science & Policy*, 51, 238-255.

- Thampapillai, D. J. & Musgrave, W. F. 1985. Flood damage mitigation: A review of structural and nonstructural measures and alternative decision frameworks. *Water Resources Research*, 21, 411-424.
- Tonmoy, F. 2014. *Assessment of vulnerability to climate change: theoretical and methodological developments with applications to infrastructure and built environment*. PhD Thesis, The University of Sydney.
- Tonmoy, F. N., El - Zein, A. & Hinkel, J. 2014. Assessment of vulnerability to climate change using indicators: a meta - analysis of the literature. *Wiley Interdisciplinary Reviews: Climate Change*, 5, 775-792.
- Tonmoy, F. N., Wainwright, D., Verdon-Kidd, D. C. & Rissik, D. 2018. An investigation of coastal climate change risk assessment practice in Australia. *Environmental Science & Policy*, 80, 9-20.
- Tuflow 2016. TUFLOW user manual. *Build 2016-03-AA*. BMT WBM.
- Turner, B. L., Kasperson, R. E., Matson, P. A., McCarthy, J. J., Corell, R. W., Christensen, L., Eckley, N., Kasperson, J. X., Luers, A. & Martello, M. L. 2003. A framework for vulnerability analysis in sustainability science. *Proceedings of the national academy of sciences*, 100, 8074-8079.
- Van Manen, S. E. & Brinkhuis, M. 2005. Quantitative flood risk assessment for Polders. *Reliability engineering & system safety*, 90, 229-237.
- Vaze, J. & Teng, J. 2007. High resolution LIDAR DEM—How good is it. *Modelling and Simulation*, 692-698.
- Vincent, K. 2004. Creating an index of social vulnerability to climate change for Africa. *Tyndall Center for Climate Change Research. Working Paper*, 56, 41.
- Vojinovic, Z. & Tutulic, D. 2009. On the use of 1D and coupled 1D-2D modelling approaches for assessment of flood damage in urban areas. *Urban water journal*, 6, 183-199.
- White, G. F. 2000. *The hidden costs of coastal hazards: Implications for risk assessment and mitigation*, Island Press.
- Wolf, T., Mcgregor, G. & Paldy, A. 2011. Integrated assessment of vulnerability to heat stress in urban areas. *Coping with Global Environmental Change, Disasters and Security*. Springer.
- Wu, S.-Y., Yarnal, B. & Fisher, A. 2002. Vulnerability of coastal communities to sea-level rise: a case study of Cape May County, New Jersey, USA. *Climate Research*, 22, 255-270.
- Zachos, L. G., Swann, C. T., Altinakar, M. S., Mcgrath, M. Z. & Thomas, D. 2016. Flood vulnerability indices and emergency management planning in the Yazoo Basin, Mississippi. *International Journal of Disaster Risk Reduction*, 18, 89-99.
- Zahran, S., Brody, S. D., Peacock, W. G., Vedlitz, A. & Grover, H. 2008. Social vulnerability and the natural and built environment: a model of flood casualties in Texas. *Disasters*, 32, 537-560.

Zhou, Q. 2014. A review of sustainable urban drainage systems considering the climate change and urbanization impacts. *Water*, 6, 976-992.

Zhou, Y., Li, N., Wu, W., Wu, J. & Shi, P. 2014. Local spatial and temporal factors influencing population and societal vulnerability to natural disasters. *Risk analysis*, 34, 614-639.

Zhu, T., Lund, J. R., Jenkins, M. W., Marques, G. F. & Ritzema, R. S. 2007. Climate change, urbanization, and optimal long - term floodplain protection. *Water Resources Research*, 43.